Evaluation of a 1.5 x 1.5 m^2 counter-flow fill performance test facility with a view to contributing to a fill performance standard

by

Timothy Paul Bertrand

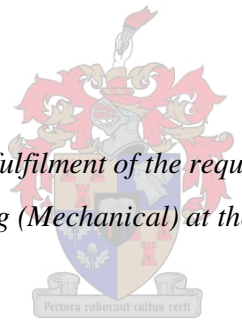

Thesis presented in partial fulfilment of the requirements for the degree Master of Science in Engineering (Mechanical) at the University of Stellenbosch

Supervisor: Prof. Detlev G. Kröger

Faculty of Engineering

Department of Mechanical and Mechatronic Engineering

March 2011

Declaration

By submitting this thesis electronically, I declare that the entirety of the work contained therein is my own, original work, that I am the owner of the copyright thereof (unless to the extent explicitly otherwise stated) and that I have not previously in its entirety or in part submitted it for obtaining any qualification.

……

Signature of candidate

……10……day of ……February……2011……

ABSTRACT

A 1.5 x 1.5 m^2 counter-flow fill performance test facility is described in detail. Instrumentation was selected and installed in the cooling tower fill test facility and calibrated to ensure measurement accuracy. A facility control program was written to simplify the operation of the test facility via a user interface. The program calculates automatically the Merkel number and loss coefficients as measures of fill thermal and flow performance respectively. A spray frame was designed and manufactured to ensure uniform water distribution to the fill. The water distribution through different fills with varying fill heights and different water flow rates was measured. The water attached to the walls of the test facility was examined.

Film, trickle and splash fills are tested in the upgraded test facility. The film and trickle fill performance determined during testing is deemed acceptable as these fills have minimal migration effects. Fills with poor distribution effects and large migration of water towards the walls of the test facility, like the splash fill tested, cannot to be tested accurately in a 1.5 x 1.5 m^2 test section as the results do not represent the performance of the fill in a relatively large cooling tower.

Other aspects examined were:

- air flow uniformity
- air fill bypass effects
- location of water inlet and outlet temperature measurement points
- location of pressure measurement probes.

It was determined that, in the current test facility:

- air uniformity is suitable for performance testing
- air bypass effects can be ignored for open fills and can be minimised for dense fills by packing sponge between the fill and walls
- water inlet and outlet temperatures should be measured in the pipe-work, resulting in a measurement method that is not influenced by the relative weightings of each thermocouple
- pressure difference over the fill height measured by the pressure measurement tap is independent of its location on the fill outlet plane provided the pressure measurement points are perpendicular to the air stream and are not against the walls.

OPSOMMING

'n 1.5 x 1.5 m² Teenvloei pakking werkverrigting toetsfasiliteit word in detail beskryf. Instrumentasie is gekies en geïnstalleer in die koeltoring pakking toetsfasiliteit en gekalibreer om akkuraatheid te verseker. 'n Fasiliteit beheer program is geskryf om die gebruik van die toetsfasiliteit te vereenvoudig. Die program het ‘n vriendelike gebruikers intervalk. Die program bereken outomaties die Merkel-getal en verlies koëffisiënte as mate van pakking termiese- en vloei-werksverrigting. 'n Sproeiraam is ontwerp en vervaardig om uniforme water verspreiding aan die pakking te verseker. Die water verspreiding deur verskillende pakkings met verskillende pakking hoogtes en water vloei snelhede is gemeet. Die water aangeheg aan die mure van die toetsfasiliteit is ook ondersoek.

Film, druppel en spat pakkings word in die opgegradeerde toetsfasiliteit getoets. Die film- en druppelpakking werksverrigting bepaal tydens die toetse is aanvaarbaar, aangesien hierdie pakkings minimale migrasie effekte het. Pakking met swak verspreiding effekte en 'n groot migrasie van water na die wande van die toetsfasiliteit, soos gevind met die spatpakking toetse, kan nie met akkuraatheid in 'n 1.5 x 1.5 m² toets seksie getoets word nie omdat die resultate nie die werkverrigting van die pakking verteenwoordig in 'n relatief groot koeltoring.

Ander aspekte wat ondersoek was:

- lugvloei uniformiteit
- lug omleiding effeckte
- die posisie van water in- en uitlaat temperatuur meetpunte
- posisie van die drukmeetapparaat.

Dit is vasgestel dat, in die huidige toetsfasiliteit

- lugvloei eenvormigheid geskik is vir prestasietoetsing
- lug omleiding effekte kan geïgnoreer word vir oop pakkings en kan verklein word vir digte pakkings deur spons tussen die pakking en mure te pak
- water inlaat- en uitlaattemperature behoort gemeet te word in die pypwerk en lei tot 'n metings metode wat nie beïnvloed word deur die relatiewe gewigte van elke thermokoppel nie
- die druk verskil gemeet deur die drupmeetpunte oor die pakkinghoogte is onafhanklik van hul posisie op die pakkinguitlaatvlak op voorwaarde dat die drukmeetpunte loodreg is teen die lugstroom en nie teen die mure nie.

ACKNOWLEDGEMENTS

I wish to express my appreciation to the following people who each played a role in assisting me to complete this degree:

To Prof Kröger: thank you for the opportunity to complete this degree under your excellent guidance. Thank you for your support and patience. I have truly learnt a lot from you. Thank you for sharing some of your knowledge with me.

To Mr Zietsman and the workshop force, particularly Julian, Nkosinathi, Calvin and Venetia: without your support, technical and non-technical, this project would not have been a success.

To Riaan Terblanche: thanks for being a sounding board for ideas and problem-solving.

To my family and friends: thank you for your continued encouragement and support.

Table of contents

LIST OF FIGURES

Page

LIST OF TABLES

Page

LIST OF SYMBOLS

A	Area, m^2
a	Surface area per unit volume, m^{-1}
c_p	Specific heat at constant pressure, J/kgK
G	Mass velocity, kg/m^2s
g	Gravitational acceleration, m/s^2
H	Height, m
h	Heat transfer coefficient, W/m^2K
h_d	Mass transfer coefficient, kg/m^2s
i	Enthalpy, J/kg
i_{fg}	Latent heat, J/kg
L	Length, m
m	Mass flow rate, kg/s
p	Pressure, N/m^2
T	Temperature, K
v	Velocity, m/s
w	Humidity ratio, kg water vapour/kg dry air
z	Elevation, m or exponent

GREEK SYMBOLS

α	Correction factor
Δ	Differential
ρ	Density, kg/m^3
σ	Standard deviation

SUBSCRIPTS

a	Air
abs	Absolute
amb	Ambient
atm	Atmosphere
av	Mixture of dry air and water vapour
ave	Average
d	Drag
f	Fluid, friction
fi	Fill
fr	Frontal or face
g	Gas
H	Height
i	Inlet, cell index
m	Mixture, mean, momentum
n	Nozzle
o	Outlet
s	Saturation
th	Throat

tot	Total
tr	Trough
tus	Upstream cross-section
v	Vapour
w	Water
wb	Wet-bulb

DIMENSIONLESS GROUPS

Cu Christiansen coefficient = $1-\frac{1}{n^2 m_{ave}}\sum\left|m_{ave}-m_i\right|$

K Loss coefficient = $\frac{\Delta p_{fd}}{\frac{1}{2}\rho v^2}$

Le Lewis factor = $\frac{h}{\left(c_{pma}h_d\right)}$

Me Merkel number = $\frac{h_d a_{fi} L_{f\,i}}{G_w}$

1. INTRODUCTION

1.1. General overview

Evaporative cooling systems are used to rid systems of waste heat. They are used in refrigeration and air conditioning equipment, chemical and petrochemical industries and power generation plants. A simple Rankine cycle is shown in Figure 1-1 and shows how evaporative cooling is integrated into a power-generation cycle.

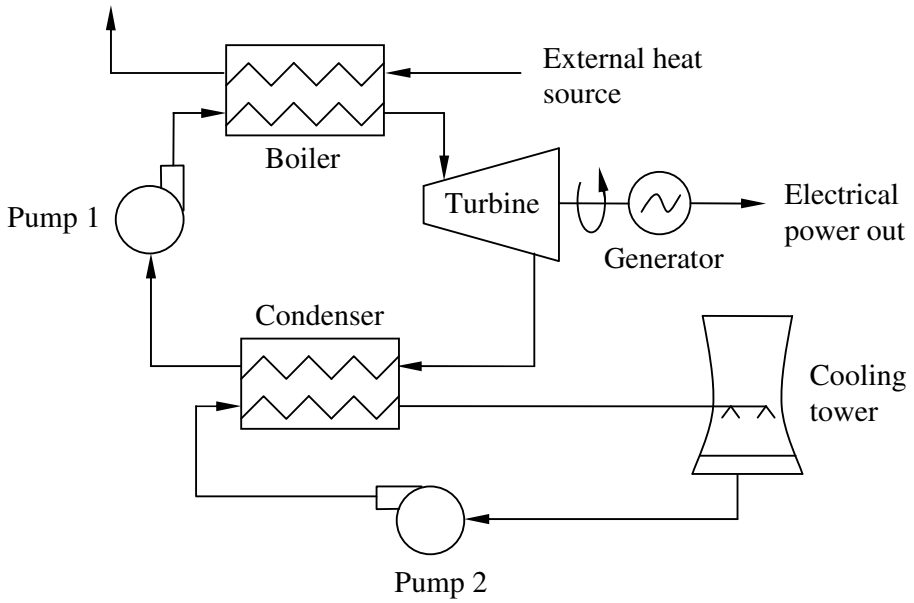

Figure 1-1: Power-generation cycle, illustrating use of evaporative cooling to remove waste heat (Çengel and Boles, 2002).

Water enters pump 1 as a saturated liquid. It is pressurised by the pump to the operating pressure of the boiler. The compressed liquid enters the boiler, where heat is transferred to the liquid from heat that originates from combustion gases, nuclear reactors or any other suitable source of heat. Superheated vapour leaves the boiler, enters the turbine and produces shaft work that turns an electrical generator. The temperature and the pressure of the steam drop in the turbine and the steam usually leaves the turbine as a saturated liquid-vapour mixture. The mixture enters the evaporator and is condensed when heat is transferred to a secondary cooling loop. In the secondary loop the warm cooling water is pumped to an evaporative cooling device where heat is rejected to the atmosphere via wet- or evaporative-cooling. The power-generation cycle is completed when the now saturated liquid in the primary loop again enters the boiler.

A typical evaporative cooling device in the form of a natural-draught counter-flow direct, or wet, cooling tower is illustrated in Figure 1-2.

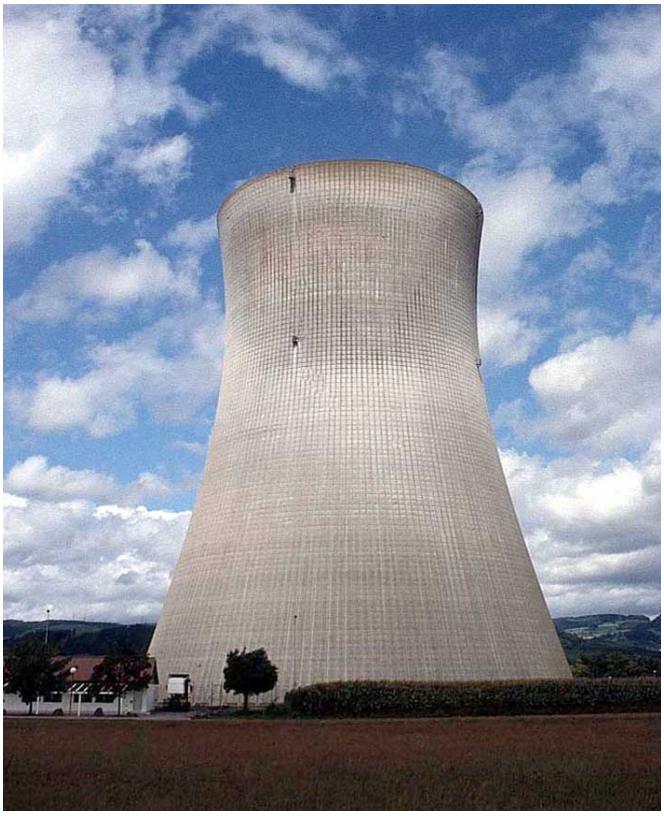

Figure 1-2: Typical natural draught wet-cooling tower used in industry.

Evaporative cooling towers are called wet systems when the cooling fluid is in direct contact with the atmosphere. This is in contrast with indirect, or dry, cooling systems where there is no contact between the cooling fluid and the atmosphere. Evaporative cooling systems are further categorised by a number of distinguishing features (Kröger, 2004).

One classification is according to draught. If the flow of air through the tower occurs as a result of the difference in air densities between the warm, moist air inside the tower and the cooler, heavier air outside the tower, then the tower is called a natural-draught cooling tower. If a fan is used to generate the draught, then the tower is termed a mechanical-draught tower. In mechanical-draught towers, if the fan is placed at the air inlet, then the tower is said to be a forced-draught tower, whereas, if the fan is located at the air outlet then the tower is said to be an induced-draught tower.

A second classification is defined by the flow directions of the water and air streams. In a counter-flow cooling tower, air travels upwards while the water flows down through the fill. In a cross-flow cooling tower, air travels horizontally while the water flows downward through the fill. The operation of a typical natural-draught counter-flow wet-cooling tower is illustrated in Figure 1-3.

Hot water in the secondary cooling loop in Figure 1-1 is pumped into the tower (1). The water is sprayed through a water distribution system (2) and falls down through the fill (3). Air passes through the fill from the bottom upward (4). Drift eliminators (5) prevent water drops which are trapped in the air stream from being blown away. Air exits the tower (6) warmer and more humid than it entered. The cooled water is collected in a basin (7) and is returned to the system (8). All this takes place in the tower shell (9), which is supported above the ground by supports (10). The area of focus in this study is the cooling tower fill (Kröger, 2004).

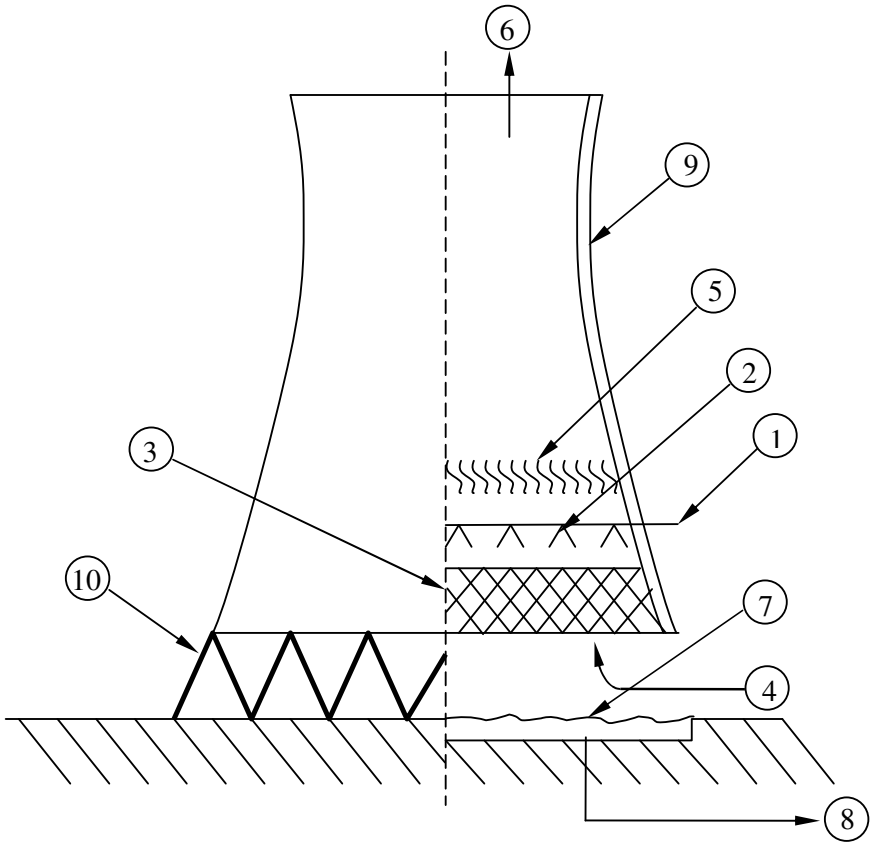

Figure 1-3: Schematic of a natural-draught wet-cooling tower (Kröger, 2004).

The function of fill is to increase the amount of energy transferred from the water to the air. This is achieved by increasing the contact surface area of the water with the air where mass and heat transfer occurs. To some degree fill also retards the

water falling through the tower, increasing the time available for heat and mass transfer. There are three main types of fill, namely film, trickle and splash fill. Examples of these three types of fill are shown in Figure 1-4 a), b) and c) respectively. Each fill type has its positive and negative aspects, but all work on the same principle of effectively increasing the surface area of the water.

a) b) c)

Figure 1-4: Examples of a) film b) trickle and c) splash-type fills.

1.2. Motivation

The use of fill greatly increases the cooling ability of evaporative cooling devices while minimising the cooling tower size. The increased cooling ability of the cooling tower leads to an improved efficiency of the system as a whole. As a result, the use of fill material has widespread acceptance in the cooling industry. While fill has a positive effect on the heat transfer in the tower, it has a negative effect on the airflow through the tower by increasing the resistance experienced by the air as it travels through the tower. A suitable way of representing the heat transfer properties and the flow resistance properties of fills is needed.

Fill is produced and tested by many parties; however, there is no standard for determining fill performance. This is made clear in performance test data available in literature by Lowe and Christie (1961), Fulkerson (1989), Johnson (1989), Johnson and Bartz (1990), Gősi et al. (1992) and Aull (2008), to mention a few. These include fill manufacturer-produced performance data for their fills, academic tests conducted on very small scales, and third-party tests of various fills to determine their performance relative to one another. All these tests contribute to a large volume of performance information available. In these tests the test facilities differ, assumptions differ, the theories used to analyse measured data differ and the parameters used to report the performance differ.

All those differences mean that data generated by one group cannot be directly compared to data generated by another. Performance data accompanied by details of the tests conducted could be usable but the details of fill tests are not generally included in performance results. Fulkerson (1989) comments that using this information is unwise due to the scarcely documented information regarding the specifics of the test facilities where the tests are performed and the theory used to process the data. Burger (1994) states that the performance information published by fill manufactures, even when backed by data, is still unhelpful as it is difficult for users to verify. All this uncertainty results in difficulties when comparing fill from different manufacturers. Burger (1994) suggests the use of an experienced consultant when selecting fill during the design process of a cooling tower. He also suggests visiting sites where the fill is used in similar applications to that of the cooling tower being designed. This is not an efficient method of designing and selecting a specific fill for use in a new cooling tower.

Standardising fill performance tests would be of great benefit when comparing and selecting a fill in the design of evaporative cooling towers. Published data obtained according to the standard would be reliable and directly comparable with other data obtained using the same conditions, test facility, assumptions and theory all specified in the standard for testing cooling tower fill.

1.3. Objectives

The goal of this thesis is to determine to what extent a 1.5 x 1.5 m² test section is suitable for determining counter-flow fill performance with reliable, accurate, repeatable results. The project ultimately aims to contribute in developing a standard for testing counter-flow cooling tower fill. To this end, this study aims to identify what standardisation achieves in the context of performance testing in general. The study examines fill performance testing methods, facilities and theoretical approaches found in literature. By examining the difference in performance determined by applying these various approaches and geometries, this study aims to motivate the need for a standard. While examining the different approaches this study aims to identify suitable parameters and formats for presenting thermal and flow performance.

This study examines test facilities which have been used to measure fill performance and examines their methods of acquiring measurements necessary to calculate the performance measures. It strives to describe in detail a test facility suitable for determining the performance of any counter-flow fill in an accurate and repeatable way. The aim is to evaluate whether the test conditions match the assumptions in the theory. This is evaluated to determine the suitability of the test facility.

This study tests the three types of fill in an upgraded test facility and aims to determine whether the results are reliable and if the facility and theoretical approach are indeed a suitable base from which to establish a standard. The study continues to suggest ways in which the test facility can be further changed in order to achieve even more reliable, meaningful results.

This thesis aims, ultimately, to contribute to the knowledge base of fill performance testing. It strives to increase the knowledge regarding effective performance testing of fill so that in the future a standard can be developed. The standard would control all aspects of fill performance testing including the test facility, temperature and pressure measurement methods and locations, parameters used to process the performance data, and the format in which this information is presented.

2. INTRODUCTION TO AND IMPORTANCE OF STANDARDS

2.1. Introduction

During the Industrial Revolution in the late nineteenth century, increasing mechanisation brought about increasing concerns about the safety and reliability of machinery, tools and technical appliances being invented. Common rules for production methods, parts and products were introduced. These rules have evolved, along with technology, into standards that control numerous aspects of the engineering industry by establishing technical definitions and criteria to ensure the reliability and quality of products. In the context of performance testing, standards outline test apparatus and methods and the operating conditions of tests. Results of tests conforming to specific standards can be directly compared with other tests conducted conforming to the same standard.

Furthermore, in the context of cooling towers there are already existing standards controlling the performance evaluation of complete cooling towers to ensure that completed towers fulfil their design specifications. Examples of these are Cooling Technology Institute's Acceptance Code for Water Towers (CTI, 2000), American Society of Mechanical Engineers' Performance Test Codes for Atmospheric Cooling Water Equipment (ASME, 2003) and British Standards Institute's Methods of Performance Testing for Water Cooling Towers (BSI, 1988). These standards protect both the supplier and the customer by ensuring that every aspect of testing the cooling tower is specified, leaving little room for subjectivity. The success or failure of the cooling tower's performance determined by these standards has financial and contractual implications for the parties concerned. However, no standards exist for determining the performance of individual cooling tower elements like fill, nozzles and drift eliminators.

2.2. Need for a counter-flow fill performance evaluation standard

Published data concerning the performance of fill is reported widely in literature. Due to a lack of any standardisation, many parameters differ between these tests. One example is the facility sizes, which range from a 0.15 x 0.15 m^2 facility (Goshayshi and Missenden, 2000) to the Houston Lighting and Power Company's H.O. Clarke Station, a 7 x 12 m^2 facility (Johnson, 1989). See Appendix C for a brief description of a sample of the test facilities where fill tests have been conducted. The difference in size has an effect on both the flow and thermal performance of the fill.

Kröger (2004) reports that the loss coefficient (a measure of the flow resistance of the dry fill) measured over a cross-fluted fill in a 0.3 x 0.3 m^2 facility can be 56 % larger than the loss coefficient of the identical fill packed into a full-scale test

facility. Kröger also notes that this difference is reduced to only 2 % in 1.5 x 1.5 m^2 test facilities.

It is reported by Gősi (1998) that the fill performance is influenced by test facility size. He suggests this is up to 10 % in a 1.5 x 1.5 m^2 facility. This effect decreases as the size of the test facility increases. This is attributed to edge effects as a result of irregular water distribution around the edges of the test section, as it is difficult to create the overlap of the spray necessary to achieve uniform water distribution over the fill inlet. Other factors that affect the measured fill performance include water distribution uniformity (Kranc, 1993), inlet and outlet water temperature measurement methods and locations, air inlet temperature measurement location, drift eliminators, and the use and size of spray and rain zones.

The theory used to process the measured data into useful performance measures is another aspect that affects the reported performance. The Merkel, Poppe and e-NTU methods are three examples of methods that could be used to evaluate the data. Kloppers and Kröger (2005b) comment that between the three approaches there may be up to a 10 % difference in the performance resulting from different assumptions made in the analysis methods.

A new standard that controls fill performance evaluation is required to specify all these factors. It is necessary for the standard to specify the test facility details, the test conditions, and the test parameters, as well as the method used to process the data and the form in which the performance measures are presented. It is necessary that methods used to measure temperatures and flow rates conform to existing standards that control these measurements.

3. COUNTER-FLOW FILL PERFORMANCE EVALUATION

3.1. Introduction

Kröger (2004) suggests that information regarding fill structural strength, assembly, chemical inactivity, fire resistance and resistance to fouling, resistance to erosion and recyclability is necessary during the selection of fill for a specific application. The primary concerns regarding fill behaviour are, however, its efficiency in removing heat from the water falling through the fill and the resistance effect that the fill has on air flowing up through the fill. The remainder of this thesis focuses on accurately measuring fill performance in a 1.5 x 1.5 m² test facility and finding suitable means of representing and determining thermal and flow performance of fill. Knowing the performance characteristics of fill is important to ensure that the behaviour of the fill under normal operating conditions is understood and the performance of the fill, and the cooling tower as a whole, can be predicted.

3.2. Thermal performance evaluation methods in literature

Merkel (1925) presented a method of determining the thermal performance of evaporative cooling towers. The theory makes various assumptions and is used widely in literature. Some examples of studies on fills that have been conducted using the Merkel theory include Lowe and Christie (1961), Savery and Hammill (1972), Hallett (1975), Fulkerson (1989), Legrand (1992), Mohiuddin and Kant (1996), Bedekar et al. (1998), Aull and Krell (2000), Goshayshi and Missenden (2000), Mirsky (1991), Gharagheizi et al. (2007), Lemouari et al (2007). Appendix B.1 looks at an elemental control volume and the derivation of the Merkel number.

A derivative of the Merkel theory is Gősi et al. (1990) who use the Merkel method to evaluate different fills but then compare all the fills tested to one reference pack. The performance of these fills is reported using three ratios, namely, relative cooling capacity, relative plan area and relative power consumption, to compare the fills tested. Two other theoretical approaches are the ε-NTU method developed by Jaber and Webb (1989), which makes the same assumptions as the Merkel theory, and the Poppe method developed by Poppe (1972). The latter method does not make the simplifying assumptions made by the Merkel theory. The differences between the theories are discussed in detail by Kloppers and Kröger (2005a, 2005b).

Bedekar et al. (1998) use the definition of cooling tower efficiency as the fill efficiency. This compares the outlet water temperature to the inlet air wet-bulb temperature. The inlet air wet-bulb temperature is used as the reference temperature as this is the minimum temperature to which water can be cooled in a

theoretical infinitely large cooling tower. Milosavljevic and Heikkilä (2001) use yet another method of representing fill thermal performance in the form of a volumetric heat transfer characteristic with the units W/m^3K. Goshayshi and Missendin (2000) report on various arrangements in corrugated film fills and report the Nusselt number for the thermal evaluation of the fill.

The derivation of the Merkel number can be found in Appendix B.2. Kloppers and Kröger (2005c) investigate the forms of the empirically determined correlation equation. They include the water inlet temperature and the height of the fill in the correlation. Van der Merwe (2006) agrees with this and finds an improved fit to test data when using the format proposed by Kloppers and Kröger. This correlation is in the form

$$Me = aG_w^{\ b}G_a^{\ c}T_{wi}^{\ d}L_{fi}^{\ e}$$

where coefficients "a" to "e" are experimentally determined.

3.3. Flow performance methods in literature

In published literature there are numerous parameters used to report on the flow performance of fills. The flow performance is often communicated simply by reporting on the measured pressure drop over the fill, as is the case in Fulkerson (1989), Mirsky (1991), and Milosavljevic and Heikkilä (2001). The measured pressure drop is a function of mean air temperature through the fill, which in turn is influenced by the fill inlet water temperature. As the temperature of the inlet water increases, so, too, does the mean air temperature. With increased temperature the density of the air decreases, resulting in an increase in the velocity and viscosity of the air passing through the fill. These all contribute to higher measured pressure drops at higher water inlet temperatures. The water inlet temperature associated with the reported pressure drop must also be reported for the pressure drop information to be useful.

Legrand (1992), however, uses a dimensionless loss coefficient for the flow resistance performance. The dimensionless properties of this parameter are desirable, as no extra information is necessary for the parameter to be useful. When comparing different fills this loss coefficient is useful, as direct comparisons of loss coefficients of fill is possible since all the impacting parameters are included in its calculation. The derivation of the loss coefficient from the draught equation can be found in Appendix B.2. Kloppers and Kröger (2003) conduct a study on the form of empirical equations used to represent the loss coefficient and suggest a two-term exponential equation in the form

$$K_{fi} = (aG_w^{\ b}G_a^{\ c}+dG_w^{\ e}G_a^{\ f})L_{fi}^{\ g}$$

which describes the performance of film, trickle and splash fills over a wider range than the other correlations in literature. Coefficients "a" to "g" are experimentally determined.

4. COUNTER-FLOW FILL PERFORMANCE TEST FACILITY

This chapter examines the Stellenbosch University counter-flow fill test facility, in which the Merkel number and loss coefficient, identified in Chapter 3, can be obtained. The description that follows separates the facility into a horizontal inlet section and a vertical counter-flow fill test section. A brief description of each section is given. The measurements made in each section are identified and discussed along with the apparatus atempting to ensure the accuracy and reliability of the measurement.

4.1. Horizontal inlet

With reference to Figure 4-2, air is drawn into a 2 x 2 m^2 wind-tunnel inlet (1) by a centrifugal fan (2). The fan is driven by a 50 kW electric motor (3) which is connected to a variable-frequency drive, allowing for controllable air speed through the tunnel. On entering the tunnel, the air flows through a cross-flow fill test section (4) and then through mixing vanes (5) and a settling screen (6). The air mixers (5) ensure the air has a uniform temperature profile over the wind-tunnel cross-section. The result is fewer temperature measurement locations needed over a cross-section to ensure that the temperatures measured are a true representation of the air flowing in the inlet tunnel. Mixers appear in pairs; one mixer mixes vertically and the other horizontally. The vertical mixer is shown in Figure 4-1. The horizontal mixer is identical to the vertical mixer but rotated through 90º.

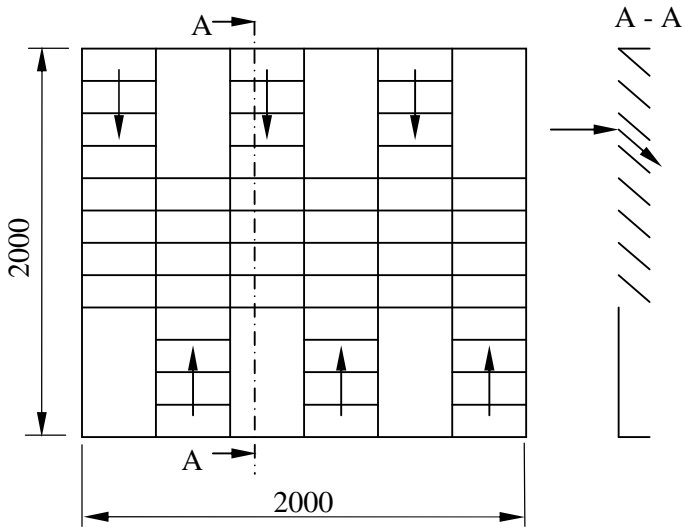

Figure 4-1: Vertical mixers.

The screen (6) located 2 m upstream of the nozzle plate settles the air by breaking up large vortices generated by the mixers and ensures the air has uniform velocity and temperature profiles as the air approaches the aspirated psychrometers (7) and nozzles (10).

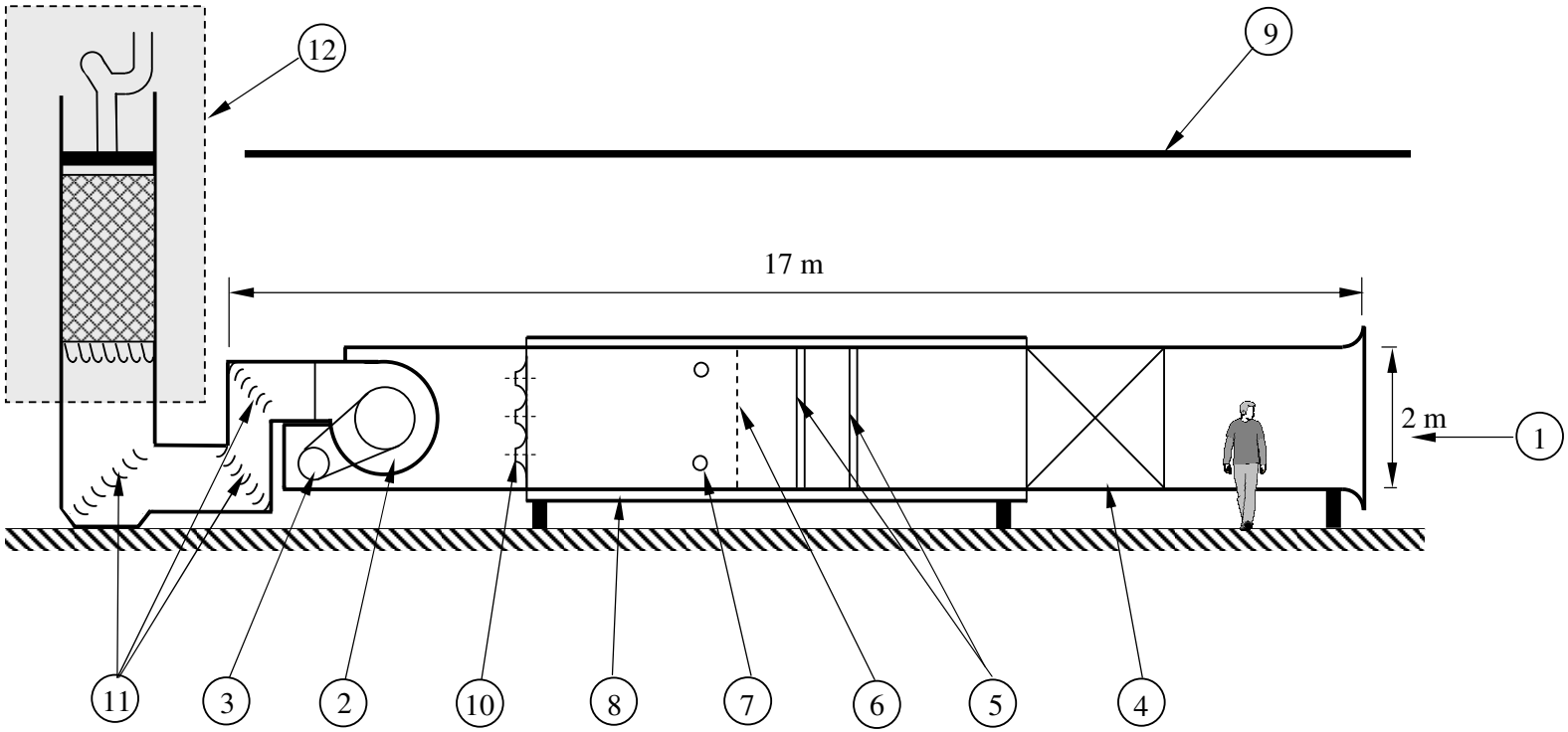

Figure 4-2: Counter-flow cooling tower fill test facility at Stellenbosch University.

Four pairs of thermocouples in aspirated psychrometers (7) measure the dry- and wet-bulb temperatures. Glass mineral wool insulation with a 100 mm thickness (8) and a roof (9) protect the facility from convective and solar radiation heat transfer to ensure accurate temperature measurements. The aspirated psychrometers (7) located downstream of the mixers are illustrated in Figure 4-3. Air is drawn over the wetted wicks at a minimum of 4 m/s by an aspiration fan. A standard to consider when measuring temperatures is ANSI (1986).

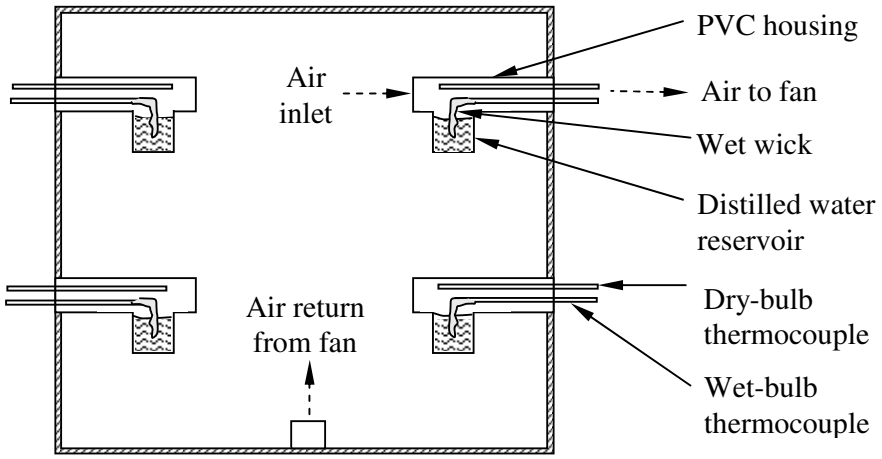

Figure 4-3: Aspirated psychrometer arrangement for measuring dry- and wet-bulb temperatures (not to scale).

The air flows through the nozzle plate (10). The pressure drop measured over the ASHRAE 51-75 elliptical nozzles is used to calculate the air mass flow rate, m_a. The nozzles and pressure tap locations are shown in Figure 4-4. The nozzles can be opened and closed to ensure that the Reynolds number is within a range specified by existing standards. The top three nozzles are opened for testing.

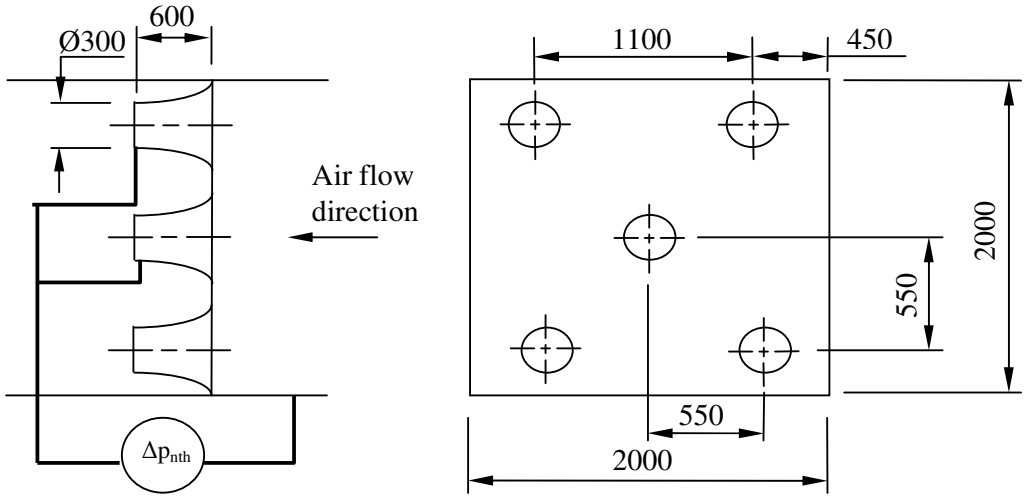

(a) Side elevation (b) Front elevation

Figure 4-4: ASHRAE 51-75 nozzles used in nozzle plate.

The pressure drop over the nozzles is measured by means of a calibrated Endress + Hauser electronic pressure transducer with a working range of 0 -10 000 N/m^2. The pressure transducer used here is pressure transducer A shown in Figure 4-5.

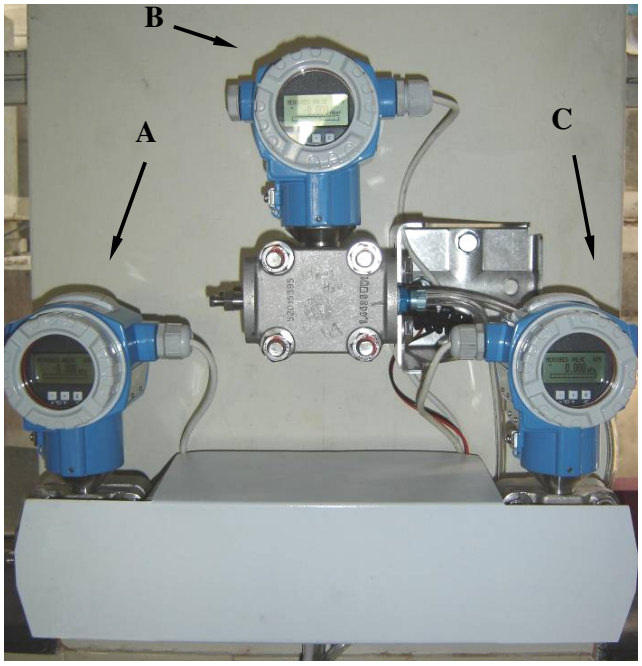

Figure 4-5: Calibrated Endress + Hauser electronic pressure transducers.

The pressure transducer is calibrated against a Betz manometer. The calibration details can be found in Appendix A3.1. A standard that specifies airflow measurement methods is ANSI (1987). ANSI (1975) and ANSI (1991) are also of interest.

The information from the abovementioned devices is used to calculate the air mass flow rate by applying Bernoulli's equation along a streamline between a point in the settling chamber upstream of the nozzles and a point in the centre of the nozzle throat. Bernoulli's equation is applied here to calculate the flow through one nozzle given by Equation (4.1)

$$m_{avm} = \frac{\sqrt{2\frac{\Delta p_{nth}}{\rho_{avn}}}}{\frac{1}{\rho_{avn}}\left(\frac{1}{A_n} - \frac{1}{A_{tus}}\right)} \tag{4.1}$$

The pressure drop over the nozzles, Δp_{nth} is measured as shown in Figure 4-4. Here A_n is the nozzle throat area and A_{tus} represents the settling chamber duct area upstream of the nozzle plate. After the nozzle plate, turning vanes (11) guide the air around 90° bends into the vertical counter-flow fill test section (12).

4.2. Vertical counter-flow fill test section

A photo of the vertical fill counter-flow fill test section (12) is shown in Figure 4-6 and the details of the test section are shown in Figure 4-7.

Figure 4-6: Photograph of counter-flow fill test facility.

Examining Figure 4-7 on page 4-6; air enters the 1.5 x 1.5 m^2 counter-flow fill test section (12). The fill height can be varied up to 5 m. Dry- and wet-bulb temperatures of the air entering the fill are measured (13). The air flows through the water extraction troughs (24), the fill (14), the distribution system (20), and ultimately the drift eliminators (15) to reduce the amount of water lost by carryover. The pressure drop across the troughs and the fill is measured using two independent calibrated electronic pressure transducers (16).

Upstream of the test section the flow rate of the hot inlet water is measured by an electromagnetic flow meter. The water is pumped into the test section (17) and flows through a cartridge filter (18). The temperature of the water is measured (19) before it is sprayed onto the fill via a distribution spray frame or applicable nozzles (20) and through a spray zone (21) as determined by the water distribution system specifications. The temperature of the water after it has travelled through the spray zone is again measured, ensuring that the temperature of the water (22) entering the fill is known. The water falls through the fill (14), is cooled, and the temperature of the water leaving the fill and entering the troughs is measured (23). The water leaving the fill is collected by two layers of water extraction troughs rotated 90° to each other (24). Trough details are shown in Figure 4-8 and Figure 4-9.

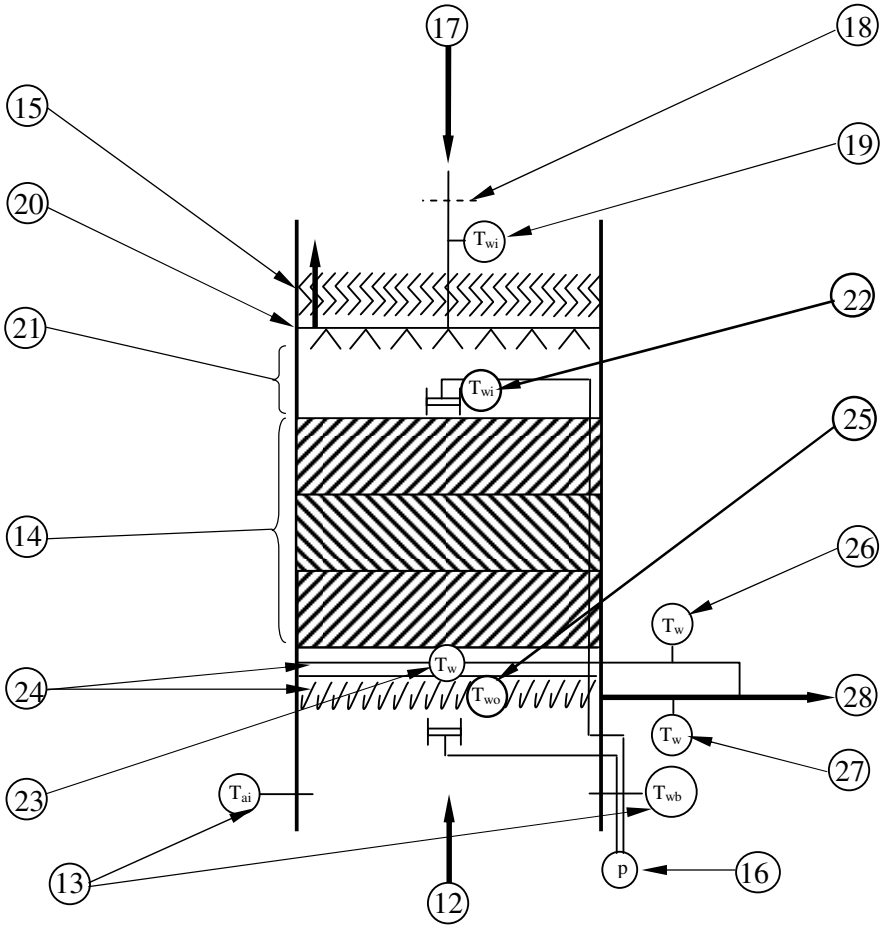

Figure 4-7: Schematic of counter-flow test section.

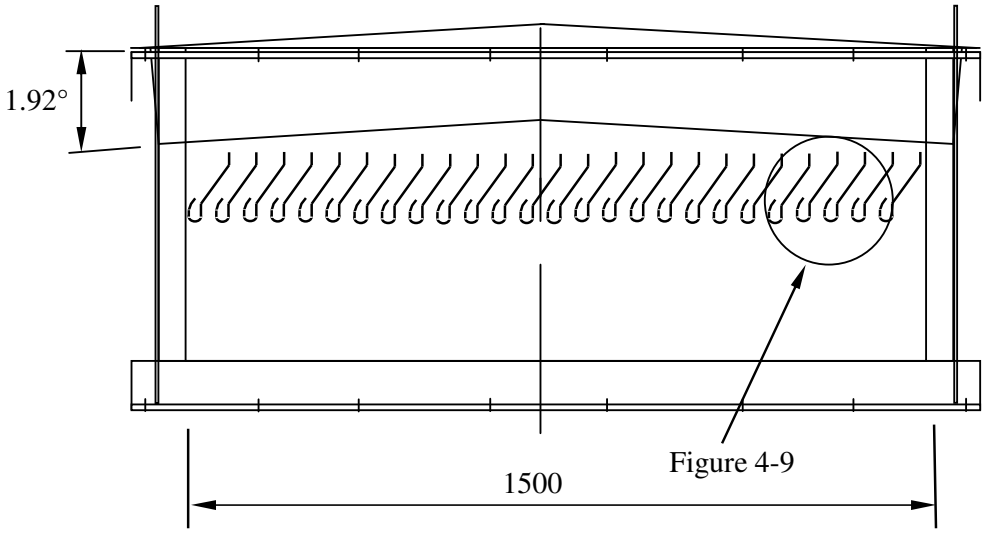

Figure 4-8: Trough assembly detail.

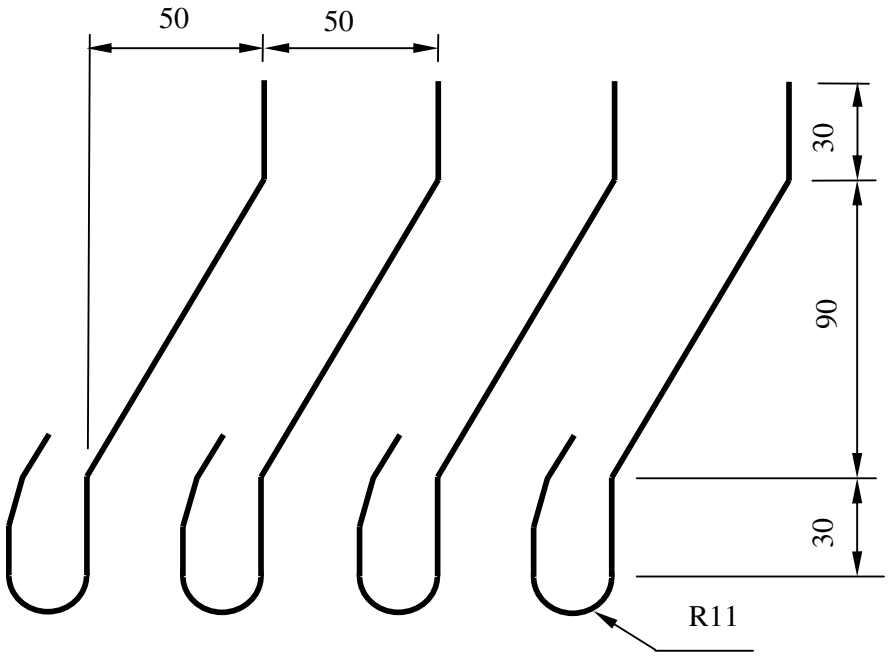

Figure 4-9: Trough detail.

The water outlet temperature is measured in the top and bottom troughs (25) as well as in the pipe work draining the top (26) and bottom (27) troughs. The water is collected in a sump, from where it is pumped back to the underground storage tank (28). There is redundancy built into the water temperature measurements to ensure a thorough understanding of all the regions of heat transfer within the test facility. All water temperature measurements are made in U-bends in pipe work or in containers designed to minimise heat transfer and ensure thermocouples are always submerged in water that is continuously flowing over the thermocouples. One of the containers used to measure the water temperature directly above and below the fill is shown in Figure 4-10.

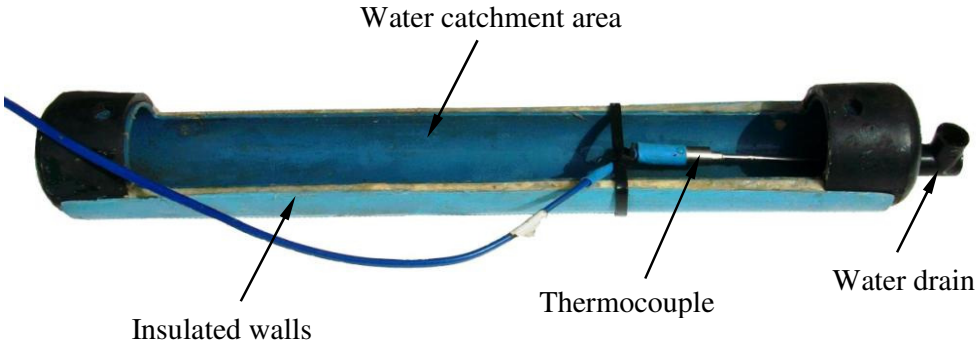

Figure 4-10: Water temperature measurement container.

4.3. Individual measurement details

4.3.1. Air inlet temperature

The dry- and wet-bulb temperatures, T_{ai} and T_{wb}, of the air entering the fill are measured upstream of the fill using four mechanically aspirated psychrometers (13). One is illustrated in Figure 4-11. A standard to consider when measuring temperatures is ANSI (1986). The standard specifies the length of wick between the thermocouple and the surface of the water and the required air velocity over the thermocouple. This is specified as a minimum of 4 m/s and checked using a hot-wire anemometer. It is desirable to have the psychrometers as close to the fill inlet as possible to minimise any heat transfer to or from the air between where the temperatures are measured and where the air actually enters the fill. This is especially necessary if the thermocouples are located in a rain zone below the fill.

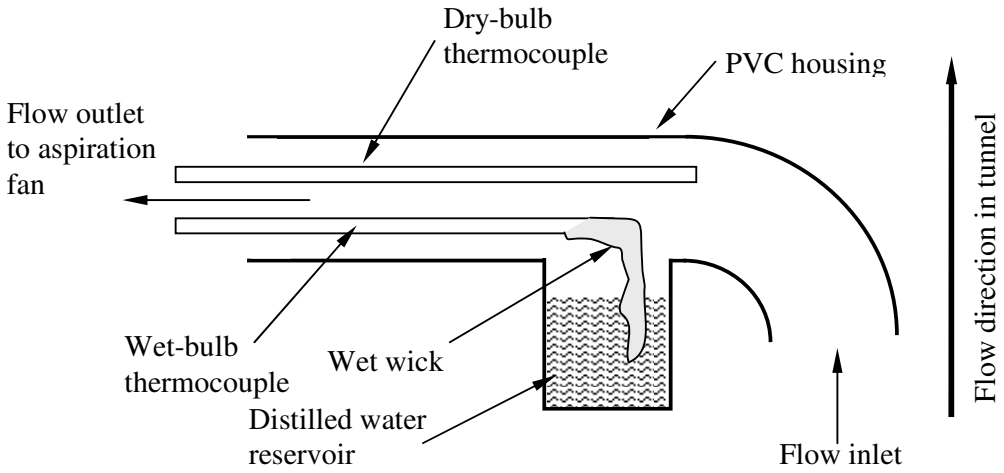

Figure 4-11: Detail of mechanically aspirated psychrometer under fill inlet.

4.3.2. Pressure drop over fill

The pressure drop over the fill is measured using two independent calibrated Endress + Hauser electronic pressure transducers. The pressure transducers are shown in Figure 4-5. Pressure transducer B has a 0 – 1000 N/m^2 range, while the pressure transducer C has a 2500 N/m^2 range. The calibration details for the fill pressure drop pressure transducers can be found in Appendix D.

Four H-tap pressure measurement devices, Figure 4-12, are used per pressure transducer. Two are located and fixed in position beneath the water extraction troughs, while two are fixed to a frame placed about the fill. The pressure devices are paired so as to measure the differential pressure over the fill.

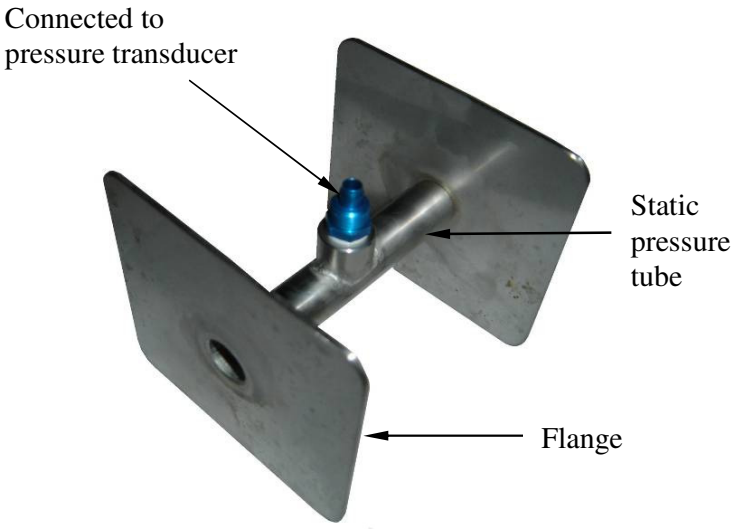

Figure 4-12: H-tap pressure measurement device.

The H-tap pressure measurement points are connected to the pressure transducers by 8 mm clear tube. The tube is clear so that any condensation in the tubes can easily be seen. If water condenses in the tubes they will become blocked and lead to erroneous pressure readings. The tube from the H-tap pressure measurements devices above the fill run down inside the test section to avoid unnecessary condensation and to avoid pressure differential errors due to buoyancy effects as a result of temperature differences. Two independent pressure transducers are used and the readings are compared with one another. Potential causes of differences could be condensate in pipes, kinked pipes, loose connections or misaligned pressure measurement devices. The average of the two measured pressure differentials is used in the performance calculation.

Note that owing to the location of the pressure H-taps the pressure drop measured includes the pressure drop over the water extraction troughs and the fill. The measured pressure drop must be corrected to ensure that the influence of the water extraction troughs is not included when reporting on the performance of the fill. A standard to consider when measuring the pressure drop over the fill would be ANSI (1989).

4.3.3. Water mass flow rate

An Endress + Hauser Proline Promag 10 electromagnetic flow meter is used to determine the water flow rate. The installed flow meter is shown in Figure 4-13. The direction of water flow through the flow meter is indicated by the blue arrow.

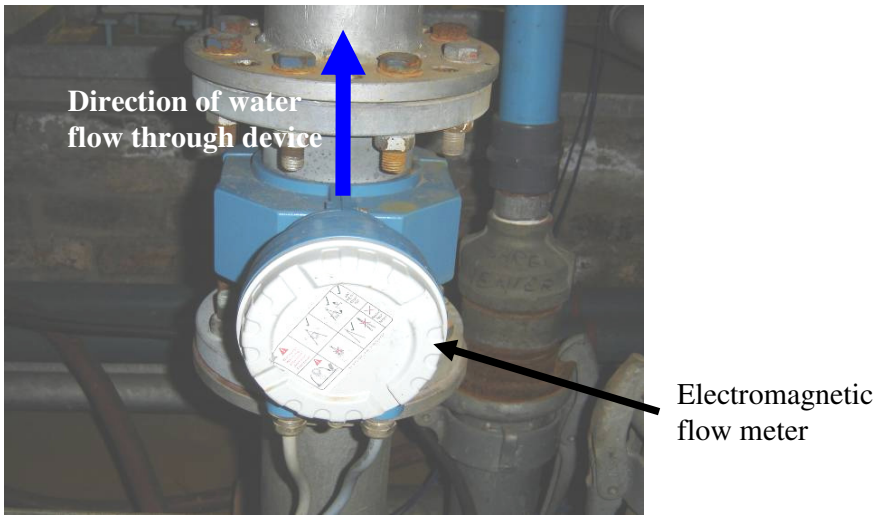

Figure 4-13: Electromagnetic flow meter installation.

The electromagnetic flow meter is installed in the pipe running between the water tank and the test section. It is installed according to the manufacturer's specifications. The specifications state that there be five pipe diameters between the flow meter and any fittings upstream of the device and two pipe diameters between the flow meter and any fitting downstream of the device. The electromagnetic flow meter is installed vertically. This is the optimum orientation for this type of flow meter, as it ensures that the flow meter is full of water during testing and mitigates any negative effects of air caught in the device. This orientation also prevents any deposits accumulating in the device and on the magnetic points.

The electromagnetic flow meter is calibrated using a calibration tank. The time taken to fill a certain volume is recorded and the flow rate calculated. The output current is recorded and the relationship between the actual flow rate and current output is determined. The details of the calibration procedure and apparatus can be found in Appendix C. The output of the device is from 4 to 20 mA, corresponding to zero and the maximum measureable volumetric flow rate of 1000 litres per minute, respectively. The output in Amperes is desirable as there are no resistance losses in wires linking the device and the data logging system. This is important in this instance, as the device is 40 m away from the data logger. British Standard (1981) is a standard that discusses and prescribes procedures when measuring flow in closed conduits and addresses a variety of methods.

4.3.4. Water inlet temperature

The arrangement of water inlet temperatures is shown in Figure 4-14. The water inlet temperature, $T_{wi(A)}$, is measured 50 mm before the water distribution system. Three thermocouples are located in the supply pipe at 120° intervals around the pipe. The average of the three measurements is used as the water inlet

temperature. The water entering the fill, $T_{wi(B)}$, is again measured. Four thermocouples measure the temperature of the water entering the fill. The average of the four thermocouples is used as the water inlet temperature. The thermocouples are located in containers that are insulated to ensure that there is no cooling of the water while it is in the measurement container. The measurement containers have a drain through which the water caught in the containers continually flows. The thermocouples are placed in these drains to ensure that the thermocouples are always completely submerged in water and that there is continuous water flow over the thermocouples (Figure 4-10). The difference between the temperatures measured in the water distribution system and the temperatures measured in the containers just before the fill is due to cooling as the water flows through the distribution system and the cooling in the 150 mm spray zone.

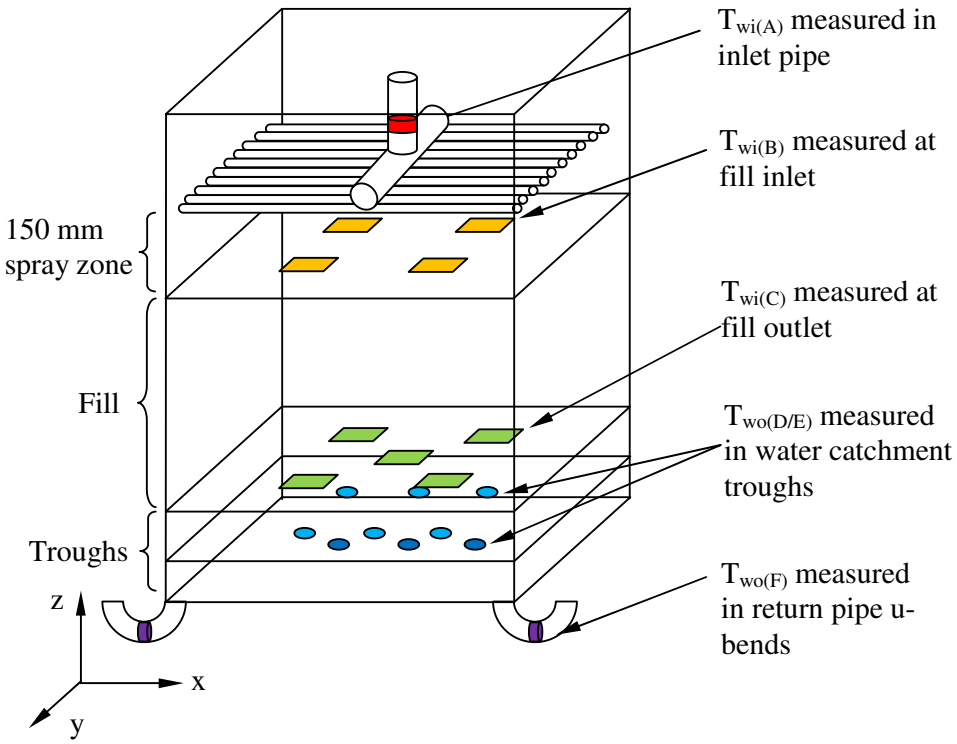

Figure 4-14: Water temperature measurement details.

The temperature of the water entering the troughs, $T_{wi(C)}$, is taken in line with the troughs in the containers shown in Figure 4-10. The water temperature is the average of five measurement points.

4.3.5. Water outlet temperature

The arrangement of water outlet temperatures is shown in Figure 4-14. The temperature of the water exiting the fill is measured in two locations. The outlet water temperature, $T_{wo(D/E)}$, is measured in the water extraction troughs. Thermocouples are located in the troughs and measure the water temperature as it

is caught by the troughs. Nine thermocouples are located in the troughs to measure the water outlet temperature. The weighting of the temperatures measured in the top and bottom row of troughs is detailed in Section 5.7. The third method used to determine the water outlet temperature, $T_{wo(F)}$, involves measuring the water temperature in the u-bends in the PVC piping that drains water from the troughs below the fill. Eight thermocouples are located in the outlet water drain pipes to measure the outlet water temperature.

The difference in the water temperatures $T_{wi(C)}$ and $T_{wo(D/E)}$ is due to cooling over the troughs. It is necessary to know this so that the contribution of the troughs to the total Merkel number can be known. The temperature difference measured between $T_{wo(D/E)}$ and $T_{wo(F)}$ is due to the cooling in the manifold system that collects the water draining from the troughs before it is drained to the sump and returned to the reservoir. It is assumed that the water flow out the left- and right-hand sides of the tunnel is equal. This assumption is made by van der Merwe (2006).

4.3.6. Atmospheric pressure

Atmospheric pressure is measured using a Thies Clima mercury barometer located in the laboratory. It has range of 80 000 – 108 000 N/m^2 and a temperature operating range of -15 to 50 °C. A standard to consider here would be ANSI (1989).

4.4. Data acquisition and processing

An Agilent data logger connected to a desktop computer is used to log measured data. A LabVIEW program written for the purpose displays and processes the measured data resulting in the instantaneous calculation and display of the dimensionless Merkel number and loss coefficient. A screenshot of the user interface is shown in Figure 4-15. The top two left-hand side plots display the dry- and wet-bulb temperatures of the nozzle and trough thermocouples respectively, while the lower plot displays the temperature difference between the inlet and outlet water. These three plots are necessary to ensure the stability of the experiment and thus the accuracy of the calculated Merkel number and loss coefficient. There are monitors on these dry- and wet-bulb measurements as well as on the measurement of the pressure drop over the fill. If any one measurement deviates beyond a specified range, the green light corresponding to the measurement device turns red, highlighting the error, which should be rectified before proceeding further with the experiment.

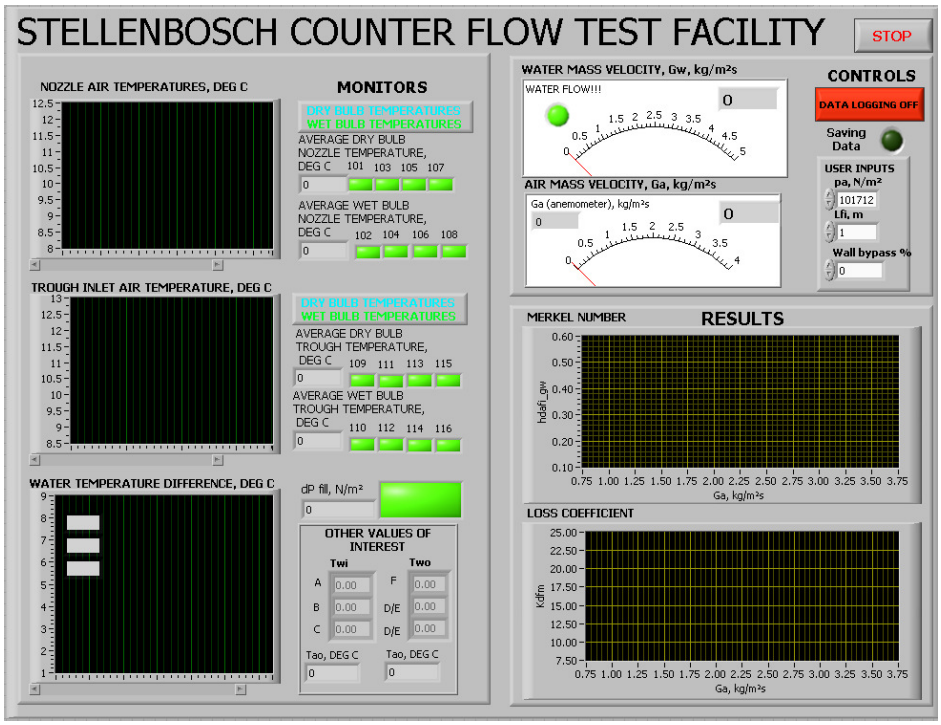

Figure 4-15: LabVIEW user interface.

Gauges indicating the water and air mass velocity being applied to the fill in the test facility are located on the right. Next to these gauges is a button controlling whether data is logged or not. This minimises the amount of data saved, as unsteady data can be ignored when air and water settings are being adjusted. Below the log on-off switch are the user inputs for the atmospheric pressure, the height of fill being tested and the expected wall water bypass percentage determined for the specific fill being tested at the specific water mass velocity. The lower two plots on the right-hand side plot the calculated Merkel number and loss coefficient for the fill versus the air mass velocity, G_a. All the measured information is saved to a Microsoft Excel file so it is available for checking, formatting and any error finding or post processing if it is deemed necessary.

5. COUNTER-FLOW FILL TEST FACILITY EVALUATION

5.1. Introduction

The test facility is evaluated to ensure that the assumptions made in the theory are indeed valid for the test setup. These assumptions are specified in Appendix B.1. Aspects examined are the water distribution uniformity and the redistribution of water through the fill height, air mass velocity uniformity, the impact of edge effects and the location of the water outlet thermocouples.

5.2. Spray frame water distribution

The selection of water distribution and its resulting water spray pattern is important as it impacts the fill performance as noted by Kranc (1983, 1993) and Fabre and Legrand (1988). Gősi et al. (1990) state that unfavourable water distribution decreases performance by 15 – 20 %. They also note that performance in cooling towers can be improved merely by modifying nozzle arrangement. Fill performance is maximised when there is a uniform distribution of water over the whole fill area. A decrease in fill performance occurs when there is too much water in an area, resulting in flooding of the fill: water flows through the fill in thick streams and the ratio of surface area to the cross-sectional area of the stream is small. Performance will also decrease when there is too little water in an area, resulting in dry spots through the fill: the air flowing up through the fill will follow this path of least resistance reducing the amount of air flowing through the wetted fill (Cooper (2006)).

Merkel theory assumes uniform water distribution over the fill. In order for the theory to be valid it is essential to have a distribution method as uniform as possible. The water distribution method impacts the uniformity of the water flow. Typically nozzles do not have excellent distribution properties over a range of water mass velocities. The distribution is uneven; there are areas of the spray that overlap and wide spray angles result in dry spots. Nozzles are also designed to operate at one flow rate. The need for a near-to-perfect water distribution and the variable flow rate used to determine the fill performance in this setup make the use of nozzles undesirable.

A 1.48 x 1.48 m^2 spray frame, shown in Figure 5-1, was designed to deliver optimal water distribution while offering minimal air flow resistance. It consists of 57 pipes arranged in two rows 50 mm apart staggered with a 50 mm pitch. Water flows from the manifold into the spray pipes that are of a pipe-in-a-pipe arrangement shown in Figure 5-2.

Figure 5-1: Spray frame designed for water distribution.

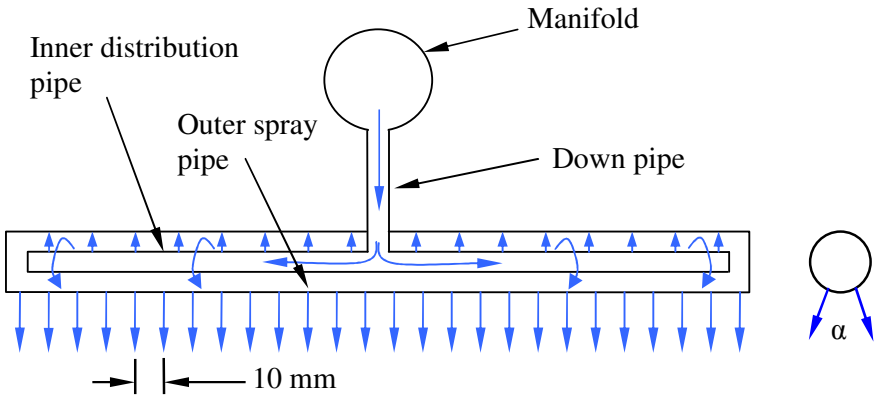

Figure 5-2: Pipe-in-a-pipe arrangement of spray frame.

The inner distribution pipes have 2 mm distribution holes drilled along the top to distribute the water uniformly into the spray pipes. The spray pipes have 1 mm holes drilled along the bottom. These 1 mm holes have a staggered pitch of 10 mm and are set at an angle α of 30° for the bottom row and 20° for the top row. These holes distribute the water over the fill. The holes are set at angles so the resulting water spray has a horizontal velocity component. This is important when testing fills with open, vertical channels. The horizontal movement prevent drops from free-falling through the fill and prevents the drops from missing the fill completely. The top and bottom rows of spray pipes are staggered with a pitch of 50 mm, as shown is Figure 5-3.

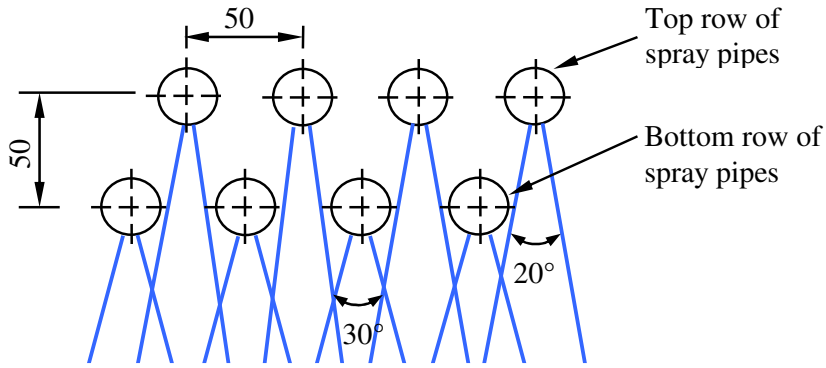

Figure 5-3: Side elevation of spray frame, showing staggered spray pipes.

The distribution beneath the spray frame is measured in the setup illustrated in Figure 5-4. An axis system is shown for referencing locations over the test cell cross-section. The origin of the axis system is aligned with the front left bottom corner of the test section.

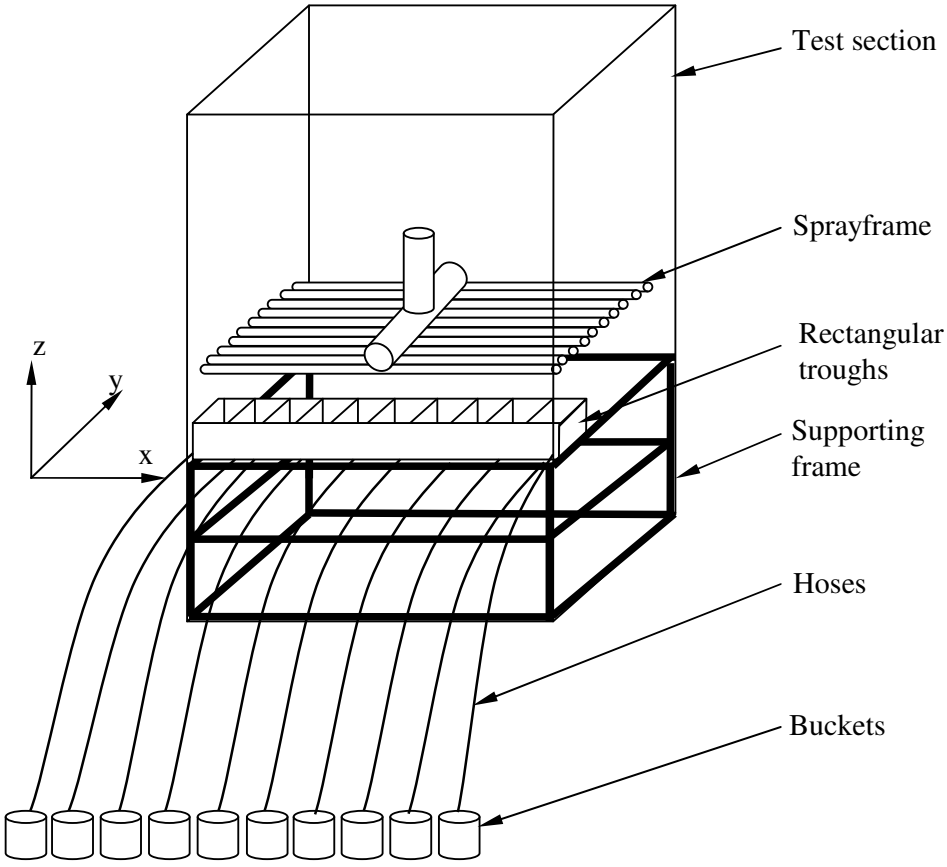

Figure 5-4: Set-up used to determine distribution under spray frame.

Water is sprayed from the spray frame and collected in rectangular troughs aligned to the x-axis as shown in Figure 5-4. The trough dimensions are shown in Figure 5-5.

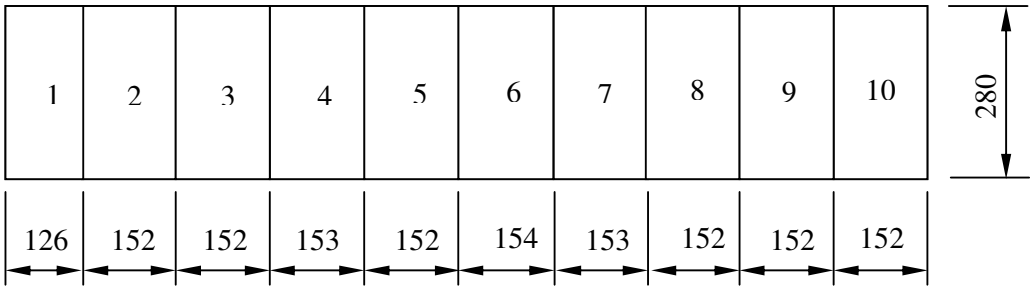

Figure 5-5: Dimensions of rectangular troughs.

The troughs drain continuously through 12 mm pipe into buckets where the mass of the water is weighed. The time taken to collect the water is recorded and the average mass flow rate over each compartment of the rectangular trough is calculated. The troughs are shifted forwards and backwards through the tunnel along the y-axis, as illustrated in Figure 5-4, to measure the flow rate under the entire area of the spray frame.

When an individual spray pipe was examined it was found that the eight internal troughs have 15 spray holes per spray pipe spraying into them, whereas the two end troughs have only 12 or 13 spray holes per spray pipe spraying into them. To compensate for this, the end troughs are scaled by a factor 13/15 when calculating the spray frame water mass velocity G_w. Without this scaling the end troughs indicate a water mass velocity that it 13 – 20 % less than the average water mass velocity over the rest of the spray frame area.

The water distribution at water mass velocities of 1.496, 2.997 and 4.485 kg/m²s is measured. The distribution is measured 150 mm below the spray frame. This is the distance between the spray frame and fill during testing allowing sufficient room for the H-taps to be installed. The results of the distribution tests are shown in Figure 5-6 through to Figure 5-11. The x-axis indicates the left-to-right position of the point under the spray frame, while the legend indicates the position of the measurement point along the y-axis under the spray frame. Note: Before completing any distribution or thermal tests it is important to operate the spray frame at a water mass velocity of at least 4.5 kg/m²s for 5 to 10 minutes. This will ensure a more uniform water distribution by flushing the spray frame of airlocks and by breaking the surface tension on the spray holes. This practice should be followed when conducting thermal performances for reasons mentioned at the start of this section. If this is not done, trapped air hinders flow to the edges of the spray frame. The result is a high water flow in the middle and low water flow around the edges of the test section.

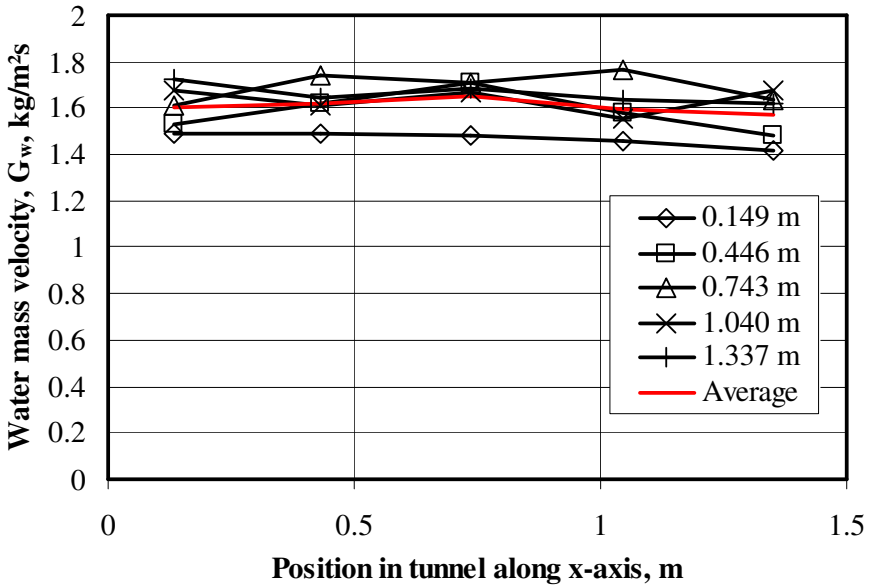

Figure 5-6: Water load distribution at 1.496 kg/m²s.

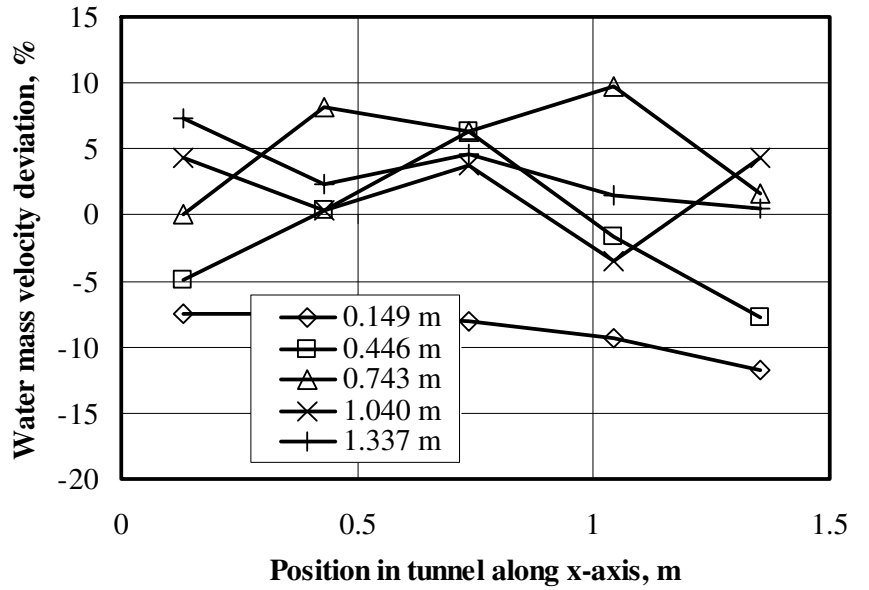

Figure 5-7: Water load deviation at 1.496 kg/m²s.

Integrated G_w	1.548 kg/m²s
Flow meter G_w	1.496 kg/m²s
G_w percentage difference	3.460 %
Christiansen coefficient	0.951

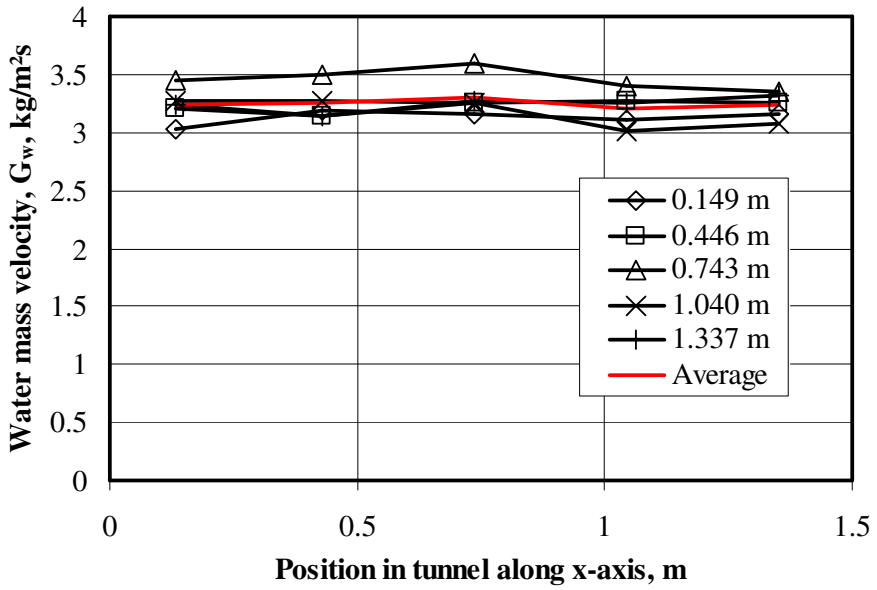

Figure 5-8: Water load distribution at 2.997 kg/m²s.

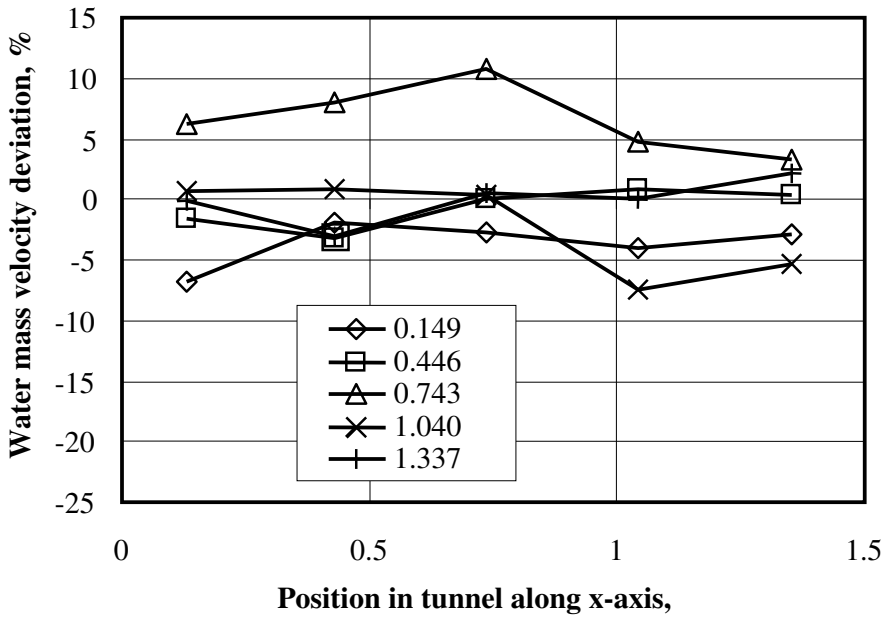

Figure 5-9: Water load deviation at 2.997 kg/m²s.

Integrated G_w	3.108 kg/m²s
Flow meter G_w	2.997 kg/m²s
G_w percentage difference	3.688 %
Christiansen coefficient	0.964

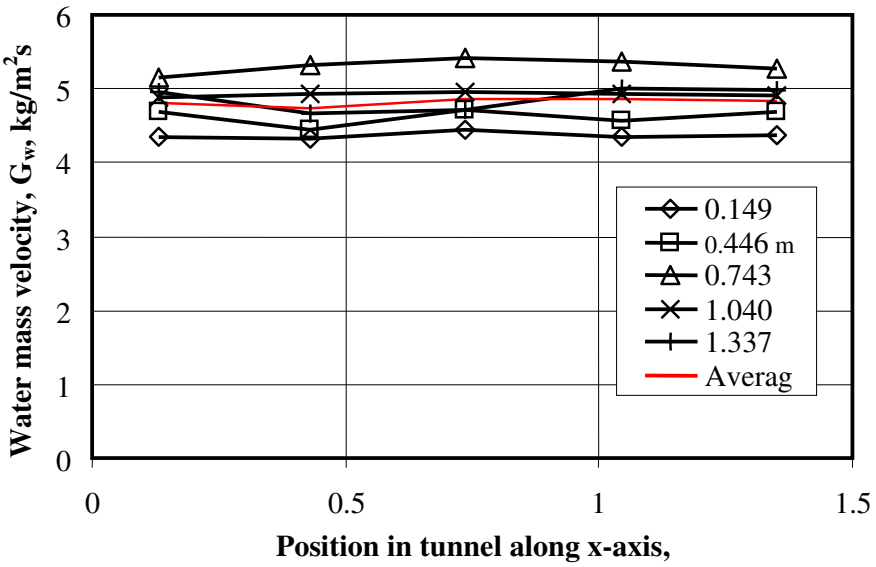

Figure 5-10: Water load distribution at 4.485 kg/m²s.

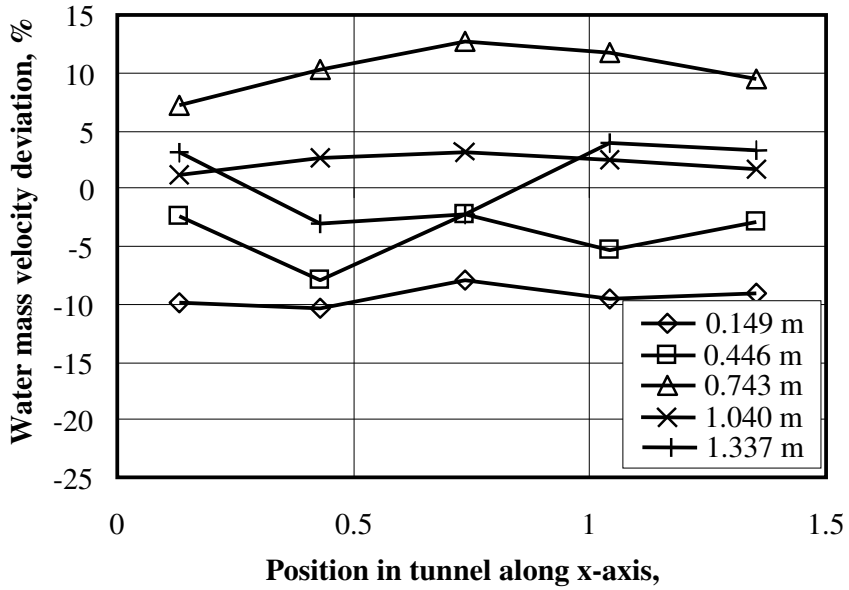

Figure 5-11: Water load deviation at 4.485 kg/m²s.

Integrated G_w	4.630 kg/m²s
Flow meter G_w	4.485 kg/m²s
G_w percentage difference	3.225 %
Christiansen coefficient	0.942

The percentage differences between the integrated water mass velocities for the three cases compared to the value recorded by the computer in each of the cases are 3.460 %, 3.688 % and 3.225 % respectively. The 1.496 kg/m²s water load has only two points outside the 10 % average. The 2.997 kg/m²s water load has only one point outside the 10 % average and the 4.485 kg/m²s water load has four points outside the 10 % average. All these points are along the outer edge of the area or in the middle of the spray frame below the manifold downpipe where a higher flow rate is expected due to the vertical downward flow of the water in the pipe supplying the manifold.

Kranc (1993) applies the Christiansen coefficient to represent water distribution uniformity in a cooling tower. The Christiansen coefficient is traditionally used in agricultural engineering to indicate how uniformly water is sprayed onto fields. The Christiansen coefficient is calculated

$$Cu = 1 - \frac{1}{n^2 m_{ave}} \sum \left| m_{ave} - m_i \right| \tag{5.1}$$

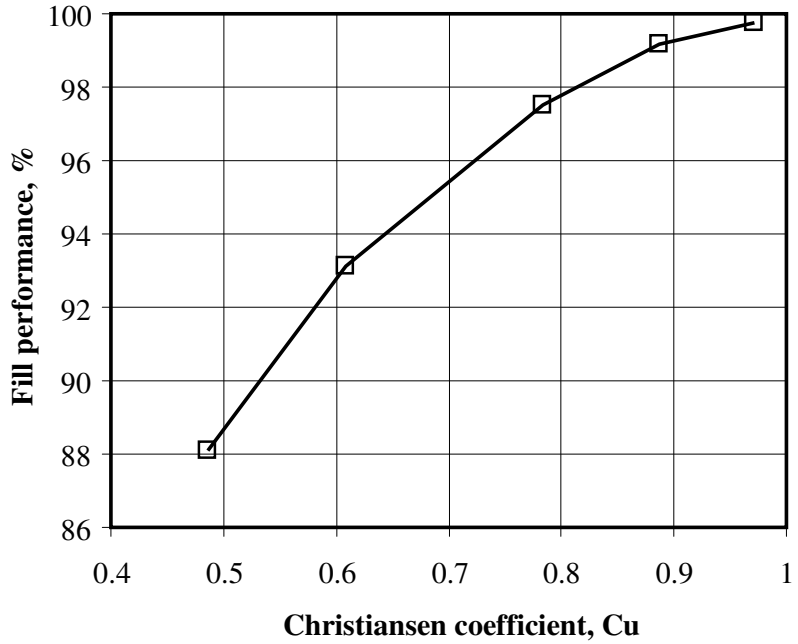

Figure 5-12: Cross-fluted fill performance as a function of Christiansen coefficient (Kranc, 1993).

Kranc states that the cooling tower will perform best when the Christiansen coefficient is equal to unity. The water loads examined here have Christiansen coefficients of 0.951 for 1.496 kg/m^{2}s, 0.964 for 2.997 kg/m²s, and 0.942 for 4.485 kg/m^{2}s. These values are close to unity. Kranc provides the graph in Figure 5-12 indicating the expected drop in performance as a function of the Christiansen coefficient for a cross-fluted, corrugated fill. The worst distribution delivered by

the spray frame, which is for 4.485 kg/m²s with a Christiansen coefficient of 0.942, according to Kranc, will result in a performance of 99.56 %. From this argument it is decided that the spray frame delivers a usable water distribution. It must be remembered that Figure 5-12 was developed by Kranc (1993) for a specific cross-fluted fill. It is assumed that trickle and splash fill perform according to a similar curve as information regarding the performance of these fills as a function or water distribution uniformity was unobtainable. Knowing this relationship for trickle and splash fills would be beneficial.

5.3. Water migration through fill

Merkel theory assumes uniform fill characteristics throughout the tower, which implies uniform water flow through the tower. Merkel theory also neglects redistribution effects over the fill height. As a result it is necessary to examine the water migration through by measuring the water flow profile at the fill outlet. The setup is illustrated in Figure 5-13.

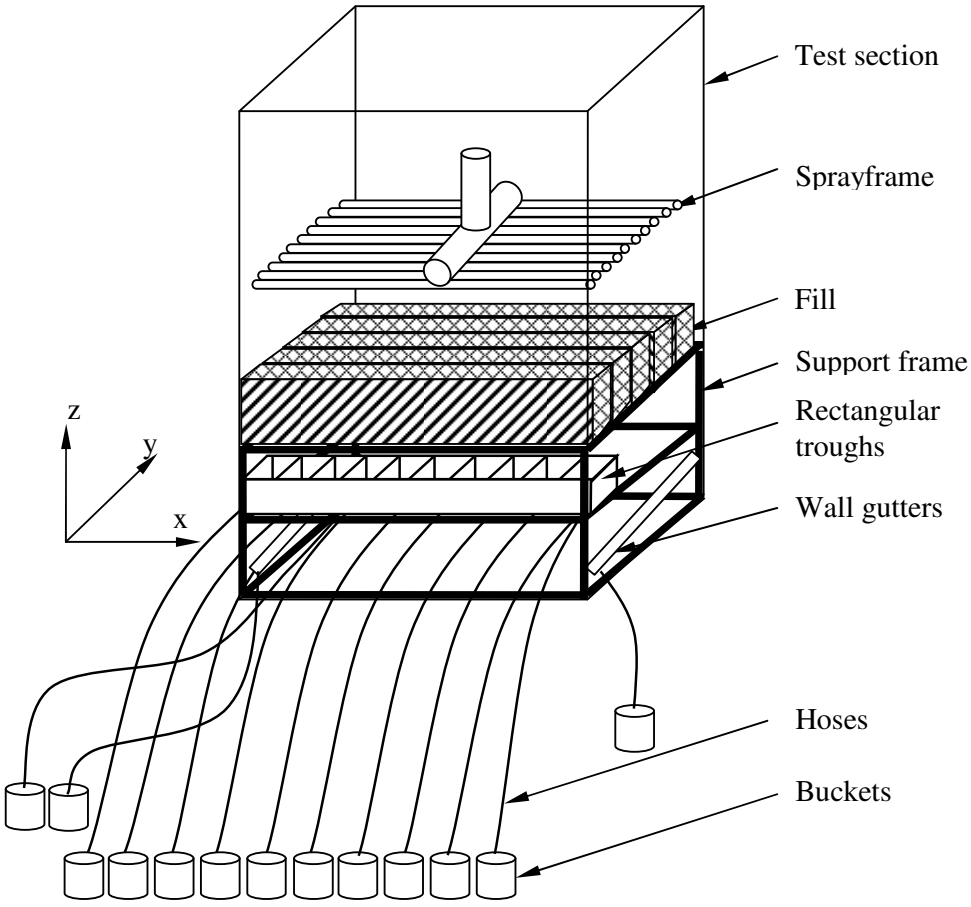

Figure 5-13: Set-up used to determine water distribution below fill.

The water distribution under different fills at different fill heights and different water mass velocities is measured. Any water running down the left, right and back walls of the tunnel is collected and measured separately. Gutters on these three walls skim the water off the wall. The gutters are drained by hoses into buckets. The water mass flow rate from each one of the walls is calculated. The door to the tunnel forms the front wall which is left open to allow the drainage pipes out; therefore, the water off the front wall is not measured. It is assumed that the flow rate of water down the front wall is the same as the water off the back wall. When conducting these distribution tests, care is taken to ensure that none of the pipes draining the rectangular troughs is kinked and that there are no air blocks in the pipes by ensuring that at no stage do any of the pipes have a positive gradient hindering the direct flow of the water between the rectangular troughs and the buckets. During the distribution tests the water mass velocity, G_w, measured by the electromagnetic flow meter and recorded. Furthermore, the water mass velocity is calculated by integrating the measured water distribution over the area. The two water mass velocities are compared.

Water distribution below the film fill with fill heights of 0.305, 0.61, 1.22 and 1.83 m is shown in Figure E-1 to Figure E-24. Migration in one layer of film fill is possible only in one direction – parallel to the length of the fill blocks. When subsequent layers are rotated 90º there is migration in both directions. This results in the dome-shaped distribution measured with a higher flow in the middle and a lower flow along the outer edges. The measured distribution does not differ drastically from the distribution delivered to the top of the fill by the spray frame and the distribution seldom exceeds 15 % from the average water flow rate. The lowest Christiansen coefficient of 0.903 is for 1.83 m fill with G_w = 2.98 kg/m^{2}s; this results in a maximum of 99 % of the ideal performance according to Figure 5-12. The performance measured for this fill will be very close to the maximum possible performance achievable in a theoretically perfect cooling tower.

Water distribution below the trickle fill with fill heights of 0.5, 1.0 and 1.5 m is shown in Figure E-25 to Figure E-43. The trickle has slightly worse distribution than that of the film fill, and distribution deviated by up to 30 % from the average water flow rate through the fill. The worst Christiansen coefficient is 0.806 for 1.5 m fill and G_w = 1.491 kg/m²s. According to Figure 5-12 the maximum performance measurable is still approximately 98 % of the ideal performance of the fill. Results measured in the 1.5 x 1.5 m² test facility will be very close to the maximum performance of the fill.

The splash fill has the worst migration effects of the three fills. These results are presented in Figure E-42 to Figure E-60 for fill heights of 2.04, 3.04 and 4.04 m. The distribution can deviate by up to 80 % from the average water flow rate through the fill. Distribution occurs in both directions, which was unanticipated. It

appears that water moves along the length of the bar while it splashes out sideways. This may be due to sagging of the v-bar between the two supports holding the bars in place. This could be improved by increasing the rigidity of the v-bar or by decreasing the distance between supports. The minimum Christiansen coefficient determined is 0.56 for 4.04 m fill with G_w = 1.508 kg/m²s. According to Figure 5-12 this can result in up to a 10 % decrease in measured performance. Accurate testing of splash fill with a high degree of migration is thus problematic in this 1.5 x 1.5 m² test facility. Results obtained for splash fill performance must be used cautiously as the results will potentially be pessimistic.

5.4. Wall water bypass and wall effects

Some tests facilities quantify wall water bypass effects by catching the water running down the wall, measuring its flow rate and temperature. Fulkerson (1989) and Fabre and Legrand (1988) are examples of where this is done. Gősi (1998) states that water distribution selection and nozzle placing can be optimised to minimise wall water bypass effects. Nozzles that spray over a large horizontal distance contribute to bigger wall effects, as the water has a high outward velocity towards the walls of the test facility. In this study, when testing the distribution of the spray frame, zero water is observed flowing down the wall. This is valid only for a spray zone of 200 mm or less. Any water flowing down the wall during fill distribution testing is therefore attributed to water migration within the fill. When conducting tests examining the migration of water through the fill, gutters along the walls catch the water flowing down the walls (see Figure E-1 to Figure E-55). This wall water was measured to be less than 5 % of the inlet water mass velocity for the maximum height of film fill (1.8 m) tested, while it is approximately 8 % for the maximum height of trickle fill (1.5 m) tested and up to 31 % for the maximum height of splash fill (4.04 m) tested.

Wall water bypass effects and the impact these have on the average water flow rate through the fill are taken into consideration during testing. This is done by modifying the water mass velocity delivered to the tunnel by half the expected amount of wall bypass water. The water mass velocity is modified only by half the expected wall bypass water, because at the fill inlet (when the spray frame is employed) there is no water flowing down the wall, whereas at the fill exit there is the maximum wall bypass water. The average water flowing down the wall needs to be used so as not to over-compensate for wall bypass effects. The impact the wall bypass water has on the measured outlet water temperature (when measuring in the outlet pipes) is not taken into consideration. When testing the splash fill it became apparent that the water off the walls negatively affects the water outlet temperature. Gutters were installed, preventing wall bypass water from mixing with the water measured in the outlet pipes. The water was directed away from the extraction troughs and allowed to fall to the bottom of the tunnel, where it was drained from the tunnel. This resulted in the wall water not impacting the outlet water temperature measured in the return pipes. However, the presence of water at

the bottom of the tunnel destabilised the air inlet temperature measurements. The air enters this section of the tunnel, to which the water is redirected, through the 90º Mitre bends. The air travelling up the left-hand side of the tunnel is in contact with the water for longer than air travelling up the right hand side of the tunnel. The differing contact time between the air and water results in the destabilising of the air inlet measurements. This is evident when comparing stable air measurements made before the gutters were installed (Figure 5-14) and measurements made with the gutters in place (Figure 5-15).

The instability of the air deems this type of gutter unhelpful. In future a gutter system must be installed that will catch the water running down the wall and completely isolate it from the air stream entering the fill. This will separate the wall water from the water temperature measurement. This will also enable the average flow rate of water through the fill to be known at all times during testing.

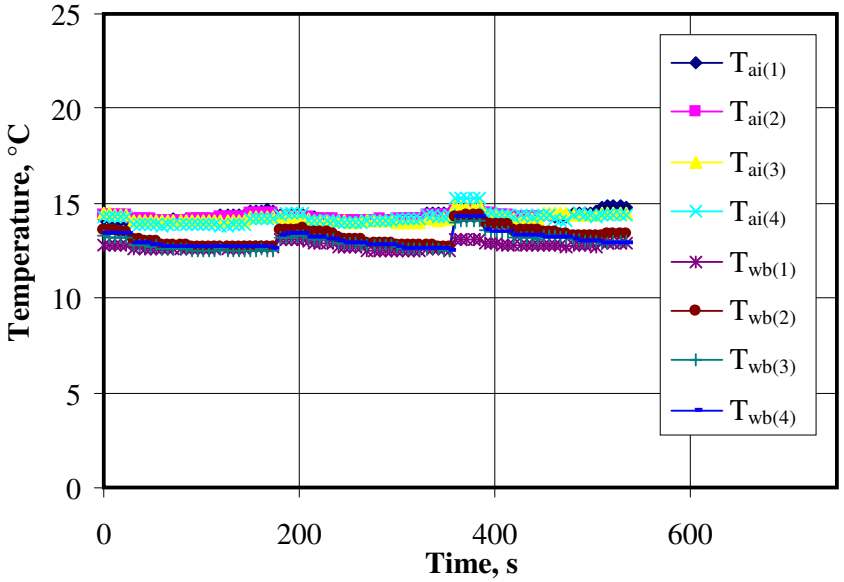

Figure 5-14: Stable air inlet measurements without wall gutters.

5.4. Air velocity profile

The distribution of the airflow through the fill is also important as this has an effect on the fill performance. Libert (2007) notes this and is able to achieve an air flow distribution percentage difference of less that 10 % over 90 % of his facility cross-section. This was achieved by optimising the design of the vanes that direct the air as it enters the fill. The guide vanes are often incorporated with a method of catching water leaving the fill. The design of this is important, and it should be designed to give a uniform air velocity profile and catch a maximum amount of water leaving the fill while minimising the rain zone below the fill.

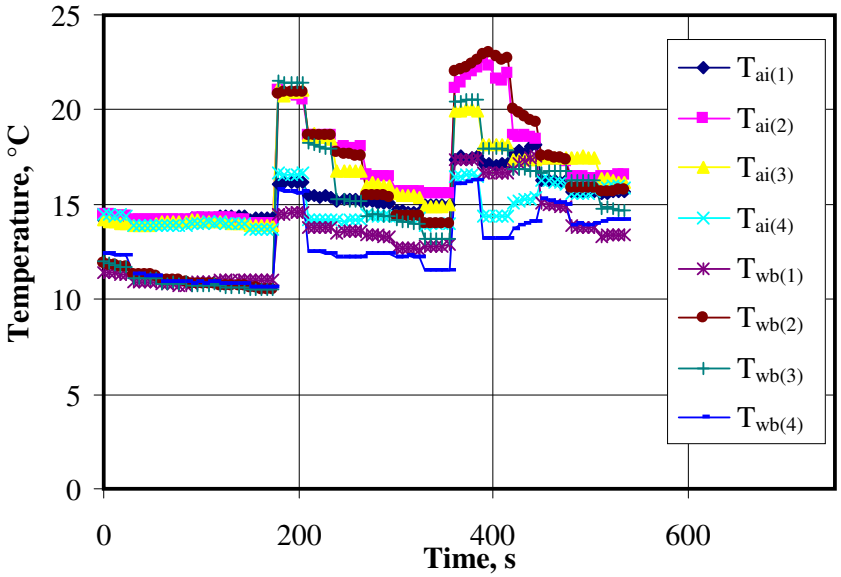

Figure 5-15: Unstable air inlet measurements with wall gutters.

The air mass velocity distribution profile over the cross-section of the tunnel at air mass velocities of 1.502 and 3.501 kg/m²s is measured using a calibrated 70 mm diameter propeller anemometer. The distributions are shown below in Figure 5-16 to Figure 5-19. The air mass velocity measured using the nozzle plate in the tunnel is compared to the air mass velocity obtained by integrating the velocity profile measured with the propeller anemometer. The momentum velocity correction factor is an indication of velocity profile uniformity as calculated by Equation (B.2.4). The assumption is made in Equation (B.2.7) that the airflow is uniform that is $\alpha = 1$. The calculated values for α_{mi} are1.011 and 1.005. They have a 1.1 % and 0.5 % deviation from the ideal. The deviations have negligible results on the calculation of the loss coefficient as found in Section B.2. This validates the airflow distribution as acceptable and validates the assumption of uniform air flow. This is a pleasing result, as the geometry of the tunnel upstream of the fill inlet is complex, with three 90° Mitre bends, as well as it being located downstream of the centrifugal fan outlet, which has notoriously bad distribution. The following graphs show that the air mass velocity measured is within 10 % over 90 % of the reported area matching the airflow distribution percentages of Libert (2007). The difference of less that 7 % between the mass velocity as determined using the propeller anemometer and the nozzle plate proves that the nozzle-plate calculated air mass velocity is correct and acceptable for testing.

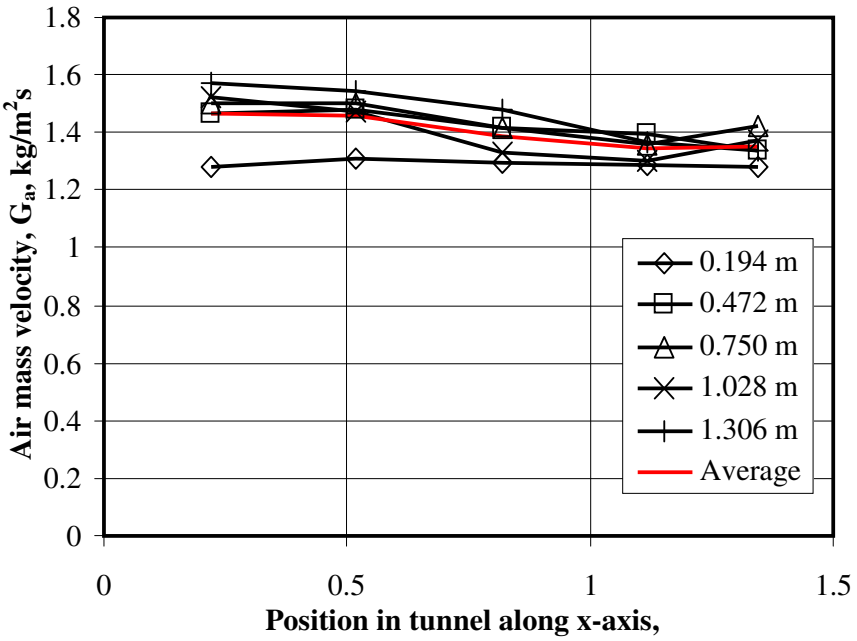

Figure 5-16: Airflow distribution for G_a = 1.502 kg/m²s.

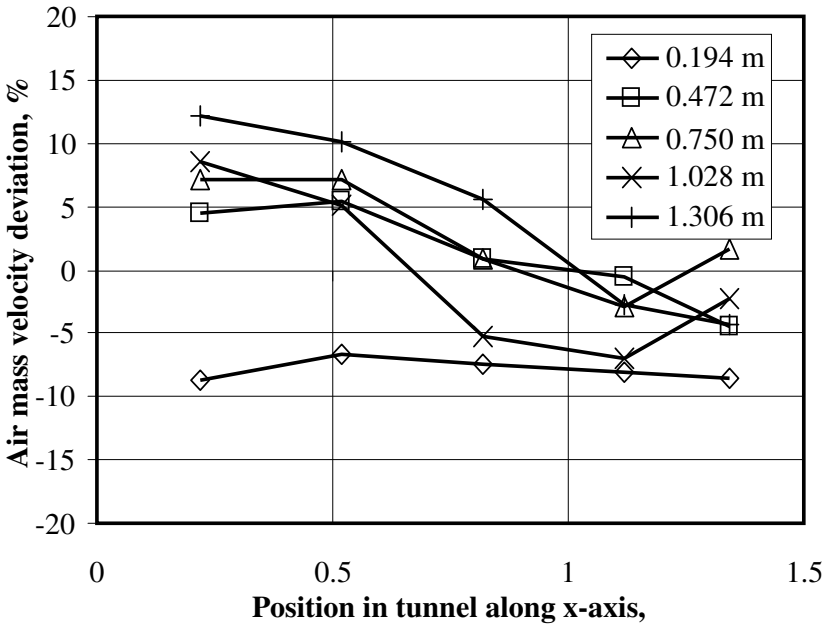

Figure 5-17: Airflow deviation for G_a = 1.502 kg/m²s.

Nozzle G_a	1.502 kg/m²s
Anemometer G_a	1.409 kg/m²s
Difference %	-6.190 %
α_{mi}	1.011

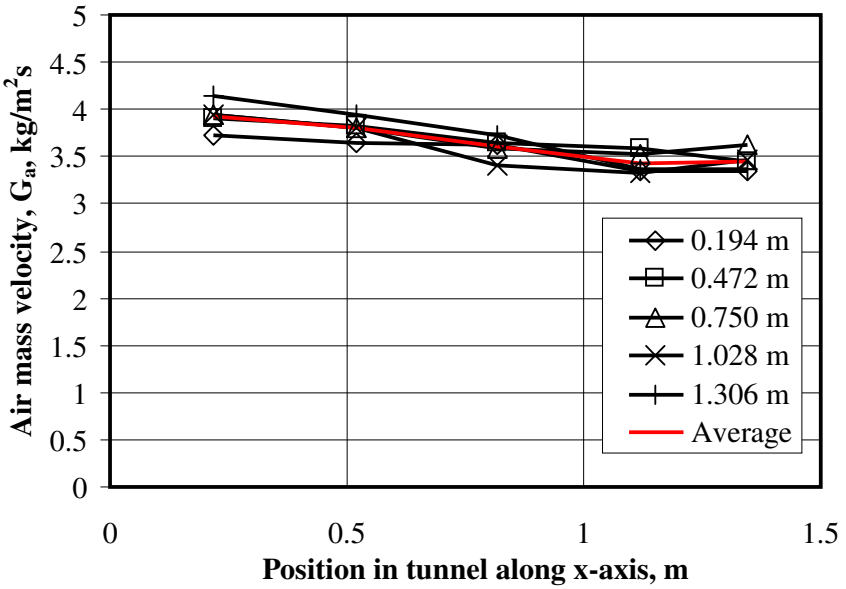

Figure 5-18: Airflow distribution for G_a = 3.501 kg/m²s.

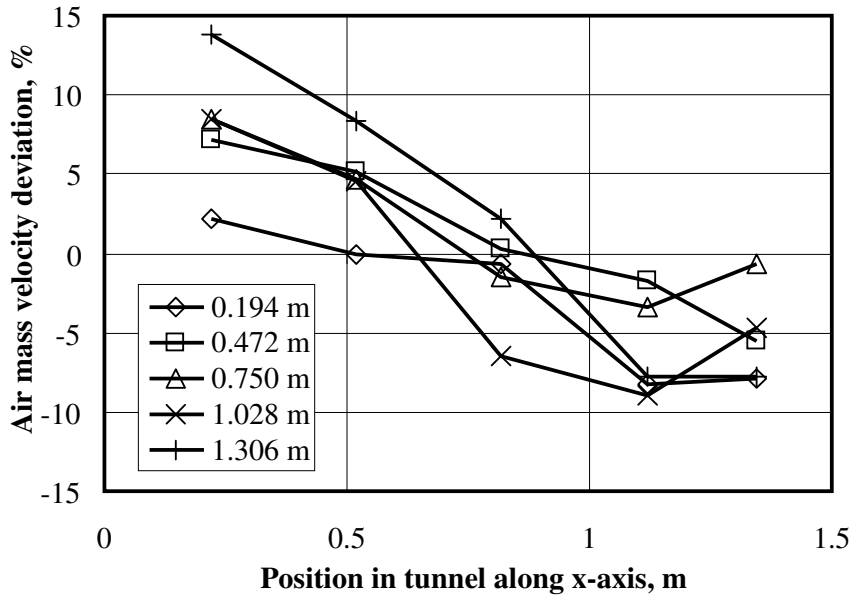

Figure 5-19: Airflow deviation for G_a = 3.501 kg/m²s.

Nozzle G_a	3.501 kg/m²s
Anemometer G_a	3.642 kg/m²s
Difference %	4.027 %
α_{mi}	1.005

5.5. Air bypass effects

The effect of air bypassing the fill is examined by measuring the pressure drop over three fill heights of film fill at various air mass velocities and then repeating, but with foam packed between the fill and the wall of the test section. The foam removes any chance of the air travelling through the test section bypassing the fill in the area between the fill and the wall. Foam of 25 mm thickness was packed on two sides of the fill, forcing the fill against the opposite wall and filling the gap between the fill and the wall. The clearance between the fill and the wall is 20 mm, as the film fill blocks have a length of 1480 mm and are packed into the tunnel with a width of 1500 mm.

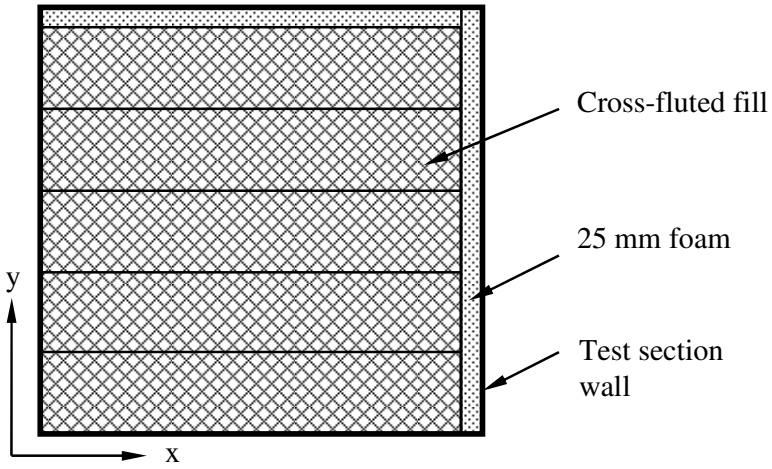

Figure 5-20: Film fill and foam to eliminate air bypass of fill.

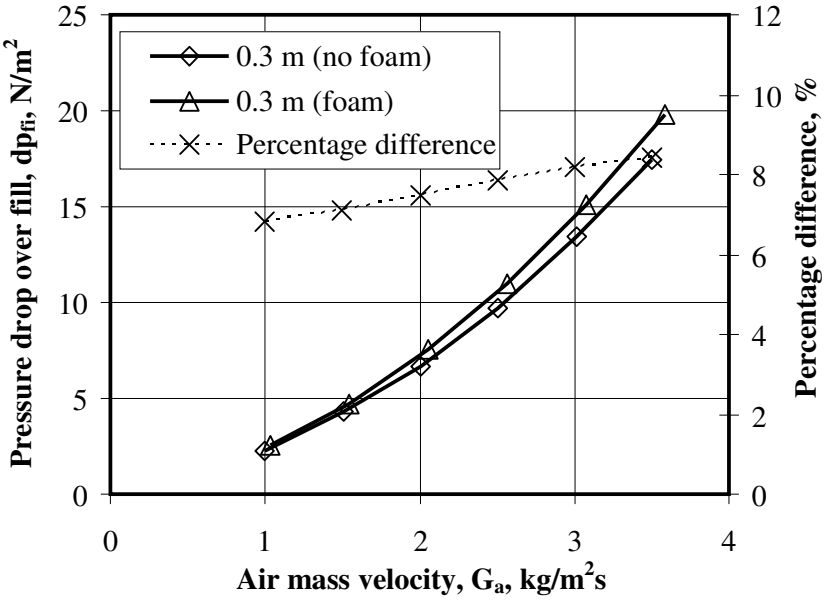

Figure 5-21: Pressure drop over 0.3 m film fill with and without foam.

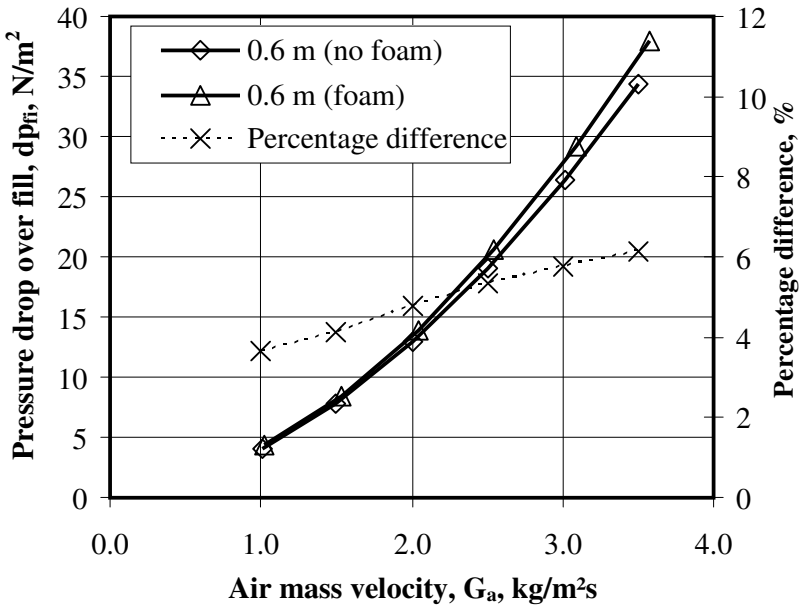

Figure 5-22: Pressure drop over 0.6 m film fill with and without foam.

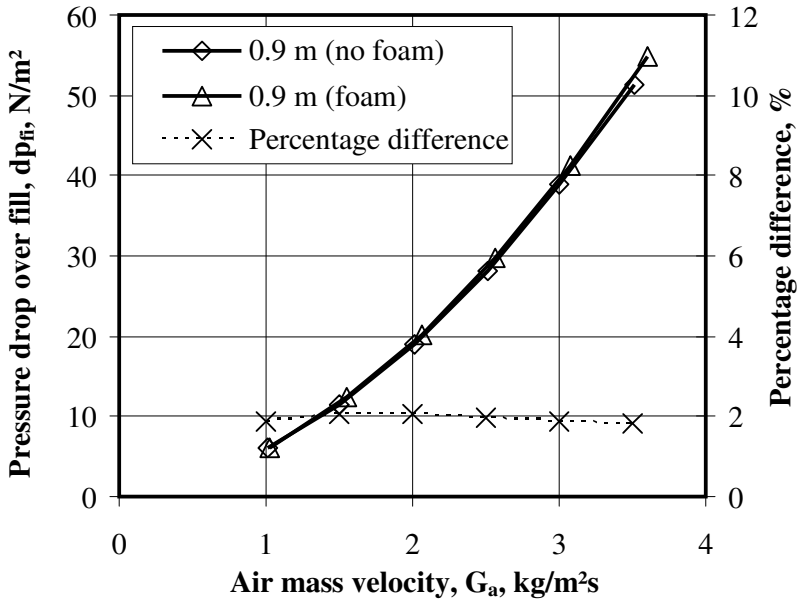

Figure 5-23: Pressure drop over 0.9 m film fill with and without foam.

The measured pressure drop over the fill indicates that bypassing of air does impact the measured pressure drop. The measured pressure drop with the foam lining is greater than the measured pressure drop without the foam lining. This result is expected, since the air bypassing the fill experiences less resistance than it were it to travel through the fill, and therefore the pressure drop is lower. Additionally, the foam lining marginally decreases the flow area, increasing the air

velocity. The effects are greater at lower fill heights and can influence the measured pressure drop by 9 %. This will have an effect on the calculated loss coefficient. As the height of the fill increases the effect is felt less and less.

The film fill is installed in blocks and clearance is needed in order to pack the fill in the test section. It was decided that when testing small fill heights of film fill the foam should be used; it is unnecessary for heights above 0.6 m. When packing the trickle fill for testing, extra layers of fill can be added to the sides of blocks of fill to ensure that the fill is packed tightly against the wall. Splash fill is a very open type of fill, and therefore bypass effects will be negligible when testing the splash-type fill. No foam lining is used when testing the trickle and splash fills.

5.6. Accuracy of water temperature measurements

The accuracy of the water inlet and outlet temperatures is vitally important when calculating the Merkel number. To ensure accuracy of the measurements it is desirable to measure at locations where there is a constant stream of water flowing over the thermocouples and where there is no heat transfer between the point where the temperature is measured and the locations that measurement is supposed to represent. As a result all water temperature measurements are made in locations where the thermocouples are always submerged, where there is continuous water flow over the thermocouples and where heat transfer is minimised.

5.7.1. Inlet water temperature measurements

The water inlet temperature is measured in two locations as described in Section 4.2. The first location of the water inlet temperature [(19) in Figure 4-7] is reliable in terms of the accuracy of the temperature that it measures. The three thermocouples are always submerged in water and the water is constantly flowing over the thermocouples and not stagnating and cooling. For the situations examined this measurement has a standard deviation, σ, of approximately 0.05 °C. This is a very acceptable level of accuracy. However, between the locations where this “fill inlet” temperature is made and the point where the water enters the fill the water still has to move through the spray frame and the spray zone. Cooling will occur in these areas, so the temperature measured here is not the actual fill inlet temperature. This cooling must be accounted for and cannot be ignored. The effect the spray frame and spray zone have on the measured Merkel number is discussed in Section 6.2.1.

The second location at which the fill inlet water temperature is measured [(22) in Figure 4-7] is a suitable location to measure the actual temperature of the water entering the fill. Insulated containers that continually drain water over submerged thermocouples, Figure 4-10, are used to ensure that the temperature measured here

is reliable. What does affect this temperature is the distribution of the water. A uniform water distribution will mean that water is evenly distributed and uniformly cooled as it is sprayed through the spray zone. This method of collecting water and measuring its temperature in a number of individual containers will only be suitable below distribution systems that deliver uniform distribution. The water inlet temperature measurement made in this location has a standard deviation of approximately 0.2 °C for all the tests that were examined. This is quite high as the Merkel number is sensitive to the water inlet temperature. This uncertainty is not a result of poor thermocouple calibration but rather a result of the sensitivity of this measurement method to the presence of water distribution profile.

The trough inlet temperature [(23) in Figure 4-7] made directly below the fill at the trough inlet is impacted very heavily by the distribution of the water leaving the fill. The development of even a slight water distribution profile will result in individual measurement containers measuring different temperatures. When testing fills with good distribution the standard deviation on this measurement can be larger than 0.55 °C. For fills with bad distribution the standard deviation can be as large as 2.4 °C as is the case for 4.04 m splash fill with G_w = 3.02 kg/m^{2}s and G_a = 2.5 kg/m^{2}s. When testing a fill with large migration effects it would be necessary to use a weighted average to calculate the water outlet temperature. During testing this weighting is not known, and, therefore, when testing fills with migration effects this method of water temperature measurement is not suitable.

5.7.2. Outlet water temperature measurements

The water outlet temperature is measured in two locations. The first is in the troughs [(25) in Figure 4-7]. Here the temperature of the water caught in the troughs is measured. This measurement is influenced by the water distribution profile and, once again, when testing a fill with large migration effects, it would be necessary to use a weighted average to calculate the water outlet temperature. This is unknown during testing. The standard deviation for this measurement is around 0.59 °C for fills with minimal water distribution effects. For the case of 4.04 m splash fill the standard deviation was calculated to be 3.05 °C. This is method of outlet water temperature measurement is unusable for fills with large water migration effects.

The second method of water temperature measurement [(26) in Figure 4-7] is an accurate method of temperature measurement as the thermocouples are always submerged and water is continuously moved over the thermocouples. The troughs are drained from two sides of the tunnel. The temperatures are measured in these two pipes. The individual pipes have standard deviations of 0.07 and 0.05 °C for the test cases examined. However the outlet water temperature used is the average of these two measurements and they have been seen to differ by up to 1.5 °C. The

resulting average would thus have a standard deviation 0.75 °C. This is only the case when there is extreme migration as is the case with the splash fill. Generally the standard deviation does not exceed 0.23 °C. Another aspect to consider is the potential for heat transfer to occur between the fill outlet and the location where the fill outlet water temperature is measured. Once the water has exited the fill it falls into the troughs, is drained through the troughs into a chamber, and is then drained by the return pipes in which the thermocouples are located. The effects of any heat transfer between the fill outlet and the location where the water temperature must be accounted for, and this is discussed in Section 6.2.1.

5.7.3. Conclusion

The methods of measuring the water inlet and outlet temperatures are presented. The method of measuring the water inlet temperatures in the supply and return pipe-work is a good method of measuring the water inlet and outlet temperatures, as the water is well mixed. This achieves a good measurement. This temperatures measured represents the temperature of the water in the respective pipes accurately. However, the heat transfer effects between the fill inlet and outlet and the locations where these temperatures are made must not be ignored. The second method, utilising catchment containers located right at the fill inlet and outlet planes. The location of these measurements is good for measuring the water inlet and outlet temperatures. The locations of these measurement points are right at the fill inlet and outlet. However, this method is very sensitive to the presence of a water distribution profile. These measurements are reliable only for uniform water distribution profiles.

When a system is used that delivers uniform water distribution to a fill and that fill has little impact on the water distribution through the test facility, the results of the two water inlet and outlet temperature methods will be very close. When non-uniform distribution is applied, or if a fill with a high degree of water migration is tested, the temperature measurements made in the return pipes are better, but not fail-safe. The cooling impact of the spray frame, spray zone, water catchment troughs and return pipes must be taken into consideration when determining the fill Merkel number. This is done is in Section 6.2.1. The large deviations in the water inlet and outlet temperatures made at locations (23) and (25) in Figure 4-7 make these methods of measurement unhelpful when establishing a standard.

5.7. Top-bottom trough split

Water exiting the fill is collected in two rows of water extraction troughs rotated 90° to each other; see Figure 4-8 and Figure 4-9. These troughs collect the water leaving the fill and direct the water to the return pump. Tests were conducted to see how much water was caught in the top row of troughs and how much was collected in the bottom row of troughs. This was conducted for an empty tunnel, 1.2 m film fill, 1.5 m trickle fill, and 4.04 m v-bar splash fill.

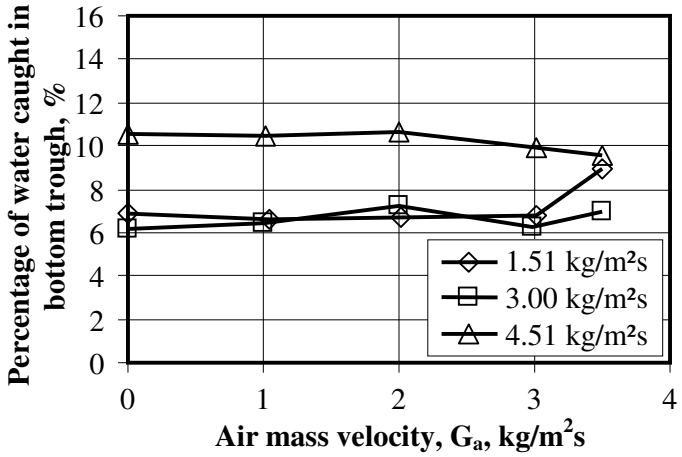

Figure 5-24: Water trough catchment ratio for empty tunnel.

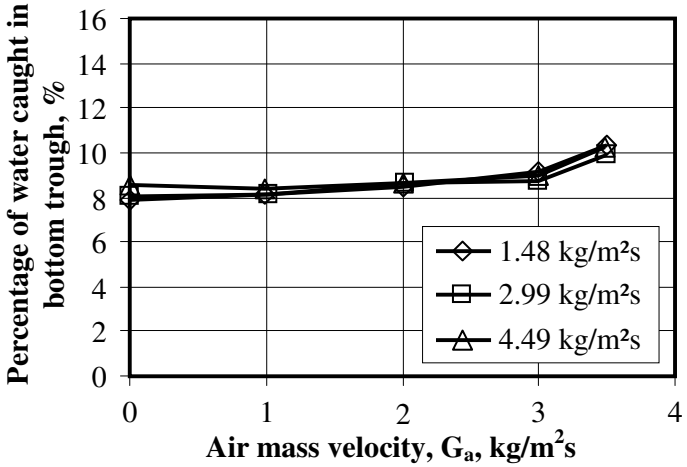

Figure 5-25: Water trough catchment ratio for 1.2 m film fill.

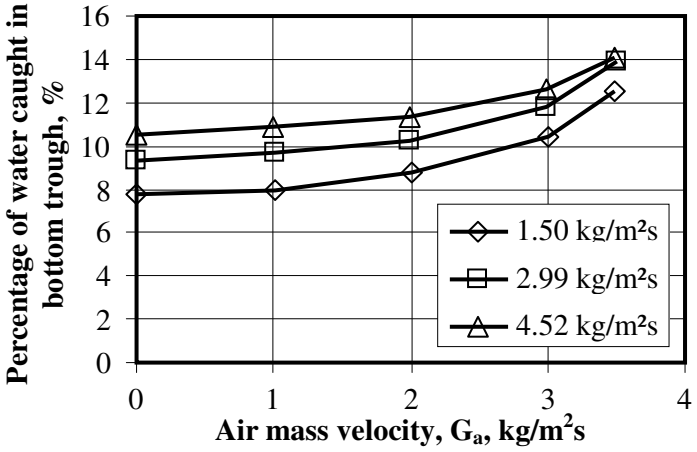

Figure 5-26: Water trough catchment ratio for 1.5 m trickle fill.

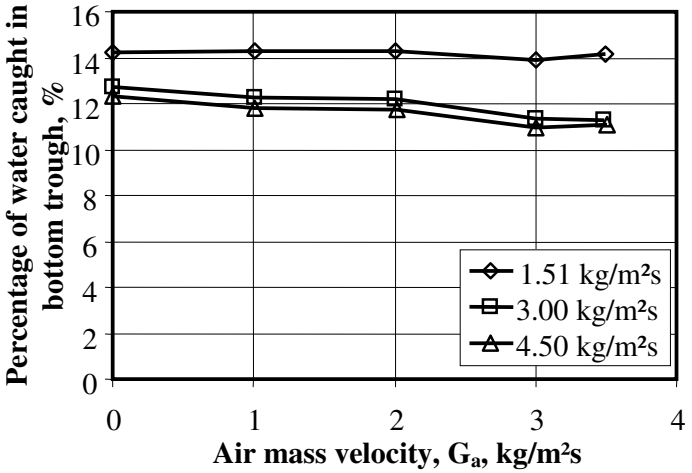

Figure 5-27: Water trough catchment ratio for 4.04 m v-bar splash fill.

This ratio is necessary to calculate the water temperature in the troughs and to compensate for any heat transfer that occurs between the air and the water as the air travels past the troughs. This compensation corrects the air properties so that the Merkel number for the fill is not too pessimistic. If the heat transfer over the troughs is ignored, and the properties of the air before the troughs are used in calculating the Merkel number, then the resulting Merkel number is low and the air entering the fill once it has travelled past the fill is more humid than it was when its properties were measured before the troughs.

5.8. Orientation and location of pressure measurement devices

The accuracy in measuring the pressure drop over the fill is vitally important when calculating the loss coefficient of the fill. The H-taps are used to measure the pressure drop over the fill. H-taps are located below the water extraction troughs and above the fill. The H-taps above the fill are fixed to a frame. It was desirable to see whether the location of the frame above the fill impacts on the pressure measurement reading. The frame was moved around above 0.6 m of cross- fluted fill, rotated and placed at an angle. The various locations of the H-tap frame are shown in Table 5-1. The images show the test section in plan view. The resulting pressure drops are graphed in Figure 5-28.

Relative to location A, locations B and C have a maximum difference of 0.63 and 0.49 N/m² respectively. These occur at G_a = 3.0 kg/m²s. This difference only of 0.63 N/m² constitutes a difference of only 2.14 %. Relative to location A, the more extreme locations D, E and F have a maximum pressure difference of 0.68, 0.21 and 0.26 N/m² respectively. The maximum pressure difference occurs at G_a = 3.0 kg/m²s for location D, and for G_a = 1.0 kg/m²s for locations E and F. These translate to 2.93, 4.72 and 5.83 % for these three cases. Placing the frame in the middle of the test section at any orientation will result in consistent pressure drops being measured.

Table 5-1: Orientation of pressure measurement devices

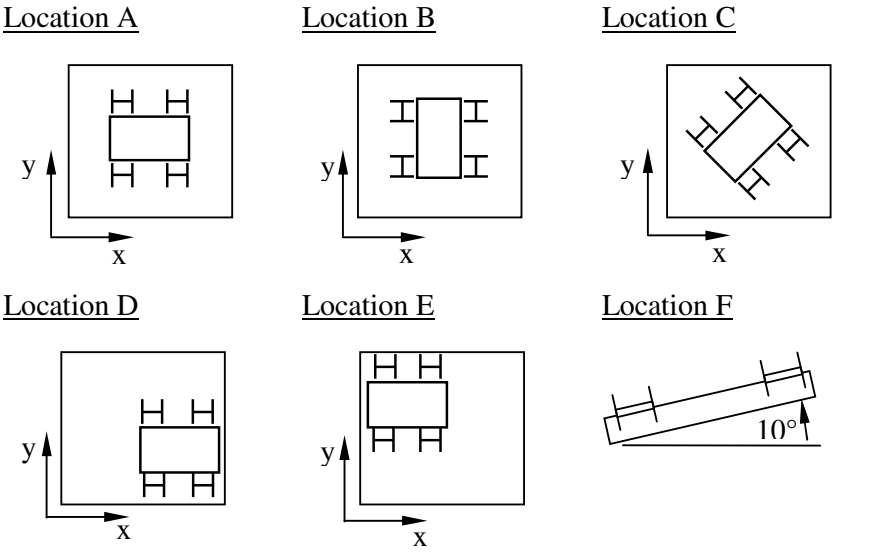

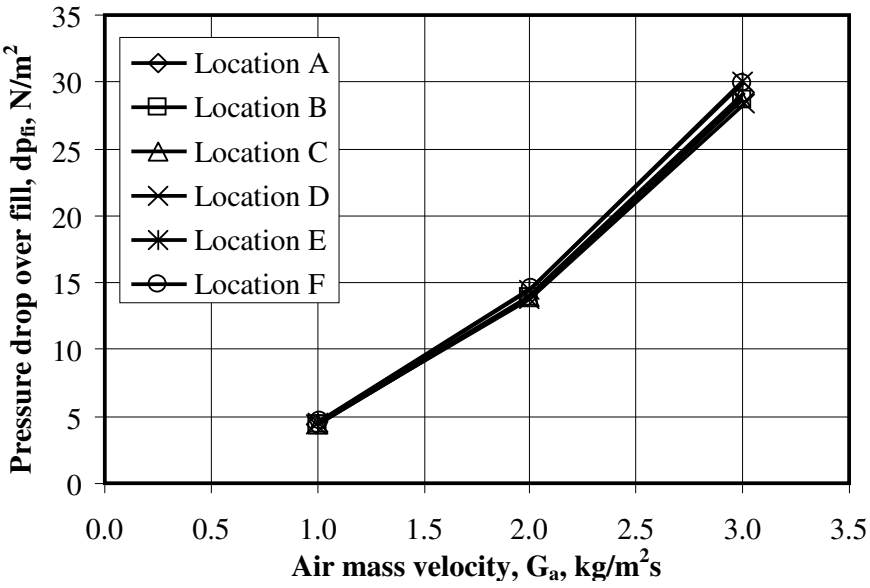

Figure 5-28: Pressure drop resulting from different H-tap frame locations.

Placing the frame at the extremes, for example close to the walls or at an inclined angle, will impact the measured pressure drop. It was therefore decided that, when placing the frame with the H-tap pressure points fixed to it, the frame must be placed above the fill in the middle of the test section. The exact location and orientation of the frame do not affect the result, provided that is it away from the wall and not at an angle.

5.9. Water mass flow rate

The water mass flow rate impacts both the Merkel and loss coefficients. It is important that the water mass flow rate through the fill is known as accurately as possible. The accuracy of this measurement depends on the accuracy of the water flow rate measurement method. From the calibration of the electromagnetic flow meter, Appendix D.3, it is seen that the flow rates determined by the flow meter and the calibration tank are within 1.25 % of each other and therefore it is assumed that the electromagnetic flow meter performs satisfactorily. The integrated flow rates determined when measuring the water distribution profiles in Sections 5.2 and 5.3 also indicate that the water mass velocity determined by the electromagnetic flow meter is good. During testing, an orifice plate flow meter is available as a comparative flow measurement to ensure that the electromagnetic flow meter is operating correctly.

5.10. Air mass flow rate

The air mass flow rate is considered accurate, as the method of determining this is in accordance with ASHRAE 51 (1975). Furthermore the integrated flow rate determined when examining the air mass flow profiles in Section 5.4 proves the air mass flow rate determined by the nozzle plate is good. During testing, a calibrated propeller anemometer is available as a comparative flow measurement to ensure that the nozzle plate flow measurement is operating correctly.

5.11. Conclusion

This chapter has examined individual elements in the test facility to ensure that each element performs satisfactorily and delivers test conditions or measurements that agree with the assumptions made in performance theory. The water distribution system was examined. It was deemed necessary to construct a water spray frame as the distribution delivered by spray nozzles is not uniform. A spray frame was designed and the water distribution delivered by the spray frame is within 10 % of the average. This satisfies the Merkel theory assumption of uniform water distribution. The Christiansen coefficient is suggested as a unit to represent the uniformity of the water flow through the tower.

The migration of water through different fills was examined. One of the Merkel assumptions is uniform performance through the fill. This means uniform water flow through the fill being tested. The film fill satisfies this assumption with the water mass velocity below the fill heights tested not deviating by more than 15 % in the film fill. The trickle fill water distribution below the fill deviates by a maximum of 30 %, while the splash fill deviates by up to 90 %. This does not satisfy the assumption of uniform water mass flow through the fill, and this must be considered when using the generated performance data.

The water distribution profiles reported on in Sections 5.2 and 5.3 are measured below the fill when there is no air flowing. Knowing the water profile through the fill is desirable but very difficult to measure. Any obstruction in the air flow causes a wake and water streams into this area of low pressure. It is assumed that the measured distributions do not change drastically during testing when there is airflow, but this is unknown.

The wall water bypass was examined. The assumption that all the water delivered to the test facility flows through the fill was evaluated. In the case of the film fill, the wall water never exceeds 5 % of the delivered water mass flow rate. In the case of the trickle fill, wall water never exceeds 8 %. These are pleasing results. In the case of the splash fill these values approach 30 % when the spray frame is used. This value increases up to 35 % when the spray nozzles are used. The case of the splash fill does not satisfy the assumption that all the water delivered to the test facility flows through the fill, and this must be remembered during testing.

The air mass velocity in the test facility was determined to ensure that the assumption of uniform air velocity through the fill is appropriate. The air mass velocity was examined at 1.5 kg/m²s and 3.5 kg/m²s. In both cases the air only rarely deviated by more than 10 % from the average, and when this did occur it never exceeded 15 % deviation. The assumption of uniform air distribution and uniform air properties was achieved in the test facility.

The methods used to determine the inlet and outlet water temperatures were examined. There are two methods of determining both measurements. One set of measurements is made in line with the fill inlet and outlet, while the second method measures the water temperature in the pipe work leading to and from the facility. The measurements made in line with the fill inlet and outlet are useful only when a uniform method of water distribution is used, and only when the fill being tested has good water flow distribution below the fill. For fills that have bad migration over the height of the fill, it is better to use the measurements made in the pipe work leading to and from the test facility, however even these measurements are not immune to severe water distribution profiles.

The method of measuring the pressure drop over the fill was examined. It was determined that the pressure measured is not too dependent on the location of the pressure measurement H-taps, provided that the taps are perpendicular to the air flow, and provided that the H-taps are placed directly next to the walls of the test facility.

Finally, the methods used to measure the water and air mass velocities delivered to the test facility were examined. From the use of a calibration tank and by integrating the water flow over the test section area it was determined that the water flow measurement made by the electromagnetic flow meter is satisfactory. Using a propeller anemometer and integrating the air mass velocity over the area determined that using the nozzle plate to calculate the air mass velocity produces a satisfactory result.

6. TEST FACILITY CONTRIBUTIONS TO FILL PERFORMACE

6.1. Introduction

In a typical counter-flow wet cooling tower there are three zones in which cooling occur. These are the spray zone, the fill and the rain zone. The spray zone above the fill is necessary to allow the development of the spray pattern from the spray nozzles. The rain zone below the fill is a result of the open space below the fill which is necessary to allow air to flow uniformly upwards through the fill. The contribution of these zones has a measureable impact on the performance of cooling towers. Kröger (2004) suggests that this can be as big as up to 10 – 20 %.

Thus the contribution of the spray and rain zones are important when determining fill performance. The majority of studies into fill performance acknowledge these effects (Lowe and Christie (1961), Brentwood (1990), Libert (2002)). Johnson (1989) compensates for these effects by measuring the water inlet and outlet temperatures right at the fill inlet and outlet planes. The contribution of the test facility geometry to the measured thermal performance must be understood and not included when reporting on fill performance.

A similar argument can be made for the flow resistance zones in the cooling tower. Libert (2002) states that the louvers installed below the fill to collect water contribute to an increased flow resistance. The flow resistance contribution of the geometry in the test facility therefore needs to be understood and not included when reporting on fill performance.

6.2. Stellenbosch test facility

The Stellenbosch test facility has been set up to minimise undesirable thermal and flow effects. The height of the spray zone above the fill has been minimised by the use of the specifically designed spray frame. The spray frame offers a better water distribution over a range of water flow rates compared to the water distribution offered by spray nozzles over a range or water mass flow rates. The use of the spray frame also results in a spray height of only 150 mm being necessary, compared to the 500 to 700 mm necessary when using nozzles. However, the contribution of the minimised spray zone is still not negligible or ignored. The height of the rain zone below the fill has been minimised by locating the water catchment troughs (Figure 4-8) below the fill. These water extraction troughs contribute a flow resistance and the impact of these troughs on the flow performance must be known.

6.2.1. Merkel number compensation

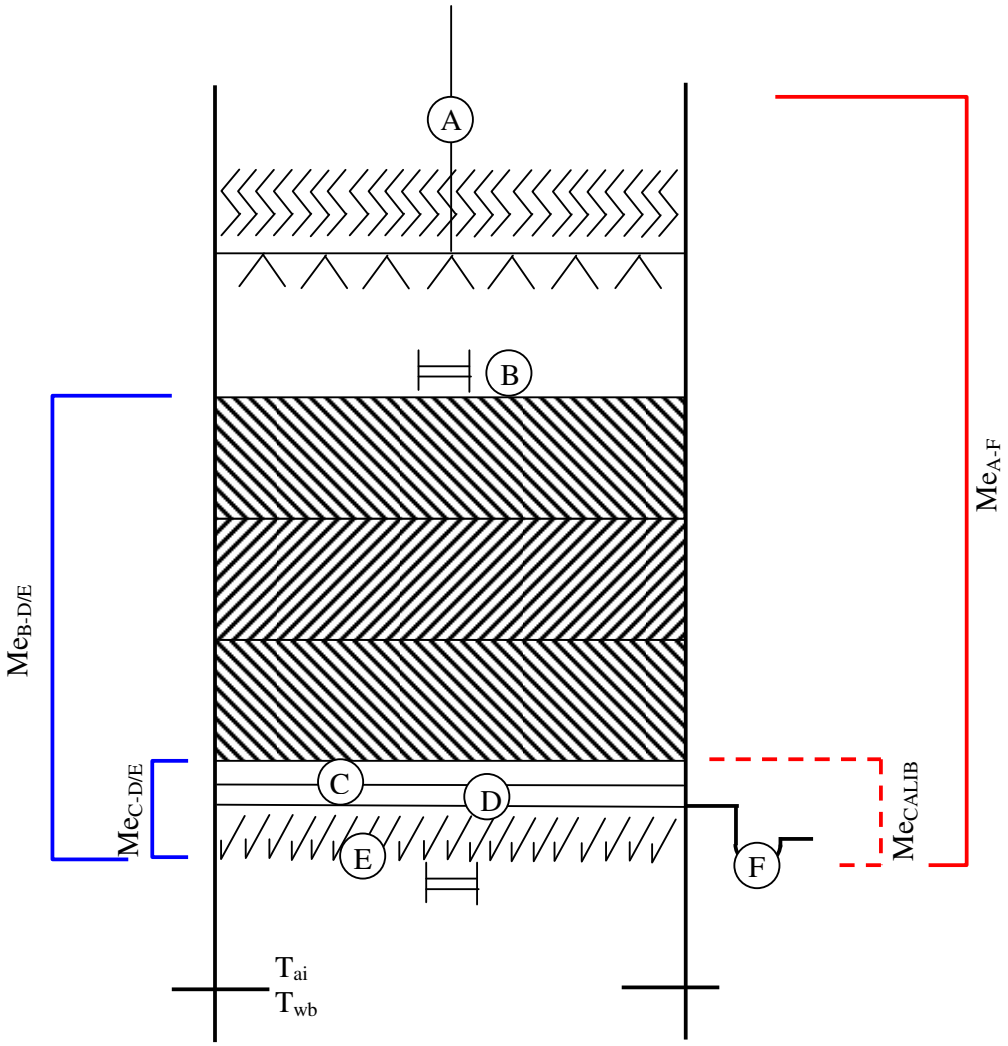

Figure 6-1: Location of thermocouples and pressure measurement H-taps during testing.

Figure 6-1 illustrates where the thermocouples and the pressure measurement H-taps are located during testing. If temperature measurement point A is used as the water inlet temperature and point F is used to measure the water outlet temperature to determine the Merkel number Me_{A-F} it is evident that, apart from the fill, the Merkel number would include heat transfer in the spray frame, in the spray zone, water extraction troughs and in the return pipe.

The effect of all these zones can be quantified by completing a test with no fill in the test facility and the spray frame 150 mm above the water extraction troughs. (This distance is necessary for the placement of the pressure H-taps between the fill and the spray frame.) A correlation for the Merkel number can be obtained and

used later to correct the Merkel number calculated when conducting fill tests as shown in Equation (6.1).

$$Me_{fill} = Me_{A-F} - Me_{CALIB} \tag{6.1}$$

This test is conducted and results are shown in Figure 6-2. A sample of the experimental data can be found in Table G-1. During testing the water cools as it is cycled through the test facility. The test is conducted three times to obtain the water inlet temperature dependency of the empty tunnel performance. Equation (6.2) represents the Merkel number for the empty tunnel as a function of water mass velocity, G_w, air mass velocity, G_a, and the inlet water temperature, T_{wi}, measured at location A.

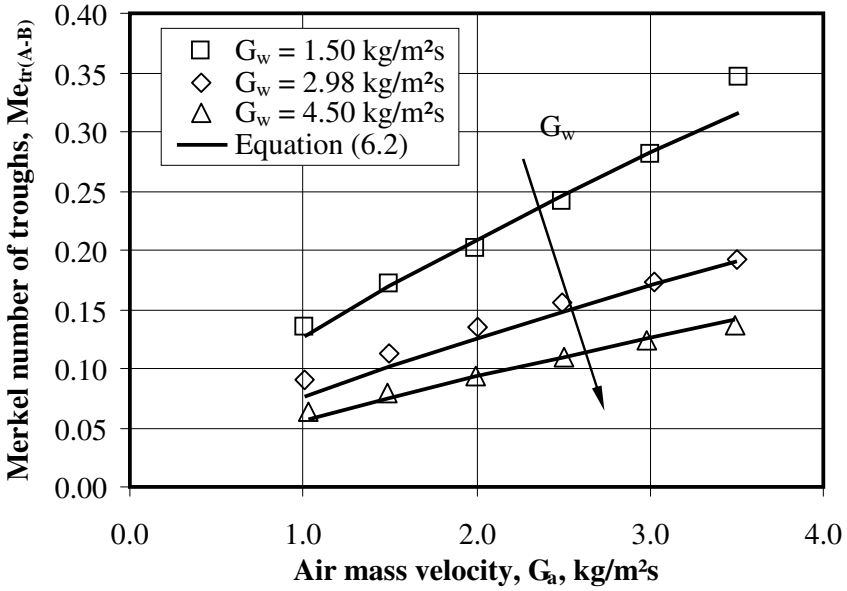

Figure 6-2: Merkel contribution of empty tunnel.

$$Me_{CALIB} = 0.386 G_w^{-0.742} G_a^{0.727} T_{wi}^{-0.225} \qquad r^2 = 0.983 \tag{6.2}$$

This correlation describes the combined Merkel number of the spray frame and spray zone and the trough and outlet pipe work. When these contribution zones are examined for 1.22 m cross-fluted fill and the Merkel number for the spray zone and troughs are calculated separately, it is calculated that approximately 70 % of the curve-corrected Merkel number is due to cooling over the troughs. This is because cooling in the spray zone is drop cooling while the cooling that occurs over the troughs is film type cooling. It follows that the Merkel number contribution of the troughs will be larger than the Merkel number contribution of the spray zone, as film cooling for a certain height is more effective than drop cooling over the same height. The height of the spray zone is typically 150 mm,

while film cooling occurs over the 320 mm troughs, and therefore it is proved that more cooling takes place over the troughs than in the spray zone. As a result, the temperature measured at C (in Figure 6-1) is used for T_{wi} in Equation (6.2). It is desirable to represent the performance of the troughs as accurately as possible, as the majority of the curve-corrected Merkel number is a result of the cooling over the troughs. This method of correcting the Merkel number will be referred to as the curve-corrected Merkel number.

Alternatively, by changing the locations of the water inlet and outlet thermocouples, the impact of some of these zones can be excluded in the Merkel number calculation. Using location B to determine the water inlet temperature, the heat transfer in the spray frame and the spray zone can be ignored, as the temperature measured here is the temperature of the water as it enters the fill and therefore is indeed the fill inlet temperature. By measuring the water outlet thermocouples at location C, the temperature of the water exiting the fill can be measured. However, if this were used as the water outlet temperature and the air properties were measured as they are [(13) in Figure 4-7], then the incorrect air properties would be assumed because, there is heat transfer over the water extraction troughs, since the air properties upstream and downstream of the troughs would be different. To compensate for this, the temperature of the water in the troughs, location D/E, is used as the water outlet temperature. The temperature at E/D is a weighted average of the water in the top and bottom layers of trough. The weighting is obtained from examining the split in the distribution for the empty tunnel and then below various fills with differing air and water mass velocities. This can be found in Section 5.7.

Another Merkel number is calculated for the troughs using location C as the water inlet and location D/E as the water outlet. The two Merkel numbers are subtracted (this is allowable because they are determined with the same air inlet properties) from each other as in Equation (6.3) to calculate the Merkel number of the fill without relying on a curve representing the troughs' performance. Ideally a test facility void of fill should not register a Merkel number measurement.

$$Me_{fill} = Me_{B-D/E} - Me_{C-D/E} \tag{6-3}$$

To illustrate that this is an effective method of compensating for the performance of the trough the test results from the empty tunnel tests (when testing is conducted with no fill and the spray frame 150 mm above the water extraction trough) are presented in Figure 6-3. Comparing this to Figure 6-2, it is evident that the thermal performance effects of the empty test facility are compensated for. This method of correcting the Merkel number will be called the measurement-corrected Merkel number. During testing the two methods are compared.

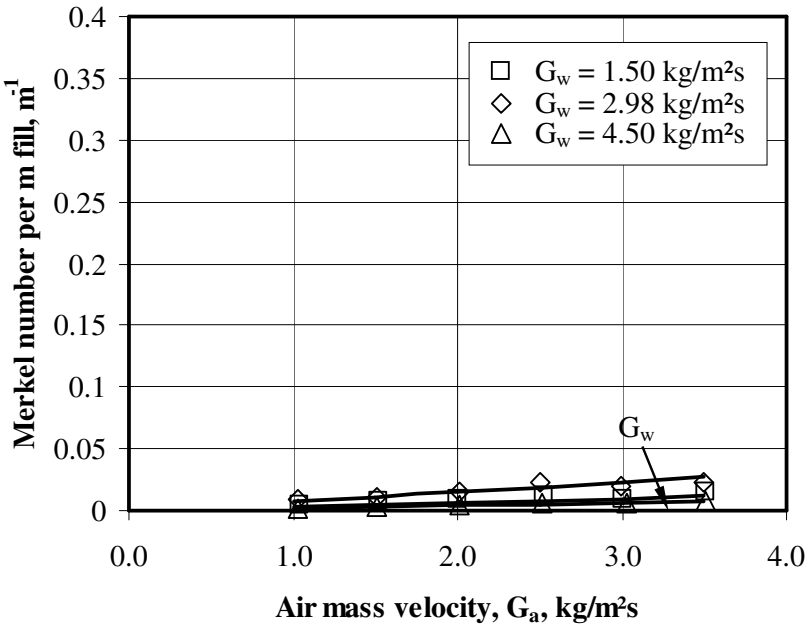

Figure 6-3: Measurement-corrected Merkel number of facility void of fill.

6.2.2. Loss coefficient compensation

In Figure 4-7 and Figure 6-1 it is evident that during testing the pressure drop measured using the pressure H-taps results in a measured pressure that includes the pressure drop over the troughs. The effect of the troughs must be subtracted from this total pressure drop so that the reported performance is that of the fill only. This is achieved by conducting a test with the spray frame 150 mm above the troughs to determine the flow performance of the troughs and the 150 mm spray zone. The drop measured over this zone is shown in Figure 6-4 and the equation describing the curve is given in Equation (6.4)

$$dp_{tr} = 1.563 G_w^{0.184} G_a^{1.693} \qquad r^2 = 0.975 \qquad (6.4)$$

The pressure drop over the troughs with no water flow is shown in Figure 6-5 with its characteristic curve Equation (6-5)

$$dp_{tr} = 1.027 G_a^{2.0015} \qquad r^2 = 0.987 \qquad (6.5)$$

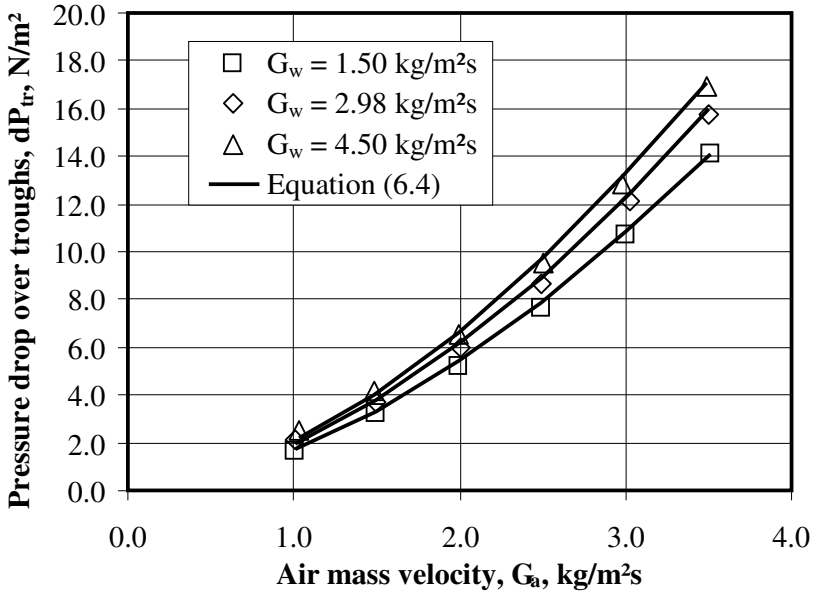

Figure 6-4: Pressure drop over troughs.

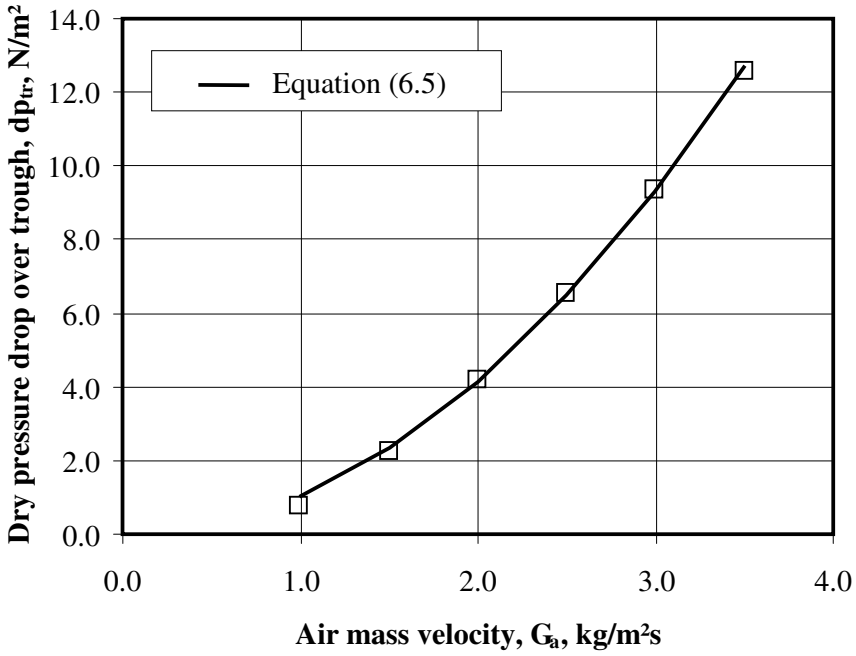

Figure 6-5: Pressure drop over trough with no water flow.

It is established in Section 3.3 that because of the dimensionless characteristics of the loss coefficient the loss coefficient is a more reliable way of representing the fill performance than would be merely reporting on the measured pressure drop.

This same argument is valid for the flow performance of the troughs. As a result the loss coefficient for the troughs is determined and shown in Figure 6-6. The equation describing the curve is shown in Equation (6.6).

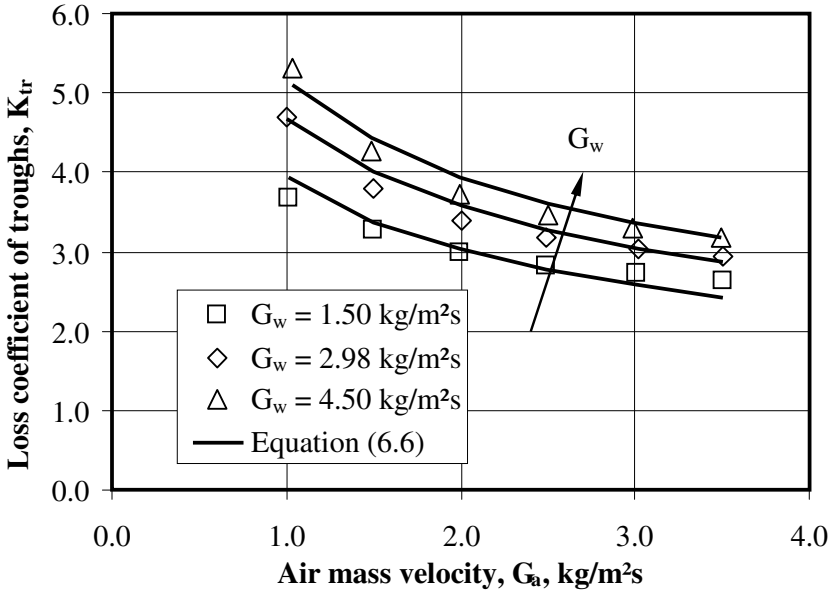

Figure 6-6: Loss coefficient contribution of empty tunnel.

$$K_{tr} = 3.581 G_w^{0.243} G_a^{-0.388} \qquad r^2 = 0.939 \qquad (6.6)$$

This information is used to correct the loss coefficient determined during testing so that the reported loss coefficient reports on the performance of the fill alone and does not include the effects of the troughs. This is achieved by

$$K_{fi} = K_{tot} - K_{tr} \qquad (6.7)$$

7. FILL PERFORMANCE EXPERIMENTAL WORK

This chapter examines the tests conducted in the Stellenbosch counter-flow fill test facility. Tests are conducted on the three types of fill, namely film fill, trickle fill and splash fill. In this chapter tunnel preparation is briefly described, testing conditions and parameters are specified, and the results of the three performance tests are presented and discussed.

7.1. Experimental preparation

Preparation for testing requires approximately two days. Preparation includes:

- heating the water
- installing the fill
- installing the water distribution system, cleaning the filter, and checking that spray holes are open
- installing fill pressure drop measurement devices
- installing water inlet temperature measurement devices
- wetting wet-bulb thermocouple wicks
- conducting a dry test to ensure air measurements are working correctly and to estimate the expected pressure drop over the fill during wet testing.

Van der Merwe (2006) presents a guide which describes the step-by-step process of tunnel preparation.

7.2. General overview

A performance test consists of three water mass velocities and six air mass velocities. These flow rates have been selected as they span the normal operating conditions of cooling towers in industry. The same set points are used for each type of fill so that results may be easily compared. The water and air mass velocities used during testing are shown in Table 7-1.

Table 7-1: Water and air mass velocities used for performance testing

Water mass velocity, G_w, kg/m²s	Air mass velocity, G_a, kg/m²s					
	1.0	1.5	2.0	2.5	3.0	3.5
1.5						
3.0						
4.5						

Water is heated to at least 46 °C prior to testing. A single test repeats the mass velocity matrix in Table 7-1 three times. Water from the reservoir is circulated through the test facility during testing. In the process the water is cooled as the testing progresses. The dependence of fill performance on the inlet water temperature can be determined. The dependence of performance on fill height is determined by testing three different fill heights.

During testing, the temperatures of the water and air streams are monitored to ensure that the system has reached a steady state of operation. The nozzle dry- and wet-bulb temperatures are monitored to ensure they remain within 0.2 °C of the average. The fill inlet dry- and wet-bulb temperatures are similarly monitored. The temperature drop over the fill and troughs are monitored to ensure that they are steady when data is logged. The pressure drop over the fill is monitored to ensure that the two pressures measured do not deviate by more than 2 N/m² from the average. A screenshot of the user interface used to monitor all these measurements is shown in Figure 4-15.

When a set point is changed the pressure drop over the fill stabilises faster than the temperature drop over the fill. The temperature drop over the fill stabilises within two minutes of changing the air and water flow settings. Data are logged for approximately 40 seconds as there is a time limit to testing. This time limit is a result of the water constantly cooling as it cycles through the test facility. Testing takes three hours to repeat the mass velocity matrix three times. In this time the water can cool from 50 °C to 24 °C.

7.3. Fill test results

Three types of fill are tested. The film fill is tested with fill heights of 0.305, 0.61, 1.22 and 1.83 m. The trickle fill is tested with fill heights of 0.5, 1.0 and 1.5 m. The splash fill is tested with fill heights of 2.04, 3.04 and 4.04 m. Samples of the experimental data can be found in Table G-2 for the film fill, Table G-3 for the trickle fill and Table G-4 for the splash fill. The resulting performance plots and curves generated from the full set of experiments are reported on in the following sections.

7.3.1. Film fill performance results

L_{fi} = 0.305 m

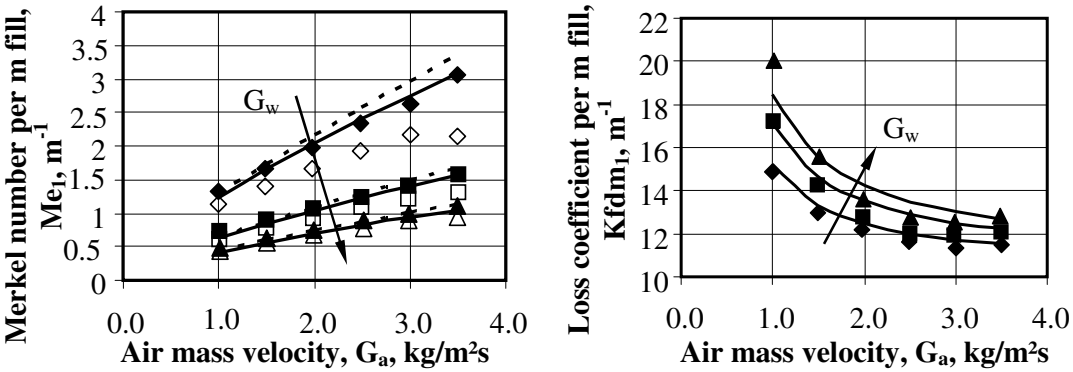

a) b)

L_{fi} = 0.61 m

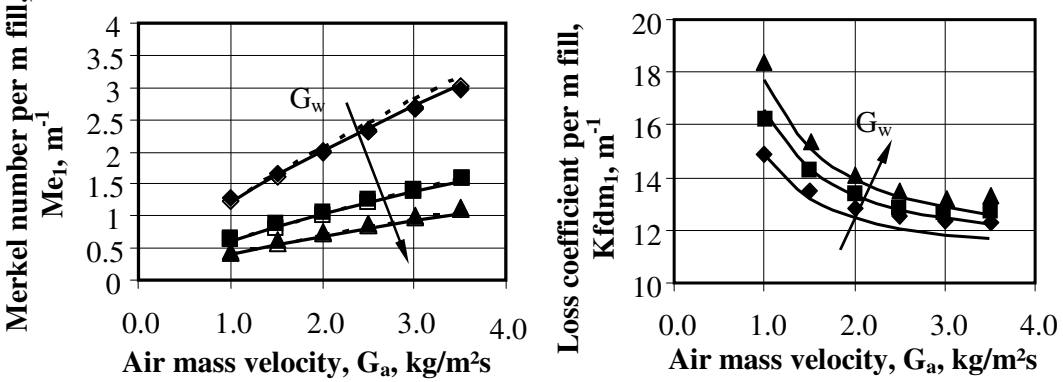

c) d)

L_{fi} = 1.22 m

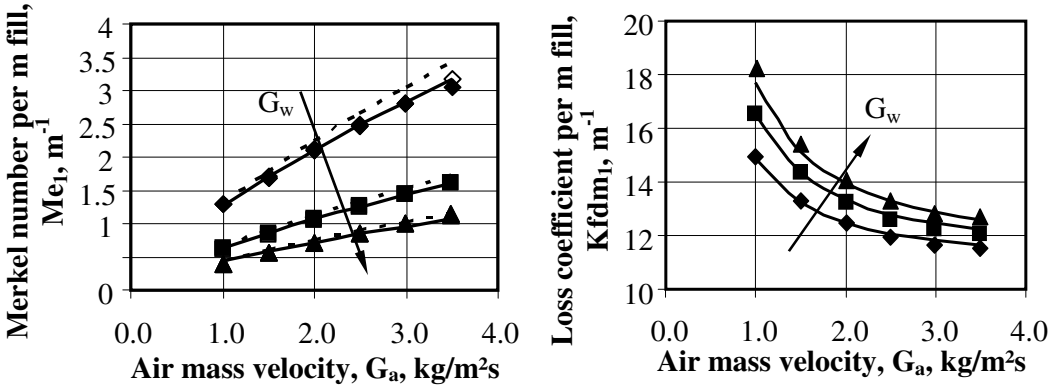

e) f)

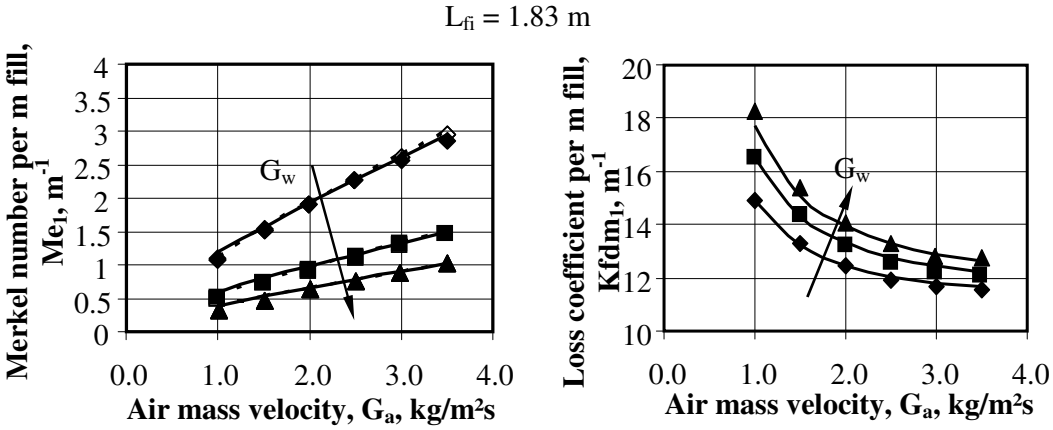

g) h)

Figure 7-1: Film fill Merkel number and loss coefficient results for 0.305, 0.61, 1.22 and 1.83 m.

Four fill heights of film fill are tested with water inlet temperatures from 54.04 to 29.35 °C. A sample of the test data can be found in Table G-1. Two methods of measuring water inlet and outlet temperatures are used to calculate two independent Merkel numbers. The Merkel number making use of the curve-correction in Section 6.2.1 is given by Equation (7.1), while the measurement-corrected Merkel number is described by Equation (7.2). The coefficients of determination, r^2, are reported on alongside the equations.

$$Me_{fill} = 2.746 G_w^{-0.984} G_a^{0.73} T_{wi}^{-0.104} L_{fi}^{-0.085} \qquad r^2 = 0.991 \qquad (7.1)$$

$$Me_{fill} = 2.64 G_w^{-0.986} G_a^{0.763} T_{wi}^{-0.104} L_{fi}^{-0.062} \qquad r^2 = 0.994 \qquad (7.2)$$

In Figure 7-1 a), c), e) and g) the Merkel number determined using the curve-correction in Section 6.2.1 is plotted by the solid markers, and the corresponding curve (Equation (7.1)) is plotted with the solid line. The measurement-corrected Merkel number is plotted by the open markers, and the corresponding curve (Equation (7.2)) is plotted with the dotted lines.

The water distribution delivered to the fill is good, but it is not perfectly uniform. This has the result that the Merkel numbers are slightly pessimistic. According to Figure 5-12 the result will be within 99 % of the maximum Merkel number achievable. Comparing the two sets of results shows there is good correlation between the two methods. This indicates that the water down the walls and the migration through the fill do not affect the measured Merkel number too significantly. This was expected as the migration effects of the fill results in a maximum of only 15 % deviation from the average flow rate through the fill. Also a maximum of only 4 % of the water attaches to the wall over the fill height.

The tests with the highest and lowest Christiansen coefficients (as reported on in Appendix E) are examined. The standard deviation, σ, of the different water in- and outlet temperature measurements are calculated as an indication of temperature measurement accuracy. The film fill highest Christiansen coefficient, $C_u = 0.922$, was for 0.61 m fill with $G_w = 4.49$ kg/m^{2}s and $G_a = 2.50$ kg/m^{2}s. The standard deviations for this case are:

- $T_{wi(A)}$; σ = 0.03 °C
- $T_{wi(B)}$; σ = 0.23 °C
- $T_{wi(C)}$; σ = 2.02 °C
- $T_{wo(D/E)}$; σ = 0.98 °C
- $T_{wo(F)}$; σ = 0.08 °C

The film fill test with the lowest Christiansen coefficient, Cu = 0.903, was for 1.83 m fill with $G_w = 2.98$ kg/m^{2}s. The situation examined has a $G_a = 2.50$ kg/m^{2}s. The standard deviations for the measurements made in this case are:

- $T_{wi(A)}$; σ = 0.06 °C
- $T_{wi(B)}$; σ = 0.29 °C
- $T_{wi(C)}$; σ = 1.94 °C
- $T_{wo(D/E)}$; σ = 0.97 °C
- $T_{wo(F)}$; σ = 0.16 °C

These results suggest that the curve-corrected Merkel method will produce more accurate performance results than the temperature-corrected method for the film fill. An uncertainty greater than 0.1 °C is deemed unacceptable. The Merkel number is most sensitive to the water outlet temperature. An uncertainty of 0.16 °C, as is the case for $T_{wo(F)}$, is unacceptable. Both measurement methods require refinement of the water outlet temperatures for accurate performance testing.

The loss coefficient reported on in Figure 7-1 b), d), f) and h) is the loss coefficient of the film fill only, as the contribution of the troughs has been subtracted as in Equation (6.7). Foam is used to prevent any short-circuiting of air around the fill in accordance with Section (5.5). The curve describing the loss coefficient of the fill is given in Equation (7.3).

$$K_{fdm_1} = \left(4.499 G_w^{\,0.359} G_a^{\,-1.122} + 9.577 G_w^{\,0.028} G_a^{\,0.056}\right) L_{fi}^{\,-0.043} \qquad r^2 = 0.982 \qquad (7.3)$$

A very small fill height effect is evident for both the Merkel number and loss coefficient. It is only the impractically small fill height $L_{fi} = 0.305$ m that causes this dependence.

7.3.2. Trickle fill performance results

L_{fi} = 0.5 m

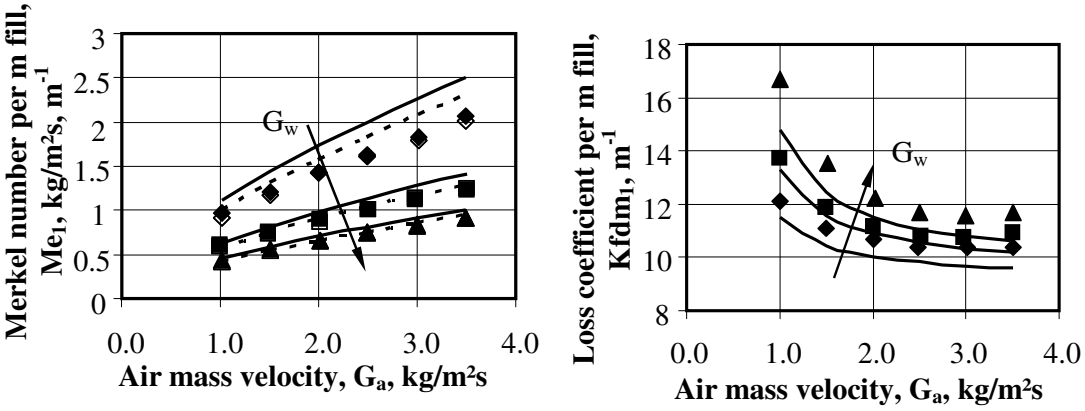

a) b)

L_{fi} = 1.0 m

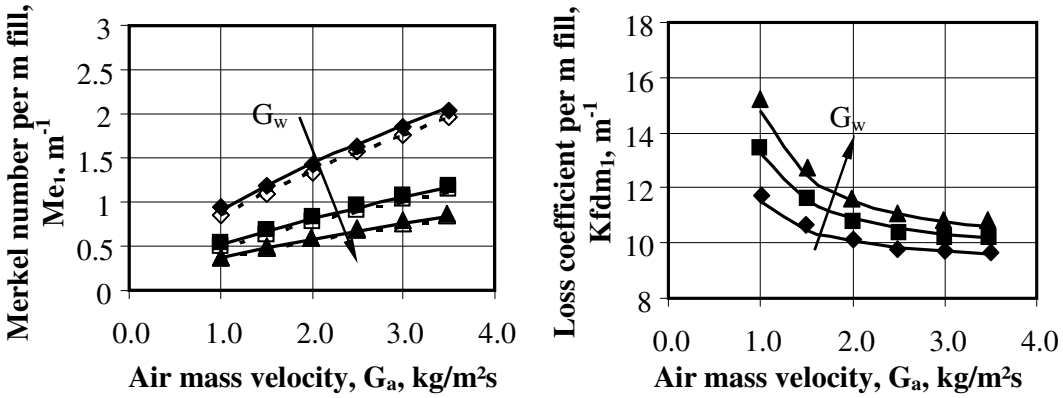

c) d)

L_{fi} = 1.5 m

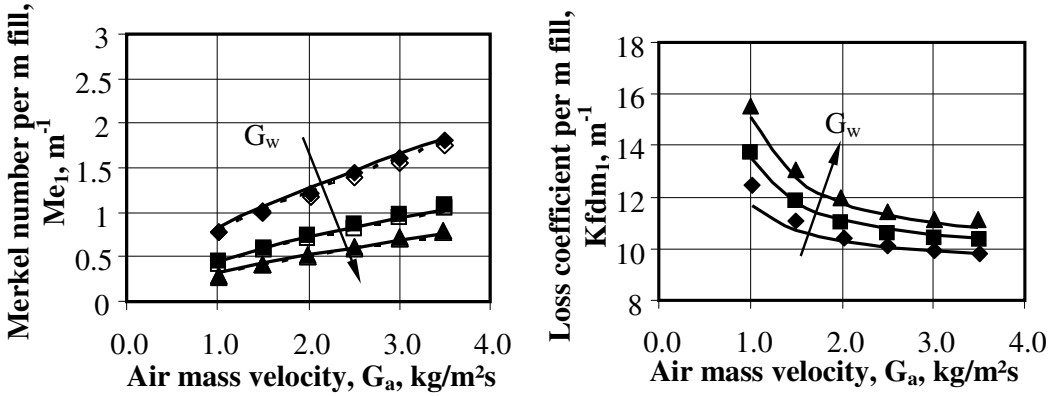

e) f)

Figure 7-2: Trickle results for 0.5, 1.0 and 1.5 m.

Three fill heights of trickle fill are tested with water inlet temperatures from 51.49 to 29.5 °C. A sample of the test data can be found in Table G-2. Two methods of measuring water inlet and outlet temperatures are used to calculate two independent Merkel numbers. The Merkel number making use of the curve-correction in Section 6.2.1 is given by Equation (7.4), whereas the measurement-corrected Merkel number is described by Equation (7.5). The coefficients of determination, r^2, are reported on alongside the equations.

$$Me_1 = 3.931 G_w^{-0.857} G_a^{0.644} T_{wi}^{-0.285} L_{fi}^{-0.294} \qquad r^2 = 0.995 \qquad (7.4)$$

$$Me_1 = 3.86 G_w^{-0.826} G_a^{0.639} T_{wi}^{-0.302} L_{fi}^{-0.239} \qquad r^2 = 0.994 \qquad (7.5)$$

In Figure 7-2 a), c) and e) the Merkel number determined using the curve-correction in Section 6.2.1 is plotted by the solid markers, and the corresponding curve (Equation (7.4)) is plotted with the solid line. The measurement-corrected Merkel number method is plotted by the open markers, and the corresponding curve (Equation (7.5)) is plotted with the dotted lines.

The migration through the trickle fill is slightly more than that of the film fill. Also, more water attaches to the wall over the fill height when compared to the film fill. This would imply that the two methods of determining the Merkel number should not agree as closely as for the film fill. This is seen Figure 7-2 a), c) and e).

The trickle fill tests with the highest and lowest Christiansen coefficients (as reported on in Appendx E) are examined. The standard deviation, σ, of the different water in- and outlet temperature measurements are calculated as an indication of temperature measurement accuracy. The highest Christiansen coefficient, 0.853, was for 1.5 m trickle fill with G_w = 2.797 kg/m^{2}s and G_a = 2.50 kg/m^{2}s. The standard deviations for the measurements made in this case are:

- $T_{wi(A)}$; σ = 0.05 °C
- $T_{wi(B)}$; σ = 0.23 °C
- $T_{wi(C)}$; σ = 1.73 °C
- $T_{wo(D/E)}$; σ = 0.9 °C
- $T_{wo(F)}$; σ = 0.11 °C

The trickle fill test with the lowest Christiansen coefficient, Cu = 0.806, was for 1.5 m fill with G_w = 1.49 kg/m^{2}s. The situation examined has a G_a = 2.50 kg/m^{2}s. The standard deviations for the measurements made in this case are:

- $T_{wi(A)}$; σ = 0.06 °C
- $T_{wi(B)}$; σ = 0.22 °C

- $T_{wi(C)}$; σ = 1.62 °C
- $T_{wo(D/E)}$; σ = 0.87 °C
- $T_{wo(F)}$; σ = 0.39 °C

These results suggest, once again, that the curve-corrected Merkel method will produce more accurate performance results than the temperature-corrected method for the trickle fill. However, the uncertainty of the curve-corrected outlet water temperature measurement, $T_{wo(F)}$, is greater than 0.1 °C and is unacceptable for accurate performance calculations. The Merkel number is most sensitive to the water outlet temperature. Both water outlet temperature measurement methods require refinement for accurate performance testing.

The loss coefficient reported on in Figure 7-2 b), d) and f) is the loss coefficient of the trickle fill only, as the contribution of the troughs has been subtracted as in Equation (6.7). The curve describing the loss coefficient of the fill is given in Equation (7.6).

$$K_{fdm_1} = \left(3.402 G_w^{\,0.067} G_a^{\,-0.022} + 1.324 G_w^{\,0.798} G_a^{\,-1.777}\right) L_{fi}^{\,0.055} \qquad r^2 = 0.978 \qquad (7.6)$$

A very small fill height effect is observed for both the Merkel number and loss coefficient. It is only the impractically small fill height L_{fi} = 0.5 m that causes this dependence.

7.3.3. Splash fill performance results

L_{fi} = 2.04 m

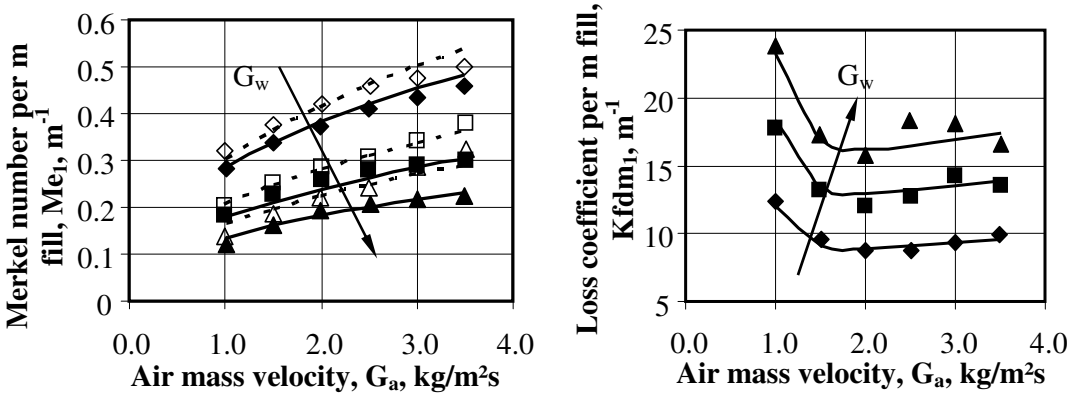

L_{fi} = 3.04 m

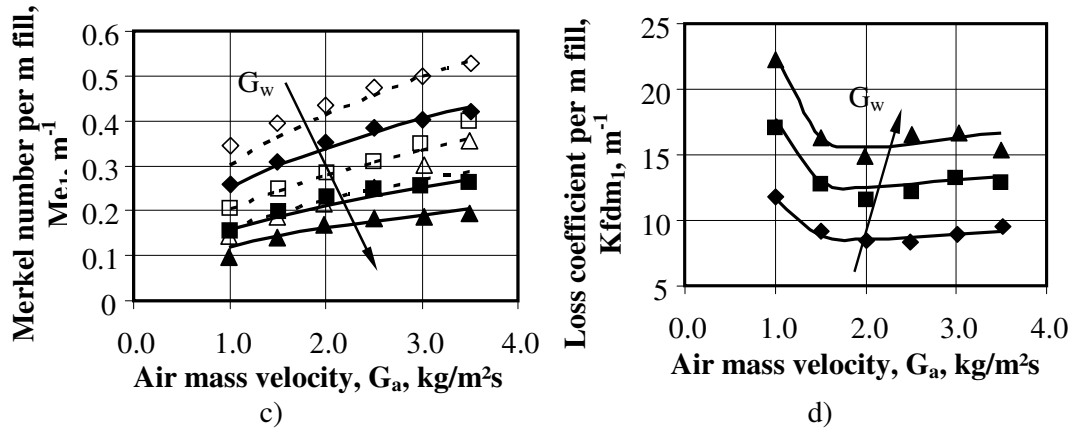

L_{fi} = 4.04 m

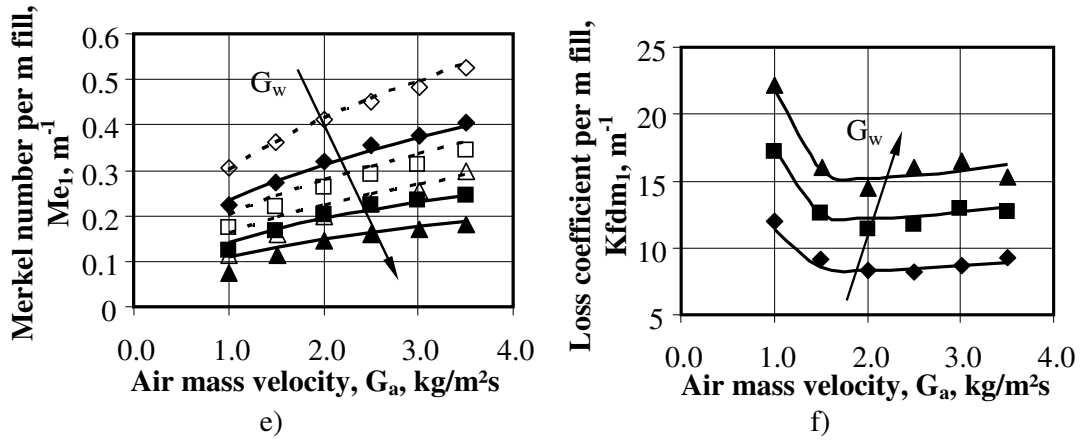

Figure 7-3: Splash fill Merkel number and loss coefficient results for 2.04, 3.04 and 4.04 m.

Three fill heights of splash fill are tested with water inlet temperatures from 48.33 to 31.03 °C. A sample of the test data can be found in Table G-3. Details of the splash fill can be found in Appendix H as it is a fill not typically used in counter-flow applications. Two methods of measuring water inlet and outlet temperatures are used to calculate two independent Merkel numbers. The Merkel number making use of the curve-correction in Section 6.2.1 is given by Equation (7.7), whereas the measurement-corrected Merkel number is described by Equation (7.8). The coefficients of determination, r^2, are reported on alongside the equations.

$$Me_1 = 0.513 G_w^{-0.683} G_a^{0.424} T_{wi}^{-0.026} L_{fi}^{-0.296} \qquad r^2 = 0.983 \qquad (7.7)$$

$$Me_1 = 0.621 G_w^{-0.568} G_a^{0.446} T_{wi}^{-0.126} L_{fi}^{-0.007} \qquad r^2 = 0.949 \qquad (7.8)$$

In Figure 7-3 a), c) and e) the Merkel number determined using the curve-correction in Section 6.2.1 is plotted by the solid markers, and the corresponding curve (Equation (7.7)) is plotted with the solid line. The measurement-corrected Merkel number method is plotted by the open markers, and the corresponding curve (Equation (7.8)) is plotted with the dotted lines.

The water distribution to the fill by the spray frame is good, but there is major migration of water through the fill and a large amount of water attaches to the wall over the fill height. The measurement-corrected method of measuring water outlet temperature is not suitable for determining the outlet water temperature, as each thermocouple below the fill experiences a different flow rate and measures a different temperature. If one knew the flow rates over each thermocouple, a weighted average could be applied. This is, however, unknown. The measurement-corrected method results in an optimistic Merkel number. The curve-corrected Merkel number measures the temperature of mixed water, representing a better average of the water leaving the fill; however, here the Merkel number includes effects of the water that has flowed down the walls of the test section. The flood of water running down the wall results in a pessimistic Merkel number for the curve-corrected method. The deviation between the two Merkel numbers increases with fill height. This is due to worsening distribution below the fill as the height of the fill increases, and the increase with wall water as the fill height increases. The actual Merkel number will lie between the Merkel numbers determined by the two methods.

The splash fill tests with the highest and lowest Christiansen coefficients (as reported on in Appendx E) are examined. The standard deviation, σ, of the different water in- and outlet temperature measurements are calculated as an indication of temperature measurement accuracy. The highest Christiansen coefficient, C_u = 0.708, was for 2.04 m splash fill with G_w = 2.99 kg/m^{2}s and

G_a = 2.50 kg/m^{2}s. The standard deviations for the measurements made in this case are:

- $T_{wi(A)}$; σ = 0.06 °C
- $T_{wi(B)}$; σ = 0.28 °C
- $T_{wi(C)}$; σ = 1.45 °C
- $T_{wo(D/E)}$; σ = 2.14 °C
- $T_{wo(F)}$; σ = 0.25 °C

The splash fill test with the lowest Christiansen coefficient, Cu = 0.560, was for 4.04 m fill with G_w = 1.508 kg/m^{2}s. The situation examined has a G_a = 2.50 kg/m^{2}s. The standard deviations for the measurements made in this case are:

- $T_{wi(A)}$; σ = 0.05 °C
- $T_{wi(B)}$; σ = 0.16 °C
- $T_{wi(C)}$; σ = 2.53 °C
- $T_{wo(D/E)}$; σ = 3.16 °C
- $T_{wo(F)}$; σ = 0.41 °C

These results suggest that the curve-corrected Merkel method will produce more accurate performance results than the temperature-corrected method for the splash fill. However, the uncertainty of the curve-corrected outlet water temperature measurement, $T_{wo(F)}$, is too high for accurate performance calculations. The Merkel number is most sensitive to the water outlet temperature and an uncertainty of 0.25 °C for $T_{wo(F)}$ is unacceptable. Furthermore, the uncertainties of measurements $T_{wi(C)}$ and $T_{wo(D/E)}$ are completely unacceptable. These large uncertainties explain the large performance differences of the two different measurement methods.

The loss coefficient reported on in Figure 7-3 b), d) and f) is the loss coefficient of the splash fill only, as the contribution of the troughs has been subtracted as in Equation (6.7). The curve describing the loss coefficient of the fill is given in Equation (7.9). A fill height effect slightly higher than for the film and trickle fills is observed.

$$K_{fdm_1} = \left(6.313 G_w^{\,0.547} G_a^{\,-0.205} + 4.017 G_w^{\,0.659} G_a^{\,-3.519}\right) L_{fi}^{\,-0.102} \qquad r^2 = 0.978 \qquad (7.9)$$

Examining Figure 7-3 b), d) and f), inflection points in the loss coefficient data points are visible. This is where the loss coefficient starts to increase with air mass velocity. In practice a fill would never operate beyond this point, as fan energy cost increases are not matched by an increase in thermal performance of the fill. The increasing loss coefficient is due to water drops becoming entrained in the air

stream, increasing the resistance of the air through the tunnel. Beyond a certain air mass velocity these droplets are blown out the top of the tower, and once again the loss coefficient begins to drop. This is still a negative phenomenon, because it means water is being wasted by being blown out the top of the cooling tower in the form of drift. The exponential equation used to describe the fill loss coefficient cannot accurately describe the performance of the fill, and the format of the equation is not suitable when testing fill with two inflection points.

7.4. Conclusion

Three fill types were tested. The Merkel number for each of the three fills was determined using two independent sets of water inlet and outlet temperature measurement. The two methods produce very similar results for fills with little migration distribution effects, and where there is little water attached to the wall over the fill height. This is the case for the film and trickle fills. Although the results are close, the uncertainties in the water outlet temperatures are too large for reliable performance results. The uncertainties of the water outlet temperatures are routinely greater than 0.1 °C for $T_{wo(F)}$ and can be over 3 °C for $T_{wo(D/E)}$. The water outlet temperatures measurements need to be refined.

The source of the large standard deviations of $T_{wi(C)}$, $T_{wo(D/E)}$ and $T_{wo(F)}$ can all be attributed to the water profile that occurs below the fills. Even a slight profile impacts heavily on $T_{wi(C)}$ and $T_{wo(D/E)}$. This is due to the different flow rates experienced by each temperature measurement location. If the flow rate over every thermocouple were known during testing, a mass weighted average could be applied. All fills produce a water distribution profile as the water flows through the fill. This means that the method of measuring temperatures in individual water catchment containers is unusable if the water mass flow rate in each container is unknown. The deviations that are measured in measurement $T_{wo(F)}$ are a result of the water being drained from the trough at two different locations. This is shown in Figure 4-14. The separate locations have deviations below 0.1 °C but the temperature difference between the two outlet pipes can be up to 0.5 °C. To eliminate this difference all the water leaving the test facility should be mixed well before any temperature measurement is made. The assumption of uniform flow from the left and right-hand sides of the tunnel made in Section 4.3.5 is proved to be incorrect for circumstances of severe water migration through the fill.

The loss coefficients determined are described well by the equations in the forms in which they appear in Equations (7.3), (7.6) and (7.9), except when there are double inflection points in the loss coefficient, as there are for the splash fill. The loss coefficients are not sensitive to the water outlet temperature and are thus deemed reliable. The loss coefficient is sensitive to pressure drop over the fill. At no stage during testing did these measurements deviate more than 1 % from the average pressure drop measured over the fill.

It must be noted that curve-fits are obtained using the sum of least squares method. This method does not constrain whether the generated equations over- or under predicts the data point. It is possible for the performance predicted by the equation to be greater than the actual performance of the fill as determined during fill performance testing. Caution must be practiced when using the generated equations in design applications. A conservative approach must be followed to ensure that the equation does not predict performance greater than the actual fill performance.

8. CONCLUSION AND RECOMMENDATIONS

8.1. Conclusions

In Chapter 2 the need for standardisation in fill performance testing was identified. It used the size of the test facility as an example to illustrate the difference in results obtained from test facilities of different sizes. The section identified aspects of the tests that are to be controlled, ensuring useable, comparable results. These included standardising the parameters calculated to represent thermal and flow performance of fills, the test facility in which data is obtained in order to calculate these parameters, and the format in which performance data are presented.

In Chapter 3 the various calculated parameters used in literature to determine fill performance were examined. The Merkel number was chosen as the measure to represent the thermal performance of the fill, while the loss coefficient was chosen as the parameter used to represent the flow performance of fills. These parameters were chosen as they are dimensionless, resulting in direct comparison of fill performance. The Merkel number and loss coefficient are widely used in literature, implying that the theory is well understood.

In Chapter 4 the 1.5 x 1.5 m² counter-flow test facility at Stellenbosch University was described. The general layout of the test facility was described, and the apparatus and methods applied to measure specific measurements as accurately as possible were discussed in detail.

Chapter 5 evaluated the test facility and compared the operation thereof to the assumptions made in the Merkel number theory as identified in Appendix B.1. The chapter examined the water distribution delivered by the specifically designed spray frame. It was decided that the spray frame delivers a usable distribution. According to Kranc (1993) it was determined that the worst distribution delivered by the spray frame will result in performance within 99 % of the maximum performance of the fill. The migration of water through the fill was examined for various fills, fill heights and water mass velocities by comparing the distribution delivered by the spray frame with the measured distribution below the fill. The cross-fluted and trickle fills had distributions that did not change dramatically over the fill heights, where as the splash fill had large-scale migration with the distribution below the fill deviating, up to 90 % from the average. In the case of the splash fill the assumptions made in the Merkel theory of uniform water distribution and uniform performance of the fill over a cross-section are not matched, contributing to possible inaccuracies in measured splash fill performance.

The amount of water that attached to the walls over the fill height was examined. The film and trickle fills had minimal water attached to the walls whereas the splash fill had, at times, 31% of the water attached to the walls. This large flow rate down the walls affects the outlet water temperature and reduces the actual water flow within the fill. The assumption of uniform fill performance over the fill cross-section is not matched when testing splash fill. This further contributes to inaccuracies in measured splash fill performance.

The air velocity profile was measured to examine whether or not the Merkel assumption of uniform air inlet conditions was matched. The air profile matched Limber's (2007) goal of obtaining less that 10 % deviation from the average over 90 % of the area. The measured air velocity profile is suitable for testing fills, as the influences of the air momentum coefficients in the calculation of the loss coefficients are minimal.

The contributions that the test facility has on measured fill performance were examined in Chapter 6. The contributions that the spray frame, spray zone, troughs and pipe work have on the Merkel number were quantified, ensuring that the performance of fill alone can be identified by ignoring the added performance of these zones. The contribution of the troughs on the loss coefficient was similarly identified so that the reported fill performance does not include the added contribution of the troughs.

Performance tests were conducted on film, trickle and splash fills and are reported on in Chapter 7. The fill Merkel number and loss coefficient dependencies on air and water mass velocities, inlet water temperature and fill height were determined by running tests where these parameters were varied. At least three heights of each fill were tested with three water mass velocities and six air mass velocities. The inlet water temperature decreased over the duration of a test because the water cycled between the underground storage tank and the test facility slowly cooled. The inlet water temperature started at no less than 48 °C and typically cooled by 25 °C over the duration of a test.

When testing fill two methods of measuring the water inlet and outlet temperatures were used and two independent fill Merkel numbers were determined. For the film and trickle fills the Merkel numbers determined according to the two methods agreed strongly. This implies that the test facility in its existing state is suitable for determining the performance of fills that have minimal migration of water through the fill and where minimal water attaches to the walls over the fill height. For the splash fill the two Merkel numbers do not agree. The splash fill has severe migration of water through the fill and a large

amount of water attaches to the wall over the fill height. This results in non-uniform performance over the fill cross-section, a changing water mass velocity through the fill over the fill height, and unreliable outlet water temperature measurements. The uncertainties in the water outlet temperatures used in the measurement-corrected Merkel method are too high. These all contribute to the uncertainty in the splash fill performance obtained in this 1.5 x 1.5 m² test facility.

This study has highlighted the importance of uniform water distribution, the migration effects of water through the fill, the degree to which water attaches to the wall over fill heights, the potential of air bypassing the fill along the walls, and the impact these have on the measured performance of the fill. In conclusion, the present 1.5 x 1.5 m² test facility at Stellenbosch University is able to generate meaningful results for fill Merkel numbers and loss coefficients only for fills that have minimal migration effects and minimal water flowing down the walls, as was the case with the cross-fluted and trickle fills tested in this study.

8.2. Recommendations for improving Stellenbosch test facility

The accuracy of the water inlet and outlet temperature is important, as the Merkel number is highly sensitive to these measurements. Measuring the water outlet temperature directly below the fill is problematic when fills with large migration effects are tested. The water distribution profile through the fill during testing is unknown, and therefore the weighted average of the measurements cannot be accurately calculated. It is recommended that the water inlet and outlet temperatures are measured in the pipe work leading to and from the test facility. This measurement is also reliable only when there is minimal water flowing down the walls of the test facility. When testing fill that does move water to the walls the installation of gutters will remove water from the wall before it is collected in the troughs, and the wall water will not influence the water outlet temperature measurement. It is also suggested that the water caught in the extraction troughs be mixed together in order to measure the outlet water temperature. This will result in it being unnecessary to know the ratio of water in the separate drain-pipes. When the water inlet and outlet temperatures are measured in the pipe work leading to and from the test section, it is essential that the impact of all the zones where heat transfer occurs, other than the fill, be identified and their impact on the measured Merkel number accurately known. The impact these zones have on the Merkel number, and the impact that the troughs have on the loss coefficient, must be used to correct the Merkel number and loss coefficient, as done in this study.

The changes to the test facility suggested previously in this chapter are summarised below and Figure 8-1 shows the basic layout of the suggested, improved facility. The three main necessary changes to be made are:

1) Installation of gutters to remove water from the walls before water is caught by the water extraction troughs, as the wall water

influences the water outlet temperature measured in the pipe work. This will also allow the water mass flow rate of the water attached to the wall below the fill to be known, allowing the average water mass velocity through the fill to be calculated.

2) All water leaving the fill and collected in troughs should be well mixed before the water outlet temperature is measured, removing the need to know the split of water in the separate drain-pipes in order to calculate a mass weighted average for the water outlet temperature.

3) Further improve the distribution of the spray frame by changing hole diameters or hole pitch to increase flow along the edges of the spray frame and to decrease flow in the middle of the spray frame below the supply manifold.

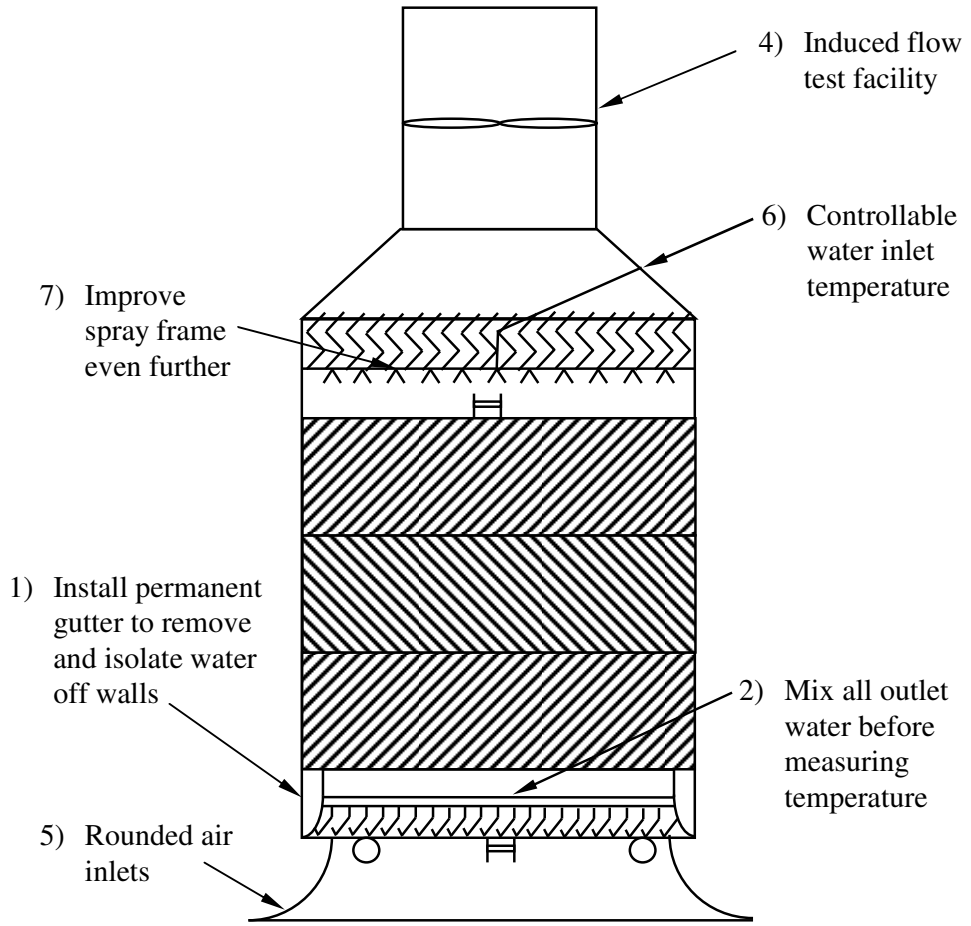

Figure 8-1: Improved test facility based on observations during this study.

Other changes that will further improve the accuracy of the results, but will not have as much of an impact as the aspects mentioned previously, are:

4) Convert the facility to an induced flow-type cooling tower. This will result in an improved air flow distribution, as the facility will not be located downstream of the centrifugal fan outlet, and the three 90° bends joining the horizontal and vertical sections of the facility will no longer be necessary.

5) Rounded inlets installed at the test section inlet would result in a uniform air inlet profile, provided the inlet is sufficiently high enough above the ground. The structure supporting the facility must be designed to have minimal blockage effects.

6) Controllable water inlet temperature would allow steady operating conditions to be achieved. With the setup as it is now, the inlet water temperature is constantly decreasing, so steady operating conditions over a long period of time are impossible to obtain. Controllable inlet water temperatures can be achieved by installing an inline boiler to heat the water so that the temperature of the water does not drop as it is cycled through the test facility, and by mixing the hot water from the underground tank with cooled outlet water from the facility to achieve a set point inlet water temperature. Some test facilities (Brentwood (2003), Libert (2003)) have controllable air inlet conditions, but that is not practical with this test facility. It is further suggested that any future facility to be built be located near a source of waste heat, such as at a power plant, where money will not be wasted on heating water for testing but can be directed from out of the turbine houses and used for the fill tests, as is the case with the Mistral test facility in France (Fabre and Legrand (1988) and Legrand).

8.3. Recommendations for standardised fill performance test facility

This study has examined many sources of erroneous measurements in fill testing. Based on these findings recommendations for the standardised test facility to minimise the uncertainty of measurements and ensure accurate performance testing are listed below. This study is unable to specify the exact design and layout a test facility for accurate fill performance, but based on observations made in this study suggested are made to form a base from which further development can continue.

- This study is unable to make a specific recommendation regarding the necessary size of the test facility. This study is able to conclude that splash fills were unable to be successfully tested in the Stellenbosch test facility. A test cell size greater that 1.5 x 1.5 m^2 is thus suggested. The test facility must be large enough so that the maximum flow rate of water attaching to

the wall is a negligible percentage of the water flowing through the test facility.

- Similar to Figure 8-1, the facility must be an induced-type cooling tower thereby eliminating the negative turbulence effects of a fan or turning vanes upstream of the fill.
- Similar to Figure 8-1, the test facility must have rounded inlets to ensure uniform airflow into the fill. The rounded inlets must be sufficiently high above the ground to eliminate any effects the ground may have on flow uniformity. Libert (2002) achieves airflow within 10 % over 90 % the test cell area.
- The inlet water temperature must be controllable. This will ensure a steady inlet water temperature when testing. Set point temperatures are achieved by mixing the inlet and outlet water streams as is done in Aull (2008) and Johnston (1989).
- The inlet water flow rate must be adjustable. The water flow rate must be measured in the water supply pipe. Redundancy measurements are necessary to ensure measurement accuracy.
- Water distribution to the fill must be uniform. It is suggested that a purpose built spray frame be used instead of spray nozzles. This allows the water flow rate to be adjusted while having minimal impact on the water distribution uniformity.
- Spray from the distribution system must not spray directly down but rather at an acute angle. This will prevent water from free-falling through open fills without coming into contact with the fill.
- The water inlet temperature must be made in the main pipe supplying water to the test facility. This measurement must be made as close to the spray frame as possible to minimise heat transfer between the measurement location and the spray frame.
- The spray zone between the spray frame and the fill inlet must be kept to a minimum.
- The walls of the test facility must be insulated so that no conductive heat transfer occurs through the walls.
- The walls of the test facility must be padded inside with sponge material to prevent any short-circuiting of air between the fill and the walls when testing dense fills.
- Water that attaches to the walls of the test facility over the height of the fill must be collected and must not be included in the outlet water temperature measurement. The flow rate of the water running down the walls must be measured.

- Water flowing through the fill must be caught in troughs directly below the fill. There must be no rain zone below the fill.
- The total surface area of the troughs must be minimised to minimise the potential for cooling of water as is flows into, and through the troughs.
- The troughs supporting fill during tests must be level so that subsequent layers of fill are level.
- Water must be drained quickly from the trough. The pipes draining the troughs must be insulated to reduce any loss of temperature as the water flows in the pipe-work.
- The water exiting the troughs must be thoroughly mixed as soon as it leaves the troughs. The temperature of the mixed water must be used as outlet water temperature.
- All measurements must be made using at least four thermocouples.
- The level of thermocouple accuracy suitable for the specific measurement made. For the outlet water temperature T-type thermocouples with an accuracy of ±1 °C are not suitable.
- Similarly to Figure 8-1, air inlet temperatures must be made directly below the water extraction troughs.
- Standards for dry- and wet-bulb temperature measurements must be adhered to. The air velocity over the wet-bulb socks must be at least 4 m/s.
- The air flow rate through the tunnel must be controllable.
- The air flow rate must be measured by a method recognised by laboratory standards for air flow measurement. Redundancy is necessary to ensure accurate measurement.
- The pressure drop measurement must be of a similar kind as used in this study. This method of pressure measurement is not affected by water flowing down the wall as is the case with pressure measurement points connected through the wall.
- Piping between the pressure measurement probes and the transducers must be located inside the test facility to remove and pressure differences measured as a result of buoyancy effects.
- Pressure measurement piping must be clear to ensure that no condensation occurs in the piping which could accumulate and block the pipe.

These are all the suggestions that are to be applied, if not considered, in the development of a standard test facility for counter-flow cooling tower fill.

9. REFERENCES

Aull, R.J. And Krell, T., Design Features of Cross-Fluted Film Fill and Their Effect on Thermal Performance, CTI Journal, Vol. 21, No. 2, pp. 12-33, 2000.

Aull, R.J., Private Correspondence, 20 August 2008.

ASME, Atmospheric Water Cooling Equipment, Performance Test Codes, ASME PTC 23-2003, New York, 2003.

ANSI/ASHRAE 41.1 – 1986, Standard Method for Temperature Measurement.

ANSI/ASHRAE Standard 41.2 – 1987 (RA 1992), Standard Methods for Laboratory Airflow Measurement.

ANSI/ASHRAE 41.3 – 1989, Standard Method for Pressure measurement.

ANSI/ASHRAE Standard 51 – 1975, Laboratory Methods of Testing Fans for Rating

ANSI/ASHRAE Standard 84 – 1991, Method of Testing Air-to-Air Heat Exchangers.

Bedekar, S.V., Nithiarasu, P. and Seetharamu, K.N., Experimental Investigation of the Performance of a Counter-Flow, Packed-Bed, Mechanical Cooling Tower, Energy, Vol. 23, No. 11, pp. 943-947, 1998.

Bourillot, C., TEFERI, Numerical Model for Calculating the Performance of an Evaporative Cooling Tower, EPRI Report CS-3212-SR, August 1983.

British Standard, Methods of Measurement of Fluid Flow in Closed Conduits, BS 1042: Section 1.1, 1981.

Brentwood Industries, Application Note: Turbosplash PAC - High Performance Splash Fill: Notes of Performance Data, 1990.

Brentwood Industries, Cooling tower products, Application Manual, 2003.

Burger, R., Select the Right Cooling Tower Fill, Hydrocarbon Processing, Vol. 73, No. 8, pp. 141 – 143, August 1994.

Cooper, J.W., Cooling Tower Designs for Tomorrow's Nuclear Power Plant, EPRI Cooling Tower Technology Seminar and Conference, Iowa, USA, 6 August, 2006.

Çengel, Y.A. and Boles, M.A., *Thermodynamics; an engineering approach, fourth edition in SI units*, McGraw-Hill, New York, 2002.

Fabre, L. and Legrand, G., Mistral New Test Bench for Cooling Tower Components (Nuclear Generation Centre of Bugey, France), 6th IAHR Cooling Tower Workshop, Pisa, Italy, 4-7 October, 1988.

Fulkerson, R.D., Comparative Evaluation of Counter-flow Cooling Tower Fills, Journal of the Cooling Tower Institute, Vol. 9, No. 2, pp. 26-32, 1989.

Gharagheizi, F., Hayati, R. and Fatemi, S., Experimental Study on the Performance of Mechanical Cooling Tower with Two Types of Film Packing, Energy Conservation and Management, Vol. 48, pp. 277-280, 2007.

Goshayshi, H.R. and Missenden, J.F., The Investigation of Cooling Tower Packing in Various Arrangements, Applied Thermal Engineering, Vol. 20, pp. 69-80, 2000.

Gősi, P., Halász, J. and Kostka, P., Comparative Evaluation of Different Packings, 8th Cooling Tower and Spraying Pond Symposium, Karlsruhe, Germany, 5-9 October, 1992.

Gősi, P., Studying Decreasing Wall-Effect in Wet Cooling Towers, IAHR 11th Cooling Tower Symposium, Cottbus, Germany, 21-23 September, 1998.

Gősi, P., Kostka, P. and Tomcsányi, G., Effect of Water Distribution Pattern of Nozzles on the Performance of Wet Packings, IAHR 7th Cooling Tower and Spraying Pond Symposium, Leningrad, USSR, 29 May – 2 June, 1990.

Hallett, G.F., Performance Curves for Mechanical Draft Cooling Towers, Journal of Engineering for Power, Vol. 97, No. 4, pp. 503-508, 1975.

http://www.brentwood-ind.com/cool/brentwood/brentwood.aspx, Application Note: Notes on Performance Curves and Data, 17 September 2009.

Ibrahim, G.A., Nabhan, M.B.W. and Anabtawi, M.Z., An Investigation into Falling Film Type Cooling Tower, International Journal of Refrigeration, Vol. 18, No. 8, pp. 557-564, 1995.

Jaber, H. and Webb, R.L, Design of Cooling Towers by the Effectiveness-NTU Method, Journal of Heat Transfer, Vol. 111, pp. 837-843, November 1989.

Johnson, B.M. (Ed.), Cooling Tower Performance Prediction and Improvement, Volume 1, Applications Guide, EPRI Report GS – 6370, Volume 2, Knowledge Base, EPRI Report GS-6370, EPRI, Palo Alto, 1989.

Johnson, B.M. and Bartz, J.A., Comparative Performance Characteristics of Selected Cross-flow and Counter-flow Cooling Tower Fills in an Engineering-Scale Test Facility, IAHR 7th Cooling Tower and Spraying Pond Symposium, 29 May – 2 June. 1990.

Kloppers, J.C. and Kröger D.G., Loss Coefficient Correlation for Wet-Cooling Tower Fills, Applied Thermal Engineering, Vol. 23, 2003.

Kloppers, J.C. And Kröger D.G., A Critical Investigation into the Heat and Mass Transfer Analysis of Wet-Cooling Towers, International Journal of Heat and Mass Transfer, Vol. 48, pp. 765-777, 2005a.

Kloppers, J.C. and Kröger D.G., Cooling Tower Performance Evaluation: Merkel, Poppe and E-NTU Methods of Analysis, Journal of Engineering for Gas Turbines and Power, Vol. 127, Pp. 1-7, 2005b.

Kloppers, J.C. and Kröger D.G., Refinement of the Transfer Characteristic correlation of Wet Cooling Tower Fills, Heat Transfer Engineering, Vol. 26, Issue 4, pp. 35-41, 2005c.

Kranc, S.C.M, Performance of Counter-flow Cooling Towers With Structured Packings and Maldistributed Water Flow, Numerical Heat Transfer, Part A, Vol. 23, pp. 115-127, 1993.

Kranc, S.C., The Effect of Nonuniform Water Distribution on Cooling Tower Performance, Journal Of Energy, Vol. 7, No. 6, pp. 636-639, 1983.

Kröger, D.G., *Air-Cooled Heat Exchangers and Cooling Towers*, *Thermal-Flow Performance Evaluation and Design*, Pennwell Corp., Tulsa, Oklahoma, 2004.

Lefevre, M.R., Eliminating the Merkel Theory Approximations – Can it Replace the Empirical Temperature Correction Factor? Paper TP-84-18, CTI Annual Meeting, 1984.

Legrand, G., Studies of Cooling Tower Components on the Mistral Test Bench, Service Réacteurs Nucléaires et Echangeurs, Département Transferts Thermiques et Aérodynamique, Groupe Thermohydraulique des Systèmes, 1992.

Lemouari, M., Boumaza, M. and Mujtaba, I.M., Thermal Performances Investigation of a Wet Cooling Tower, Applied Thermal Engineering, Vol. 27, pp. 902-909, 2007.

Libert, J.P., Design and Operation of a Counter-flow Fill and Nozzle Test Cell: Challenges and Solutions, CTI Annual Conference, Corpus Christi, Texas, 4-7 February, 2007.

Lowe, H.J., Christie, D.G., Heat Transfer and Pressure Drop Data on Cooling Tower Packings and Model Studies of the Resistance of Natural Draft Towers to Airflow, Proceedings of the International Heat Transfer Conference, Boulder, Colorado, U.S.A., 1961.

Merkel, F., Verdunstungskühlung. VDI-Zeitschrift, Vol. 70, No. 70, pp. 123-128, 1925.

Milosavljevic, N. And Keikkilä, P., A Comprehensive Approach to Cooling Tower Design, Applied Thermal Engineering, Vol. 21, pp. 899-915, 2001.

Mirsky, G.R., Film Fill Recent Research and Application Data, CTI Journal, Vol. 12, No.1, pp. 31-45, 1991.

Mohiuddin, A.K.M. and Kant, K., Knowledge base for the systematic design of wet cooling towers. Part II: Fill and other design parameters, International Journal of Refrigeration, Vol. 19, No. 1, pp. 52-60, 1996.

Poppe, M., Wärme und Stoffübertragung bei der Verdunstungskühlung in Gegen- und Kreuzstrom, Doctoral thesis, Technische Universität, Hannover, 1992.

Savery, C.W. and Hammill, M.P., Evaporative Cooling Tower Performance Predictions, ASME Winter Annual Meeting, New York, 26–30 November, 1972.

Poppe, M. and Rogner, H., Berechnung von Rückkühlwerkern, VDI-Wärmeatlas, pp. Mi1-Mi15, VDI-Verlag, Düsseldorf, 1991.

Van Der Merwe, D., Evaluation of Natural Draught Wet-Cooling Tower Performance Uncertainties, Master's Thesis, University of Stellenbosch, 2006.

APPENDIX A. THERMOPHYSICAL PROPERTIES OF FLUIDS

A.1. Introduction

These equations are used to determine the fluid properties needed to complete the calculation of the Merkel number and loss coefficient. They are sourced from Kröger (2004).

A.2. Thermophysical properties of dry air

The following properties for dry air are valid from 220 K to 380 K at standard atmospheric pressure (101325 N/m^2)
Density:

$$\rho_a = (278.08\ T),\ kg/m^3 \tag{A.1.1}$$

Specific heat:

$$c_{pa} = 1.045356 \times 10^3 - 3.161783 \times 10^{-1}\ T + 7.083814 \times 10^{-4}\ T^2 - 2.705209 \times 10^{-7}\ T^3,\ J/kgK \tag{A.1.2}$$

A.3. Thermophysical properties of saturated water vapour

The following properties for saturated water vapour are valid from 273.15 K to 380 K.
Vapour pressure:

$$p_v = 10^z,\ N/m^2$$

$$z = 10.79568(1 - 237.16/T) + 5.20808\log_{10}(273.16/T) + 1.50474 \times 10^{-4}\ [1 - 10^{-8.29692\{(T/273.16) - 1\}}] + 4.2873 \times 10^{-4}[10^{4.76955(1 - 273.16/T)} - 1] + 2.786118312 \tag{A.2.1}$$

Specific heat:

$$c_{pv} = 1.3605 \times 10^3 + 2.31334T - 2.46784 \times 10^{-10}T^5 + 5.91332 \times 10^{-13}T^6,\ J/kgK \tag{A.2.2}$$

A.4. Thermophysical properties of air and water vapour mixtures

Density:

$$\rho_{av} = (1 + w)\ [1 - w/(w + 0.62198)]p_{abs}/(287.08T),\ kg/m^3 \tag{A.3.1}$$

Specific heat:

$$c_{pav} = (c_{pa} + wc_{pv})/(1 + w),\ J/K\ kg\ air\text{-}vapour \tag{A.3.2a}$$

or the specific heat of the air-vapour mixture per unit mass of dry air:

$c_{pma} = (c_{pa} + wc_{pv})$, J/K kg dry air (A.3.2b)

Humidity ratio:

$$w = \left(\frac{2501.6 - 2.3263 \cdot (T_{wb} - 273.15)}{2501.6 + 1.8577(T - 273.15) - 4.184(T_{wb} - 273.15)} \right) \left(\frac{0.62509\, p_{vwb}}{p_{abs} - 1.005\, p_{vwb}} \right) - \left(\frac{1.00416(T - T_{wb})}{2501.6 + 1.8577(T - 273.15) - 4.184(T_{wb} - 273.15)} \right) \quad \text{(A.3.3)}$$

Enthalpy:

$i_{av} = [c_{pa}(T - 273.15) + w\{i_{fgwo} + c_{pv}(T - 273.15)\}]/(1 + w)$, J/kg air-vapour (A.3.4a)

or the enthalpy of the air-vapour mixture per unit mass of dry air:

$i_{ma} = c_{pa}(T - 273.15) + w[i_{fgwo} + c_{pv}(T - 273.15)]$, J/kg air-vapour (A.3.4b)

where the specific heats are evaluated at (T + 273.15)/2 and the latent heat i_{fgwo} is evaluated at 273.15K according to Equation (A.4.3).

A.5. Thermophysical properties of saturated water liquid

The following properties of saturated water liquid are valid for 273.15 K to 380 K

Density:

$$\rho_w = (1.49343\times10^{-3} - 3.7164\times10^{-6}T + 7.09782\times10^{-9}T^2 - 1.90321\times 10^{-20}T^6)^{-1}, \text{ kg/m}^3 \quad \text{(A.4.1)}$$

Specific heat:

$$c_{pw} = 8.15599\times10^{3} - 2.80627\times10T + 5.11283\times10^{-2}T^2 - 2.17582\times10^{-13}T^6, \text{ J/kgK} \quad \text{(A.4.2)}$$

Latent heat of vaporization:

$$i_{fgw} = 3.4831814\times10^{6} - 5.8627703\times10^{3}T + 12.139568T^2 - 1.40290431\times10^{-2}T^3, \text{ J/K} \quad \text{(A.4.3)}$$

APPENDIX B. DERIVATION OF PERFORMANCE MEASURES

B.1. Derivation of Merkel method, Kröger (2004)

Consider a control volume at the surface of a typical fill in a wet-cooling counter-flow tower as in Figure B-1.

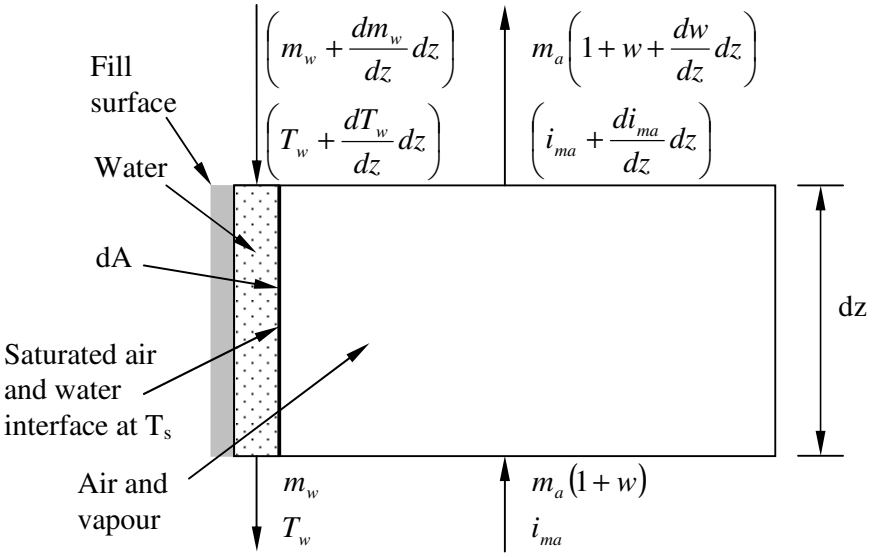

Figure B-1: Control volume on surface of wet-cooling counter-flow fill.

Three initial assumptions are made: the interface water temperature T_s is the same as the bulk water temperature T_w; air and water properties are constant over a horizontal cross-section; and the area, dA, available for heat and mass transfer is identical.

The control volume mass balance is,

$$m_a(1+w)+\left(m_w+\frac{dm_w}{dz}dz\right)=m_a\left[1+\left(w+\frac{dw}{dz}dz\right)\right]+m_w$$

or

$$\frac{dm_w}{dz}=m_a\frac{dw}{dz} \tag{B.1.1}$$

where m_a is the air mass flow rate.

The control volume energy balance is

$$m_a i_{ma}+\left(m_w+\frac{dm_w}{dz}dz\right)c_{pw}\left(T_w+\frac{dT_W}{dz}dz\right)=m_a\left(i_{ma}+\frac{di_{ma}}{dz}dz\right)+m_w c_{pw}T_w \tag{B.1.2}$$

with T_w in °C.

Neglecting the second order terms results in

$$m_w c_{pw} \frac{dT_w}{dz} + c_{pw} T_w \frac{dm_w}{dz} = m_a \frac{di_{ma}}{dz} \tag{B.1.3}$$

i_{ma} is the enthalpy of the air-water vapour mixture per unit mass of dry air given in Equation (A.3.4b) as

$$i_{ma} = c_{pa} T_a + w\left(i_{fgwo} + c_{pv} T_a\right) \tag{B.1.4}$$

where i_{fgwo} is evaluated at 0°C and c_{pa} and c_{pv} at T_a/2°C.

Substituting Equation (B.1.1) into (B.1.3) to find

$$\frac{dT_w}{dz} = \frac{m_a}{m_w}\left(\frac{1}{c_{pw}}\frac{di_{ma}}{dz} - T_w \frac{dw}{dz}\right) \tag{B.1.5}$$

The total enthalpy transfer at the air-water interface consists of an enthalpy transfer associated with the mass transfer due to the difference in vapour concentration and the heat transfer due to the difference in temperature.

$$dQ = dQ_m + dQ_c \tag{B.1.6}$$

where the subscripts m and c refer to the enthalpies associated with the mass transfer and convective heat transfer respectively. The mass transfer at the interface is expressed by

$$\frac{dm_w}{dz} dz = h_d \left(w_{sw} - w\right) dA \tag{B.1.7}$$

where w_{sw} is the saturation humidity ratio of air evaluated at the local bulk water temperature T_w.

The corresponding enthalpy transfer is

$$dQ_m = i_v \frac{dm_w}{dz} dz = i_v h_d \left(w_{sw} - w\right) dA \tag{B.1.8}$$

The enthalpy of the water vapour, i_v, at the bulk water temperature T_w is given by

$$i_v = i_{fgwo} + c_{pv} T_w$$

where T_w is in °C and c_{pv} is evaluated at T_w/2°C.

The convective transfer of the sensible heat at the interface is given by

$$dQ_c = h\left(T_w - T_a\right) dA \tag{B.1.9}$$

The enthalpy of the saturated air evaluated at the local bulk water temperature is given by

$$i_{masw} = c_{pa}T_w + w_{sw}\left(i_{fgwo} + c_{pv}T_w\right) = c_{pa}T_w + w_{sw}i_v$$

which may be re-written as

$$i_{masw} = c_{pa}T_w + wi_v + \left(w_{sw} - w\right)i_v \tag{B.1.10}$$

where c_{pa} is evaluate at $T_w/2°C$.

Subtract Equation (B.1.4) from Equation (B.1.10). The resultant equation can be simplified if the smaller differences in the specific heats, which are evaluated at the different temperatures, are ignored, that is

$$i_{masw} - i_{ma} \approx \left(c_{pa} + wc_{pv}\right)\left(T_w - T_a\right) + \left(w_{sw} - w\right)i_v$$

or

$$T_w - T_a = \left[\left(i_{masw} - i_{ma}\right) - \left(w_{sw} - w\right)i_v\right] / c_{pma} \tag{B.1.11}$$

where $c_{pma} = c_{pa} + wc_{pv}$.

Substitute Equations (B.1.8), (B.1.9) and (B.1.11) into Equation (B.1.6) and rearrange, resulting in

$$dQ = h_d\left[\frac{h}{c_{pma}h_d}\left(i_{masw} - i_{ma}\right) + \left(1 - \frac{h}{c_{pma}h_d}\right)i_v\left(w_{sw} - w\right)\right]dA \tag{B.1.12}$$

where $h/\left(c_{pma}h_d\right)$ = Le_f, which is known as the Lewis factor, and is an indication of the relative rates of the heat and mass transfer in an evaporative process.

Noting that the enthalpy transfer must be equal to the enthalpy change of the air stream, one has from Equation (B.1.12)

$$\frac{di_{ma}}{dz} = \frac{1}{m_a}\frac{dQ}{dz} = \frac{h_d}{m_a}\frac{dA}{dz}\left[Le_f\left(i_{masw} - i_{ma}\right) + \left(1 - Le_f\right)i_v\left(w_{sw} - w\right)\right] \tag{B.1.13}$$

For a one-dimensional model of the cooling tower fill, where the available area for heat and mass transfer is the same at any horizontal section through the fill, the transfer area for a section dz deep is usually expressed as

$$dA = a_{fi}A_{fr}dz \tag{B.1.14}$$

where a_{fi} is the wetted area divided by the corresponding volume of the fill (area density) and A_{fr} is the corresponding frontal area or face area.

Substitute Equations (B.1.14) into Equation (B.1.13) and find

$$\frac{di_{ma}}{dz} = \frac{h_d a_{fi} A_{fr}}{m_a}\left[Le_f\left(i_{masw} - i_{ma}\right) + \left(1 - Le_f\right)i_v\left(w_{sw} - w\right)\right] \tag{B.1.15}$$

When the air with a high humidity enters the fill the air becomes saturated with water vapour prior to exiting the fill. In this case the abovementioned equations fail to describe the evaporative process in the fill. Since the temperature of the saturated air at the interface is still higher than the temperature of the now-saturated free stream air, a potential for heat and mass transfer will still exist. The excess water vapour transferred to the free stream air will condense as a mist.

Assume that the heat and mass transfer coefficients for the mist zone will be the same as those for the unsaturated air (Bourillot (1983), Poppe and Rögener (1991)). The evaporation rate in the mist zone will depend on the difference in moisture content of the saturated air at the interface, which is at the local bulk water temperature, and the moisture content of the free stream air, thus

$$\frac{dm_w}{dz} = h_d a_{fi} A_{fr}\left[w_{sw} - w_{sa}\right] \tag{B.1.16}$$

where w_{sa} is the humidity ratio of saturated air at temperature T_a.

Since the excess water vapour will condense, the enthalpy of the supersaturated air is expressed by

$$i_{ss} = c_{pa}T_a + w_{sa}\left(i_{fgwo} + c_{pv}T_a\right) + \left(w - w_{sa}\right)c_{pw}T_a \tag{B.1.17}$$

Proceeding along the same lines as in the case of unsaturated air, find

$$\frac{di_{ma}}{dz} = \frac{h_d a_{fi} A_{fr}}{m_a}\begin{bmatrix} Le_f\left(i_{masw} - i_{ma}\right) + \left(1 - Le_f\right)i_v\left(w_{sw} - w_{sa}\right) \\ + Le_f\left(w - w_{sa}\right)c_{pw}T_a \end{bmatrix} \tag{B.1.18}$$

In addition to the assumption stated earlier, Merkel (1925) assumes the Lewis factor is equal to unity and that the evaporation loss is negligible. Introducing these two assumptions, the governing Equations (B.1.15) and (B.1.5) simplify respectively to

$$\frac{di_{ma}}{dz} = \frac{h_d a_{fi} A_{fr}}{m_a}\left(i_{masw} - i_{ma}\right) \tag{B.1.19}$$

and

$$\frac{dT_w}{dz} = \frac{m_a}{m_w}\frac{1}{c_{pw}}\frac{di_{ma}}{dz} \tag{B.1.20}$$

With only the above equations, it is impossible to calculate the state of the air leaving the fill, since to do this at least two properties must be known. Hence, the exit air temperature is unknown. Merkel assumes that the air leaving the fill is saturated with water vapour. This enables him to determine the temperature and density of the air.

Traditionally, Equations (B.1.19) and (B.1.20) are combined and integrated to yield

$$\frac{h_d A}{m_w} = \frac{h_d a_{fi} A_{fr} L_{fi}}{m_w} = \frac{h_d a_{fi} L_{fi}}{G_w} = \int_{T_{wo}}^{T_{wi}} \frac{c_{pw} dT_w}{(i_{masw} - i_{ma})} \qquad \text{(B.1.21)}$$

which is commonly referred to as Merkel's equation. The non-dimensional coefficient of the performance or transfer characteristic $h_d a_{fi} L_{fi}/G_w$ is known as the Merkel number. In this equation L_{fi} is the height of the fill and $G_w = m_w/A_{fr}$. In the literature the notation frequently used for the Merkel number is KaV/L, where K = h_d, a = a_{fi}, V = $A_{fr}L_{fi}$ and L = m_w.

The implications of some of the approximations made in deducing Equation (B.1.22) are evaluated by Lefevre (1984) and Ibrahim et al. (1995).

Merkel assumptions are summarised below, as done by Johnson (1989). These assumptions are to be kept in mind when evaluating the test setup used in fill performance tests.

1) Merkel Assumptions – use of the enthalpy driving force, Equation (B.1.21).
    a) Lewis number equal to one.
    b) Evaporation losses of water can be neglected.
    c) Outlet air from fill is saturated.
2) Driving force for mass transfer is the difference in absolute humidity at the water surface and in the air next to the surface.
3) Neglects separate effects of heat and mass transfer.
4) Neglects possible misting of the air within the tower.
5) Assumes airflow is constant throughout the tower.
6) Assumes uniform inlet conditions, that is G_a, G_w, T_{ai}, T_{wb}, T_{wi}.
7) Assumes uniform fill characteristic and uniform pressure drop throughout the tower.

8) Assumes the surface temperature of the water is the same as the bulk temperature.

9) Neglects back-mixing of airflow in spray and rain zones of counter-flow tower.

10) Neglects redistribution of water due to mixing (entrance effects), segregation (air/water segregation to lower energy flow configurations), and air drag.

11) Neglects changing rate of heat and mass transfer with time since phases were mixed.

B.2. Derivation of loss coefficient from the draught equation

The derivation of pressure drop equation according to Kröger (2004) follows with illustrations from van der Merwe (2006). The test section with an elementary control volume is shown in Figure B-2.

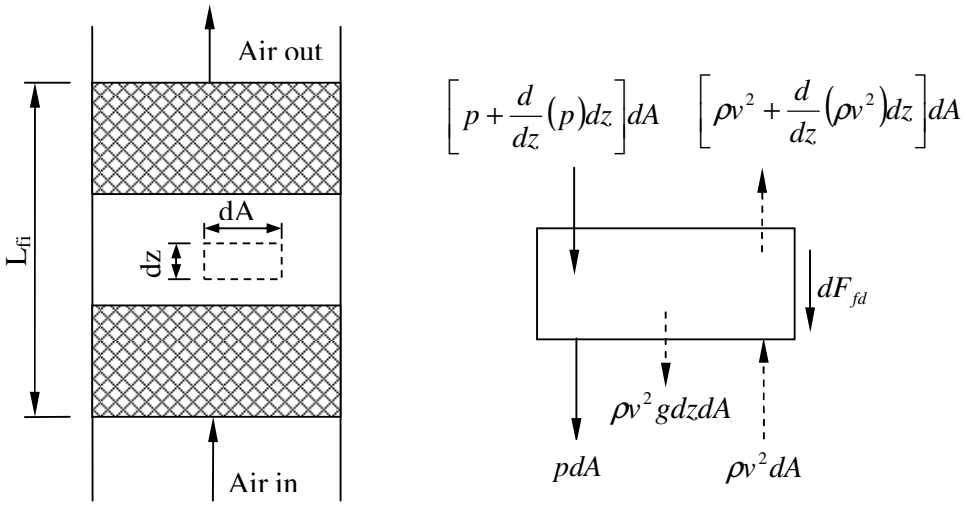

Figure B-2: Test section with elementary control volume.

From continuity we get

$$m = \int \rho v dA = \rho v_m A = \text{constant} \tag{B.2.1}$$

Applying Newton's second law of motion the sum of the forces acting on the air inside the control volume is equal to the change in momentum of the air. This gives

$$pdA - \left(p + \frac{dp}{dz}dz\right)dA - \rho_m dz g dA - \frac{dF_{fd}}{dz}dz = \frac{d}{dz}\left(\rho v^2\right)dz dA \tag{B.2.2}$$

Simplifying Equation (B.2.2) and integrating over the cross-sectional area results in

$$\begin{aligned} -dpdA - \rho_m dzgdA - dF_{fd} &= d\left(\rho v^2\right)dA \\ -pdA - \rho_m dzgA - dF_{fd}A &= d\left(\int \rho v^2 dA\right) \\ &= d\left(\alpha_m \rho v_m^2 A\right) \\ &= \rho v_m A d\left(\alpha_m v_m\right)dz + \alpha_m v_m d\left(\rho v_m A\right)dz \end{aligned} \tag{B.2.3}$$

where the momentum velocity correction factor, α_m, is given by

$$\alpha_m = \frac{\int v^2 dA}{v_m^2 A} \tag{B.2.4}$$

Simplifying Equation (B.2.3) and noting that from continuity the second term on the right-hand side is equal to zero, gives

$$-dp - \rho_m dzg - dF_{fd} = \rho v_m d\left(\alpha_m v_m\right) \tag{B.2.5}$$

Integrating the Equation (B.2.5) between the inlet and outlet of the fill yields

$$-\left(p_o - p_i\right) - \rho_m L_{fi} g - F_{fd} = \rho v_m \left(\alpha_{mo} v_{mo} - \alpha_{mi} v_{mi}\right) \tag{B.2.6}$$

Realising that $\rho v_m = \rho_i v_{mo} = \rho_i v_{mi}$ = constant, yields

$$\Delta p_{fi} = \Delta p_{fd} + \left(\alpha_{mo}\rho_o v_{mo}^2 - \alpha_{mi}\rho_i v_{mi}^2\right) + \rho_m L_{fi} g \tag{B.2.7}$$

where Δp_{fd} is the pressure drop due to friction and drag effects.

When the airflow through the fill is uniform, the value of α_m from Equation (B.2.4) is equal to unity and the air pressure drop equation reduces to

$$\Delta p_{fi} = \Delta p_{fd} + \left(\rho_o v_{mo}^2 - \rho_i v_{mi}^2\right) + \rho_m L_{fi} g \tag{B.2.8}$$

If the pipe between the static pressure tap above the fill and the pressure transducer is inside the test section, as illustrated in Figure B-3, the buoyancy effects as a result of the difference in temperature inside and outside the test section is negligible and the third term on the right-hand side in Equation (B.2.8) can be ignored, as the difference in height is effectively equal to zero.

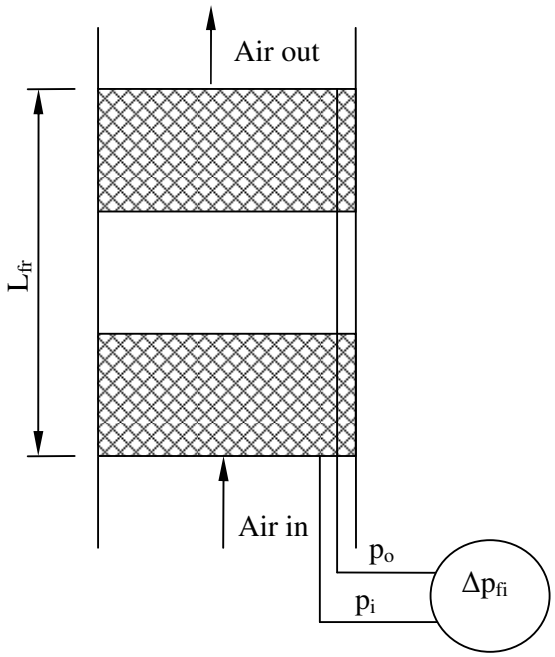

Figure B-3: Pressure measurement pipes inside test section.

Equation (B.2.8) now becomes

$$\Delta p_{fi} = \Delta p_{fd} + \left(\rho_o v_{mo}^2 - \rho_i v_{mi}^2\right) \tag{B.2.9}$$

A dimensionless loss coefficient representing the friction and drag components of the fill is desired. Using Equation (B.2.1) as in Legrand (1992) yields

$$K_{fd} = \frac{2\Delta p_{fd}}{\rho v^2} = \frac{2\left[\Delta p_{fi} - \left(\rho_{avo} v_{avo}^2 - \rho_{avi} v_{avi}^2\right)\right]}{\rho v^2} \tag{B.2.10}$$

Different reference conditions can be used for the denominator. For this study the mean air-vapour properties will be used.

APPENDIX C. TEST FACILITIES

There are many test facilities used to determine the performance of fill as well as other cooling tower elements. The test facilities differ in many ways. This appendix briefly discusses a select few of the test facilities to highlight the differences between them.

C.1. Brentwood test facility, Reading, USA

Brentwood Industries (Aull (2008), Brentwood (2003)) operates a counter-flow fill test facility consisting of two identical test cells which have a cross-section of 0.61 x 0.61 m^2 and can accommodate a fill height of 1.83 m. For all tests a square-patterned Bete nozzle located 225 mm above the fill sprays water on the top of the fill. Below the fill there is a 210 mm rain zone. The sides of the test section are made of clear, high-strength polycarbonate material that allows for observation of the water falling through the fill during testing. The Brentwood facility is illustrated in Figure C-1 below.

Figure C-1: Brentwood counter-flow test facility in Reading, Pennsylvania.

Air is induced by a centrifugal fan controlled by a variable frequency drive. An air speed of 5 m/s can be achieved in the test cells. The air velocity is measured using an orifice plate designed according to ASME specifications.

Inlet and outlet dry- and wet-bulb temperatures are measured with platinum, 3-wire resistance temperature detectors (RTD's) calibrated to mercury-in-glass thermometers whose calibration is in line with National Institute of Standards and Technology (NIST) calibration specifications.

The fill pressure drop is measured using paired, static H-taps, one at the spray nozzle elevation above the fill and one directly below the fill. H-tap pairs are connected to draught-range pressure transducers.

Water is pumped by a centrifugal pump controlled by a variable frequency drive. Specific water mass velocities of 1.9 – 6.7 kg/m^{2}s can be achieved. Two calibrated Brooks magnetic flow meters measure the water flow.

Water for the tests is heated by a 350 kW hot-water generator. During testing, the hot water temperature is maintained at a constant value by a microprocessor-based PID controller that operates three mixing valves.

For all fills tested a 3x3 water and air test matrix is used. For dense fills water mass velocities are 4.071, 5.425 and 6.782 kg/m^{2}s, with air velocities of 1.5, 2.5 and 3.5 m/s. For less dense fills the highest water mass velocity is replaced with a mass velocity of 2.775 kg/m^{2}s, with the same air velocities.

Inlet air conditions are not controlled, so steady ambient conditions are required for reliable results. During testing five scans per minute for a minimum of 15 minutes are logged for every water mass velocity and air velocity.

The data are logged automatically using an Agilent data logger. Data are processed using purpose-written Visual Basic code. The Merkel equation with the four-point Chebyshev method of numerical integration, as described in the Cooling Technology Institute (CTI) method of combined heat and mass transfer analysis, is used to calculate the performance index as described in CTI's "Cooling Tower Performance Curves".

It is reported that information is collected under "very stable conditions" with "very uniform air and water distribution", but detailed information is not made available.

C.2. EvapTech test facility, Kansas, USA

Libert (2002) reports on a test facility at EvapTech Inc in Kansas, USA, with a cross-section of 2.4 x 1.8 m^2, and which can accommodate a fill height of 2.1 m. The test facility is illustrated in Figure C-2. The test cell is designed to minimise

the thermal transfer in the rain zone below the fill. This is achieved by optimising the water extraction system so that it minimises the thermal performance of the rain zone while its effect on the airflow velocity profile of the air entering the fill is minimal.

Air is supplied to the cell by two horizontal tubular inline fans in parallel driven by two 30 kW 3-phase electric motors connected to variable frequency drives. Airflow is measured using a bank of elliptical nozzles and piezometer rings that measure static and differential pressure. The air flow measurement and the chamber construction are in accordance with ANSI/AMCA Standard 210. Air velocities in the test cell are varied between 1.5 and 3.5 m/s.

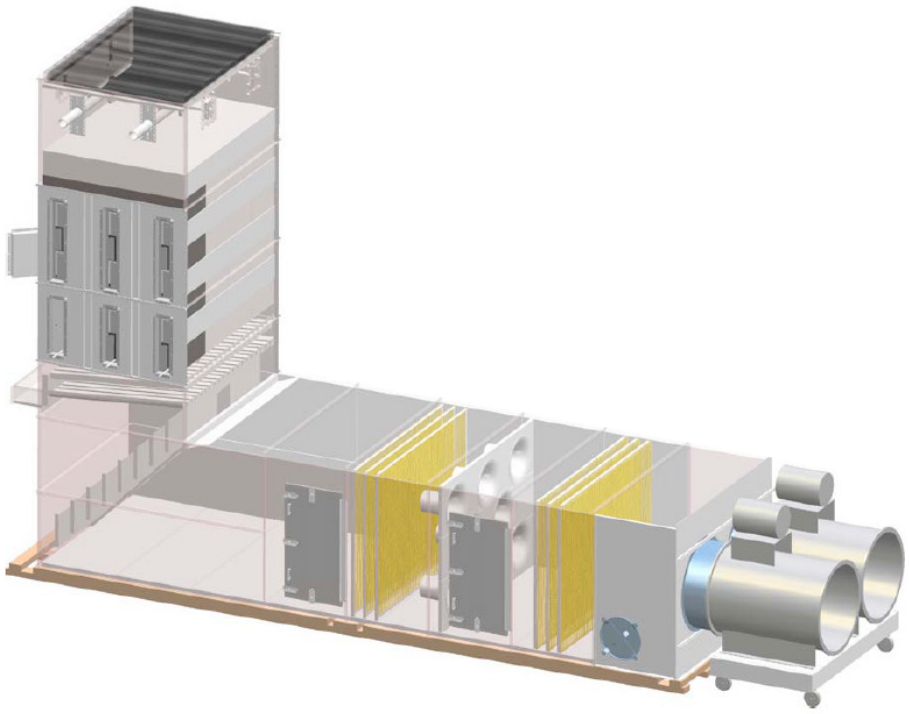

Figure C-2: EvapTech Inc counter-flow test facility Kansas, USA.

A plate heat exchanger is used to heat the water for testing. A heat load of 880 kW is available, but this can be doubled if necessary. A horizontal centrifugal pump supplies the water flow. The water flow rate is measured by a calibrated Venturi flow meter coupled with a water-over-fluid U-manometer, also by a calibrated magnetic flow meter. A straight length of pipe with fitted Pitot taps is available as a third method of water flow measurement. Water mass velocities of 2.77 - 8.333 kg/m^{2}s are used in the test cell.

Water is distributed over the fill by two pipes fitted with square-pattern spray nozzles. No specifics regarding the spray distribution profile are given, but

Libert (2002) does highlight the need for uniform water distribution and how nozzle selection can influence this. The spray zone height can be adjusted from 0.3 to 0.9 m.

Cold water is collected as it leaves the fill and flows to a tank with a make-up float valve. Outlet water temperatures are made once the water exiting the fill has been mixed in a mixing box. The water running down the walls of the test cell, bypassing the fill, is collected separately by narrow gutters and wall slots. This allows the quantity and temperature of this bypass water to be measured before it is returned to the cold water basin.

The test cell is housed in an environmental test chamber where the inlet air conditions are controlled. Fans and dampers mix the exhaust air from the test cell with fresh air to achieve steady-state conditions during testing.

Tests are run for a minimum of an hour once steady-state operation has been realised. An HP data logger measures one-minute averages from more than twenty sensors. The test data are processed and a heat transfer coefficient is calculated. The fill static pressure drop is reported on as well. It is noted that consistence between test data interpretation and performance prediction of the full-scale operation of the fill in a cooling tower is dependent on the water distribution delivered to the fill. Equations are fitted through the data points and are used to represent fill performance.

No information is provided regarding how the pressure drop over the fill is measured, where the water inlet temperature is measured, the location and method of measuring inlet dry- and wet-bulb temperatures, or whether outlet air conditions are measured.

A 19 mm cross-corrugated film fill is used as the baseline test to verify the performance of the test cell.

C.3. Mistral test bench, Lyon, France

The Mistral cooling tower test facility (Fabre and Legrand (1988) and Legrand (1992)) is located at the Nuclear Power Plant of Bugey, France. It was built to replace the Nantes-Chevire test facility that was decommissioned in 1987. The Mistral test facility has over 3000 hours of operation since its commissioning in that same year. The test facility has a counter- and a cross-flow facility, but the focus here will be on the counter-flow section. It is illustrated in Figure C-3.

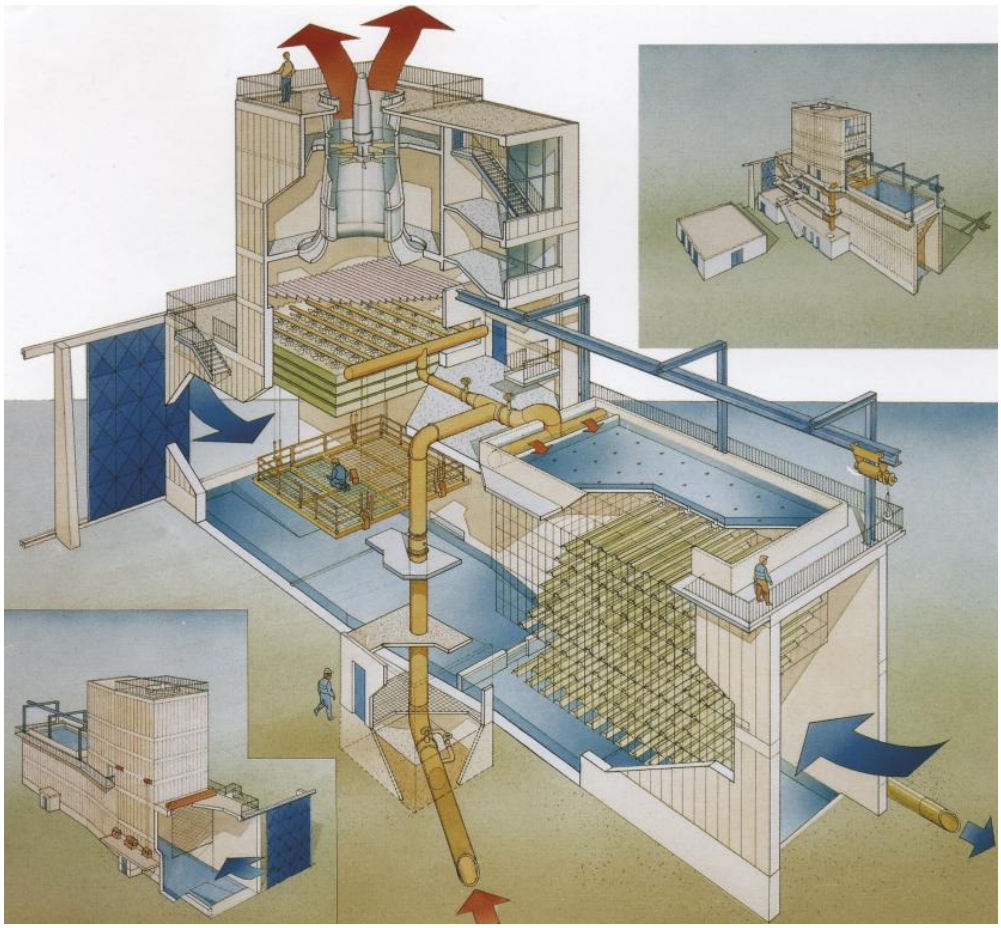

Figure C-3: Mistral test facility at Nuclear Power Plant of Bugey, France.

The counter-flow test section has a cross-sectional area of 7 x 7 m^2 with an available height of 3.5 m. Hot water is fed to the test facility from the cooling water circuit of two of the units at the power plant. The maximum water load is 25 MW for a water flow rate of 0.6 m^3/s. The water flow rate is measured using an electromagnetic flow meter located in the hot water supply line. Nozzles are used for water distribution above the fill. The water falls through the fill and is collected in the basin.

The water falling through the central core area of the tower and water falling through the periphery areas are collected separately and their flow rate and temperature are measured so as to determine separately the performance of these zones. This is a novelty of the Mistral test bench, and is a useful tool as the boundary effects decrease the performance of the fill even in large setups like Mistral, as noted by Fabre and Legrand (1988), Fabre (1992) and Gősi (1998). Being able to quantify this is very desirable.

The air is supplied by a draught fan driven by a 250 kW motor. The flow rate is controlled by a variable-frequency drive and the flow rate is measured by means of a nozzle located between the inlet and the fan. An airflow rate of 225 m^3/s can be achieved.

The air inlet and outlet temperatures are measured as are the water inlet and outlet temperatures. One-hundred-and-twenty sensors measure meteorological readings, water inlet and outlet temperatures, air inlet and outlet temperatures, air inlet and outlet velocities, and static pressure readings over the equipment. Measurements are logged by a data acquisition system.

This is a large test facility, and setup for testing takes three weeks. Thermal performance tests take two weeks to complete, with five to ten measurement points being made a day. The system takes approximately 45 minutes to stabilise.

The motivation for such a large test facility is to minimise edge effects and to be able to consider meaningfully water maldistribution effects due to spray nozzles. This large size comes at an expense, though, and setup and testing a single fill takes weeks. If a smaller test facility that is able to minimise and quantify edge effect is designed this would greatly reduce the complexity of the experiment.

C.4. Parish Station small-scale test facility, Houston, USA

A small-scale test facility is located at the Parish Station of Houston Lighting and Power Company in the USA (Johnson (1989)). The facility is shown in Figure C-4. The facility tests both counter- and cross-flow fills. The counter-flow test section has a cross-sectional area of 2.4 x 2.4 m^2 and is able to test a maximum fill height of 3.6 m. The air entering the fill is conditioned by means of commercial HVAC unit that is able to control the air temperature and humidity. Air mass velocity can be set between 1.8 and 4.8 kg/m^2s, with wet-bulb temperatures from 1.7 to 32°C.

The hot water supply is from a nearby cooling tower. Water is tapped from the top and bottom of the tower and mixed to obtain the desired water temperature for testing. The water mass velocity can be set at between 1.4 to 14 kg/m^2s, with an inlet water temperature of between 35 and 51°C.

The water outlet temperature is measured two ways. The first method is to measure the water flowing out of each collection trough below the fill. The second is to measure the mixed outlet water temperature. This is the temperature used in all performance tests of field-erected cooling towers, but includes wall effects and the cooling of water after it exits the fill.

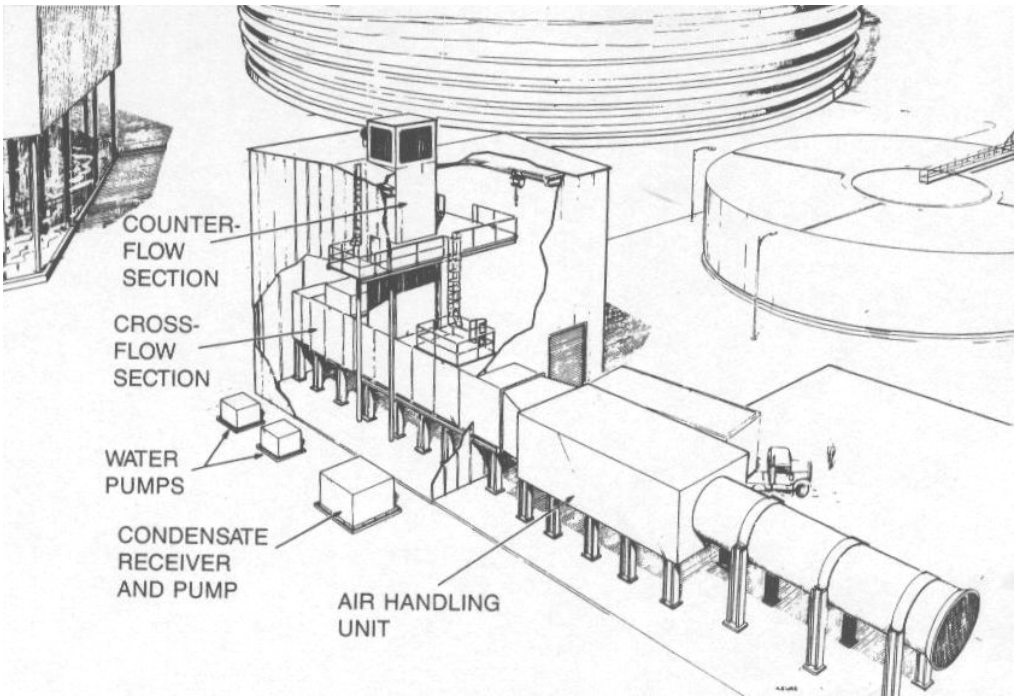

Figure C-4: Small-scale test facility at Parish Station of Houston Lighting and Power Company USA.

Temperatures are measured using RTD's; absolute and differential pressures are measured using transducers; and the air velocity is measured by nine propeller anemometers over a plane in the inlet to the test section. The water flow rate is measured by an ASME Venturi. All the data are logged automatically by a data acquisition system.

C.5. Clarke Station large-scale test facility, Houston, USA

A large-scale counter-flow fill test facility is located at Houston Lighting and Power Company's H.O. Clarke Station (Johnson (1989)). The test facility is the end cell of the full-scale counter-flow cooling facility that has been fitted with measurement devices for experimental purposes. The cell has a cross-sectional area of 7.2 x 12.5 m² and is able to accommodate fill with a height between 0.9 to 1.5 m.

The water mass velocity can be set between 2.2 and 5.3 kg/m²s by adjusting a manually operated butterfly valve. The water flow rate is measured by a sonic flow meter installed in the pipe work leading to the facility. The temperature of the water entering the fill is measured by collecting water in four troughs arranged above the fill. The outlet water temperature is measured in a similar manner, except six troughs are used.

Airflow is induced in the cell by two variable pitch fans that allow for air mass velocities of between 1.7 and 2.9 kg/m^{2}s. Air inlet conditions are measured at four locations, while outlet conditions are measured at six locations above drift eliminators. The inlet air conditions are not controlled. The pressure drop over the inlet louvers, fill, drift eliminators and the fan are all measured.

Meteorological information is measured in a weather station 23 m from the test facility. All data are recorded by a Hewlett-Packard data acquisition system.

C.6. Direct-comparison test facility, Budapest, Hungary

VEIKI Research Institute for Electric Power Co. Ltd. in Budapest, Hungary operates a test facility that is able to compare fills directly by using two identical, parallel test cells that operate simultaneously with identical inlet conditions (Gősi (1998) and Baard (1998)). This setup is able to show accurately and reliably small differences between fills packed in each of the cells.

Each cell has a cross-sectional area of 1.5 x 1.5 m^2. Water is heated in a heat exchanger by steam and sprayed through nozzles onto the top of the fill. The water mass flow rate is controlled by a series of valves. Air is supplied to the test cells by induced-draught fans connected to variable-frequency drives to control the air mass flow rate. Measurements are logged by a Hewlett-Packard data acquisition system. Redundant analogue measurement devices are also installed into the facility.

Tests with water mass velocities of 1.3 to 2.5 kg/m^{2}s and air mass velocities between 1.9 and 3.3 kg/m^{2}s are reported on by Gősi (1998).

Details of the water extraction apparatus, water mass flow measurement, types and locations of thermocouples, et cetera are not elaborated on.

APPENDIX D. CALIBRATION DETAILS

D.1. Pressure transducer calibrations

The pressure transducers are calibrated using a Betz manometer. A pressure difference is applied over the pressure transducers and the voltage output of the pressure transducer is recorded. A correlation between the pressures and voltage outputs is obtained.

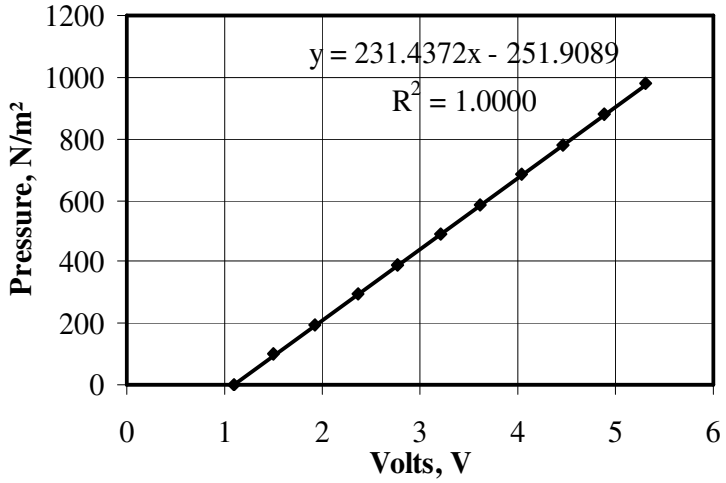

Figure D-1: Calibration of 0 – 10 000 N/m² pressure transducer used for pressure drop over nozzle bank.

Table D-1: 0 - 10000 N/m² transducer calibration.

Pressure, N/m²	Output, V
0.000	1.0790
3908.304	2.7690
3419.766	2.5584
2931.228	2.3475
2442.690	2.1365
1954.152	1.9252
1465.614	1.7139
977.076	1.5026
488.538	1.2911
0.000	1.0791

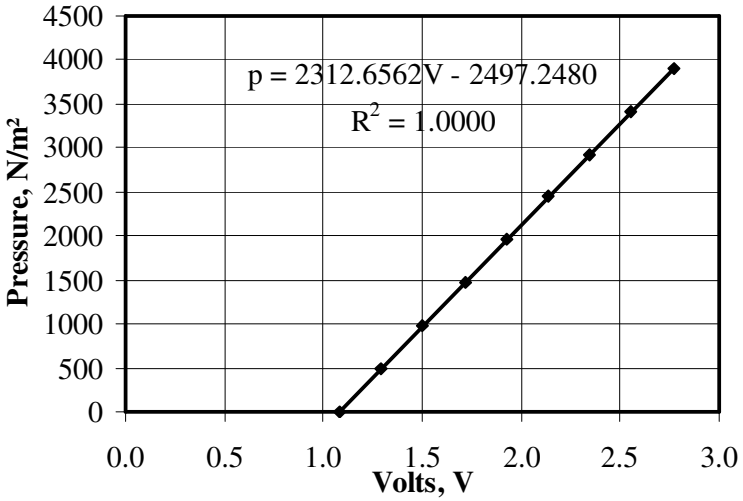

Figure D-2: Calibration of 0 - 1000 N/m² pressure transducer.

Table D-2: 0-1000 N/m² transducer calibration.

Pressure, N/m²	Output, V
0.000	1.0870
977.076	5.3057
879.368	4.8884
781.661	4.4655
683.953	4.0458
586.246	3.6223
488.538	3.2023
390.830	2.7787
293.123	2.3594
195.415	1.9302
97.708	1.5075
0.000	1.0870

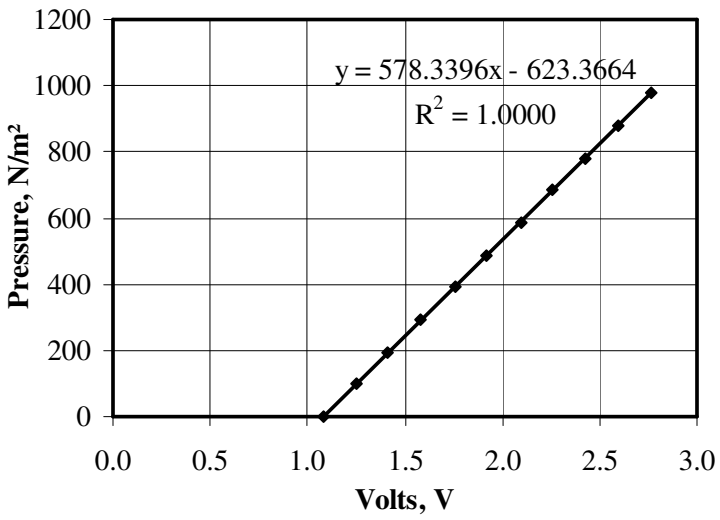

Figure D-3: Calibration of 0 - 2500 N/m² pressure transducer.

Table D-3: 2500 N/m² pressure transducer calibration data.

Pressure, N/m²	Output, V
0.0000	1.0777
977.0760	2.7660
879.3684	2.5981
781.6608	2.4301
683.9532	2.2612
586.2456	2.0928
488.5380	1.9224
390.8304	1.7543
293.1228	1.5839
195.4152	1.4142
97.7076	1.2477
0.0000	1.0777

D.2. Thermocouples

All the thermocouples were placed in a container of water. The thermocouples were left in the water and allowed to cool to room temperature. The measured temperatures were recorded. An average temperature of the 32 thermocouples was calculated. The thermocouples readings were corrected by adding or subtracting constants.

Prior to these corrections the thermocouples were within the specified limits for T-type thermocouples, which is typically ±0.5 ºC from the average measured temperature. After the corrections the thermocouples measured within an error of ±0.05 ºC of the average measured temperature. The correction applied to each thermocouple identified by its channel number is shown in Table D-4. The corrected and uncorrected errors measured by each thermocouple are shown in Figure D-4.

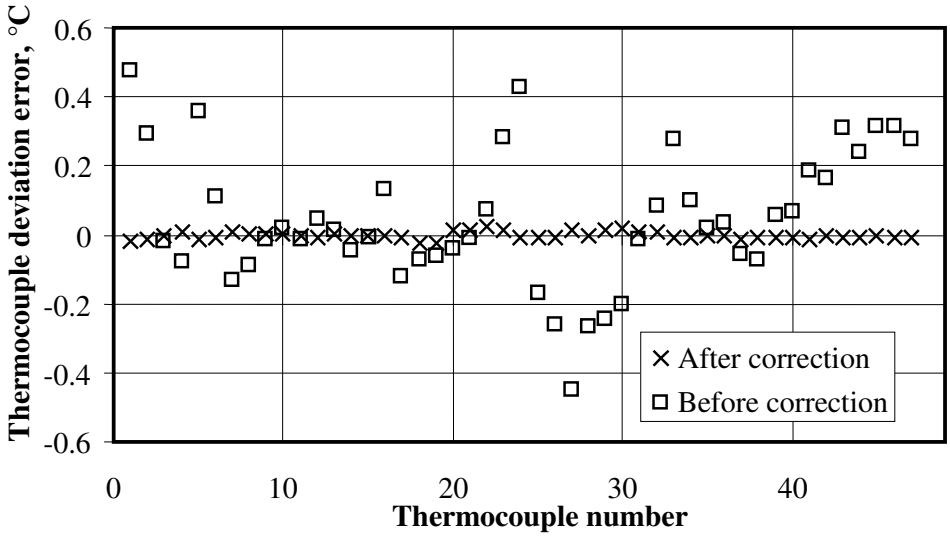

Figure D-4: Measured error of thermocouples before and after corrections.

Table D-4: Thermocouples correction constants

Reference	Channel	Correction, °C	Reference	Channel	Correction, °C
1	101	0.47891	25	209	-0.20079
2	103	0.29525	26	210	-0.01342
3	105	-0.02063	27	211	0.08176
4	107	-0.07884	28	213	-0.03786
5	102	0.35602	29	214	-0.01607
6	104	0.10879	30	215	0.07176
7	106	-0.13338	31	217	0.28207
8	108	-0.08933	32	218	0.42707
9	109	-0.01151	33	301	0.25217
10	111	0.02114	34	302	0.07452
11	113	-0.01261	35	303	0.00397
12	115	0.04800	36	304	0.02167
13	110	0.01279	37	305	-0.06079
14	112	-0.04582	38	306	-0.07324
15	114	-0.00368	39	307	0.05172
16	116	0.13281	40	308	0.06622
17	201	-0.12091	41	309	0.19122
18	202	-0.07165	42	310	0.17127
19	203	-0.06365	43	311	0.33332
20	204	-0.17188	44	312	0.26007
21	205	-0.26315	45	313	0.33287
22	206	-0.45082	46	314	0.34522
23	207	-0.26795	47	315	0.31442
24	208	-0.24244	25	209	-0.20079

D.3. Electromagnetic flow meter

The electromagnetic flow meter is calibrated by diverting water which would normally flow into the test cell to a calibration tank shown from the front view in Figure D-5. The time taken to fill a certain volume of the tank is recorded. A clear PVC pipe allows the level of the water to be measured. The tank has a width of 700 mm.

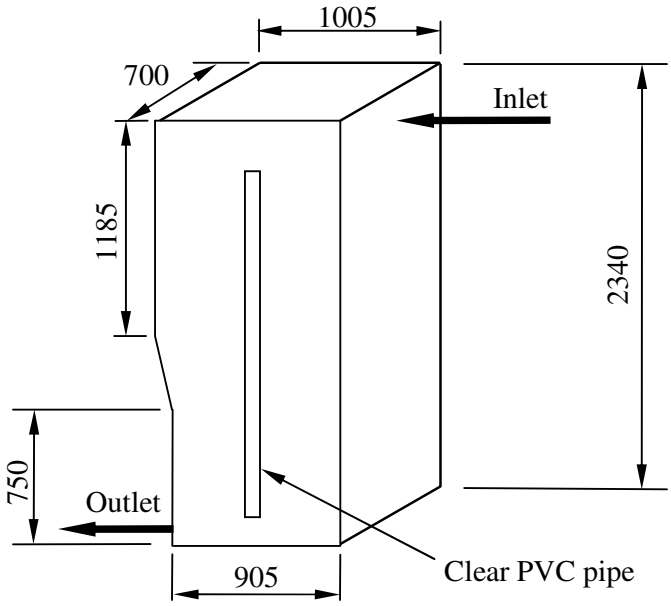

Figure D-5: Dimensions of tank used to calibrate electromagnetic flow meter.

The volumetric flow rates measured by the electromagnetic flow meter and calculated using the calibration tank are plotted in Figure D-6. The figure shows that the two methods are in very good agreement, with a maximum of 1 % deviation.

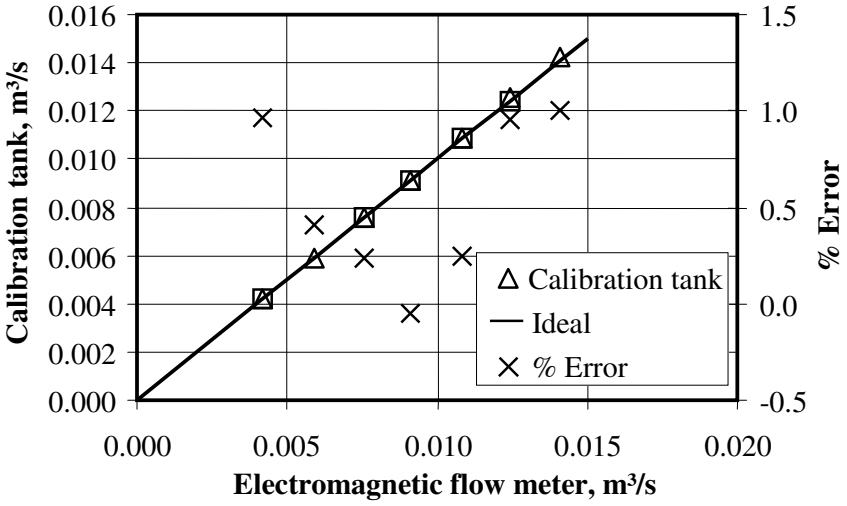

Figure D-6: Electromagnetic flow meter calibration curve.

APPENDIX E. DISTRIBUTION OF WATER THROUGH FILL

The distribution below the fill in the cooling tower test facility at the University of Stellenbosch is measured. This is done to determine whether there is any significant migration of the water as it flows through the fill. This is desirable to know, as it determines the effectiveness of the 1.5 x 1.5 m² test section in reproducing operating conditions of full-scale cooling towers. In industrial cooling towers there is (ideally) a uniform distribution of water delivered to the fill and (ideally) a uniform distribution of water through the fill. The optimal performance of a fill occurs when there is uniform water flow through the fill (as mentioned in Section 5.2).

The water flow profiles below the three fills tests are measured for at least three fill heights and at the three water mass velocities. At the same time, as discussed in Section 5.3, the water bypassing the fill and flowing down the wall is collected and measured to gauge how much water accumulates along the wall and how much water remains in the fill.

The figures showing the water distribution below the cross-fluted fill for 0.305 m, 0.61 m, 1.22 m and 1.83 m are shown in Figure E-1 to Figure E-24. The cross-fluted fill is the fill with the least migration, and very seldom is there a measurement made that deviates by more than 15 % from the average. The cross-fluted fill is also the fill with the least water attaching to the walls, with this amount never reaching or exceeding 5 % of the total water flow delivered to the test facility. From the distribution tests alone it is possible to say that the fill performance determined for the cross-fluted fill in the Stellenbosch test facility will be representative of the fill performance in a larger cooling tower.

The figures showing the distribution below the trickle fill for 0.5 m, 1.0 m and 1.5 m are shown in Figure E-25 to Figure E-43. The trickle grid does not have ideal migration through the fill height, but measured flow rates seldom deviate more than 30 % from the average. Wall water does not reach or exceed 8 % of the total water flow rate delivered to the test facility.

The v-bar splash fill has very bad migration. These results are presented in Figure E-42 to Figure E-60 for the spray frame and nozzle distribution. The distribution under the fill deviates by up to 80 % from the average water flow rate. Combined with up to 31 % of the water flow attaching to the wall, the resulting Merkel number must be scrutinised before any design decisions are made using performance results obtained in this 1.5 x 1.5 m² test facility.

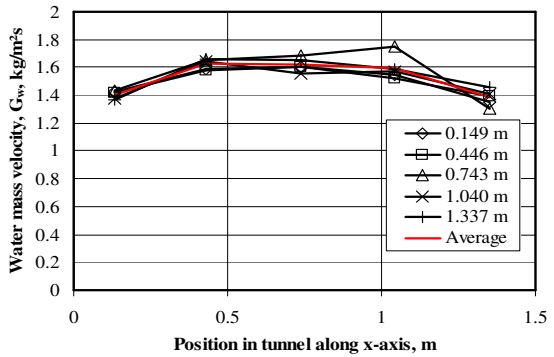

Figure E-1: Water mass velocity distribution under 0.305 m film fill with G_w = 1.447 kg/m²s.

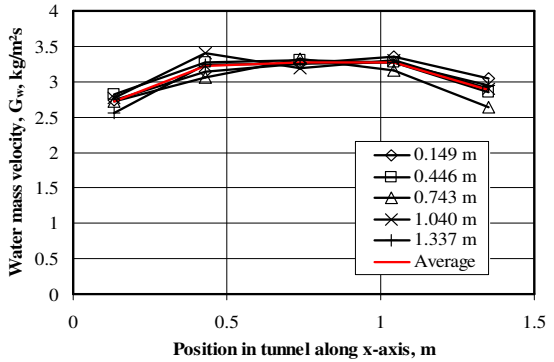

Figure E-2: Water mass velocity deviation under 0.305 m film fill with G_w = 1.447 kg/m²s.

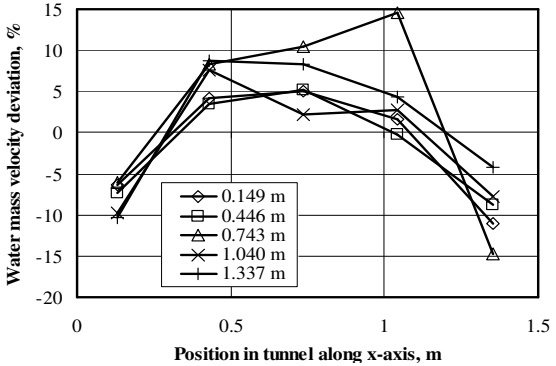

Figure E-3: Water mass velocity deviation under 0.305 m film fill with G_w = 1.447 kg/m²s.

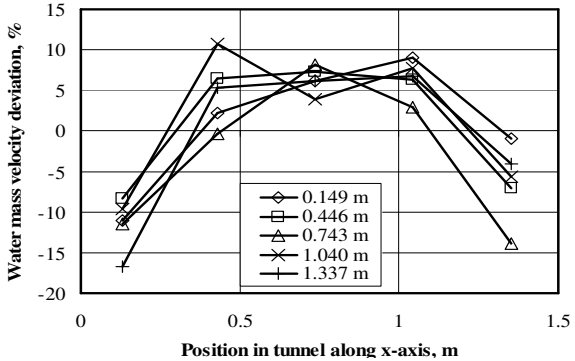

Figure E-4: Water mass velocity deviation under 0.305 m film fill with G_w = 3.000 kg/m²s.

Integrated G_w	1.540 kg/m²s
Flow meter G_w	1.447 kg/m²s
Percentage difference	6.399 %
Wall bypass G_w	0.015 kg/m²s
Percentage wall bypass	1.002 %
Christiansen coefficient	0.911

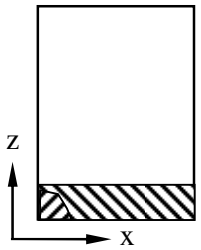

Integrated G_w	3.140 kg/m²s
Flow meter G_w	3.000 kg/m²s
Percentage difference	4.678 %
Wall bypass G_w	0.070 kg/m²s
Percentage wall bypass	2.328 %
Christiansen coefficient	0.909

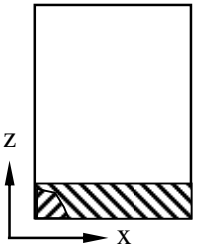

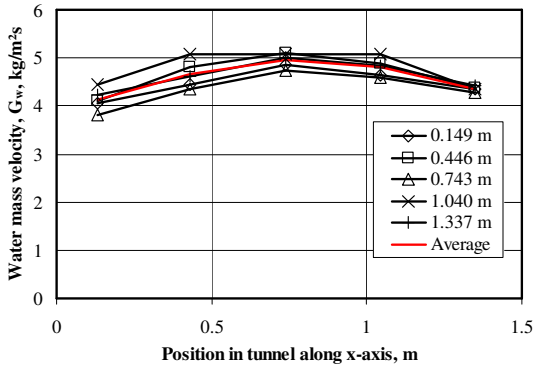

Figure E-5: Water mass velocity distribution under 0.305 m film fill with G_w = 4.488 kg/m²s.

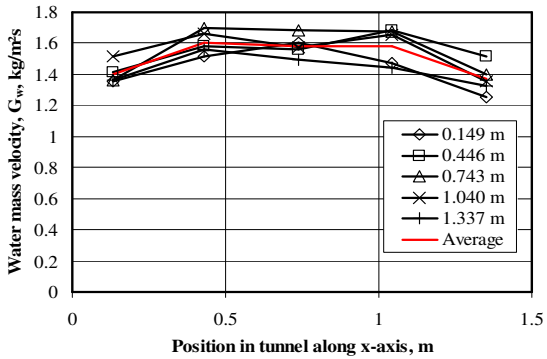

Figure E-6: Water mass velocity distribution under 0.61 m film fill with G_w = 1.501 kg/m²s.

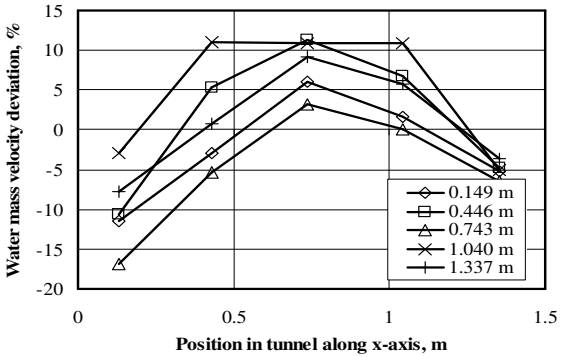

Figure E-7: Water mass velocity deviation under 0.305 m film fill with G_w = 4.488 kg/m²s.

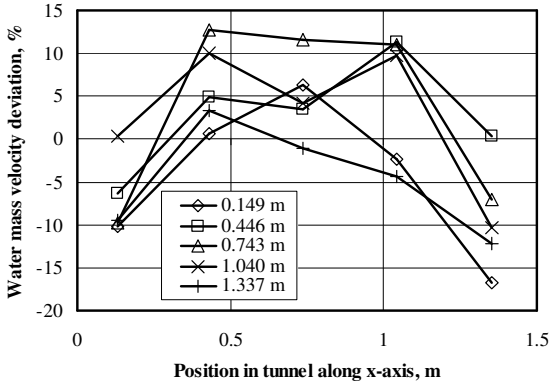

Figure E-8: Water mass velocity deviation under 0.61 m film fill with G_w = 1.501 kg/m²s.

Integrated G_w	4.696 kg/m²s
Flow meter G_w	4.488 kg/m²s
Percentage difference	4.636 %
Wall bypass G_w	0.118 kg/m²s
Percentage wall bypass	2.623 %
Christiansen coefficient	0.915

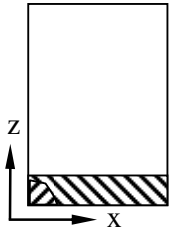

Integrated G_w	1.539 kg/m²s
Flow meter G_w	1.501 kg/m²s
Percentage difference	2.548 %
Wall bypass G_w	0.031 kg/m²s
Percentage wall bypass	2.034 %
Christiansen coefficient	0.909

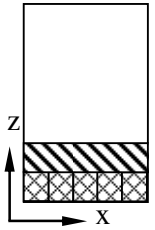

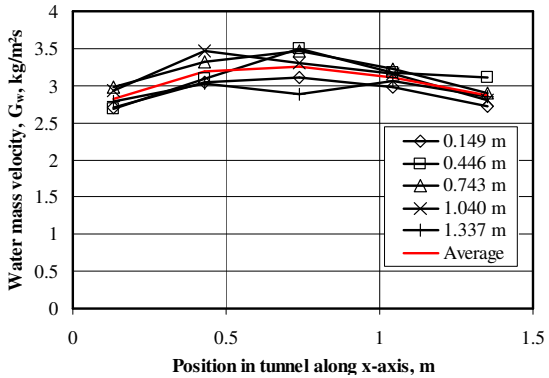

Figure E-9: Water mass velocity distribution under 0.61 m film fill with G_w = 2.981 kg/m²s.

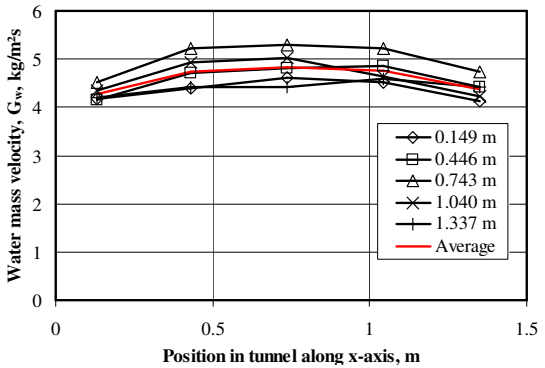

Figure E-10: Water mass velocity distribution under 0.61 m film fill with G_w = 4.463 kg/m²s.

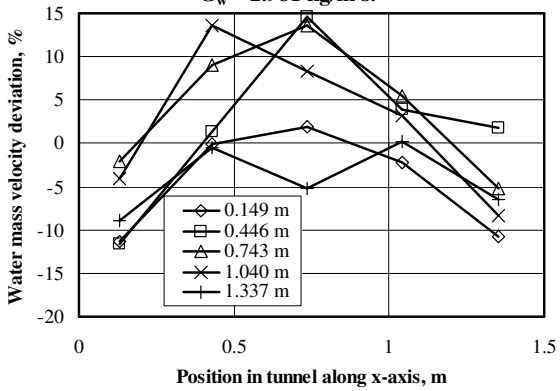

Figure E-11: Water mass velocity deviation under 0.61 m film fill with G_w = 2.981 kg/m²s.

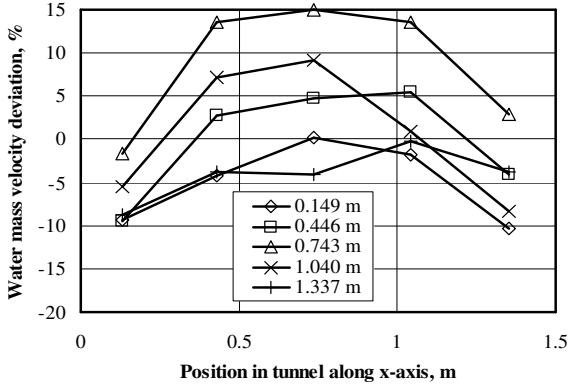

Figure E-12: Water mass velocity deviation under 0.61 m film fill with G_w = 4.463 kg/m²s.

Integrated G_w	3.134 kg/m²s
Flow meter G_w	2.981 kg/m²s
Percentage difference	5.144 %
Wall bypass G_w	0.084 kg/m²s
Percentage wall bypass	2.817 %
Christiansen coefficient	0.920

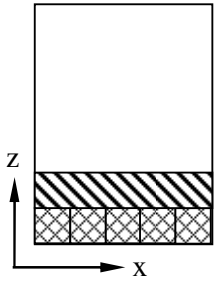

Integrated G_w	4.715 kg/m²s
Flow meter G_w	4.463 kg/m²s
Percentage difference	5.636 %
Wall bypass G_w	0.115 kg/m²s
Percentage wall bypass	2.585 %
Christiansen coefficient	0.922

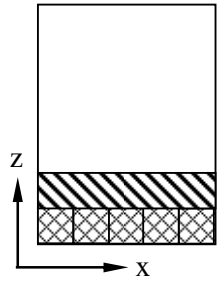

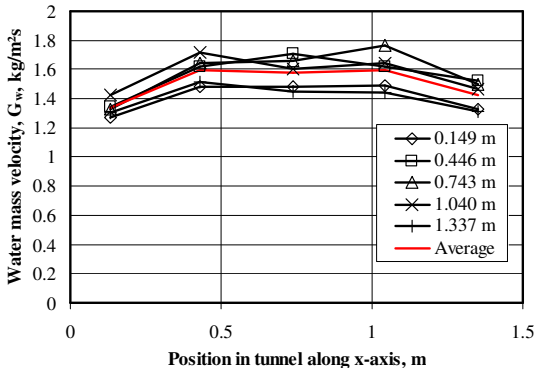

Figure E-13: Water mass velocity distribution under 1.22 m film fill with G_w = 1.5 kg/m²s.

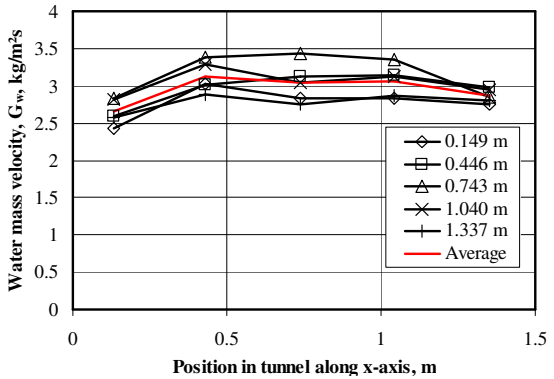

Figure E-14: Water mass velocity distribution under 1.22 m fill with G_w = 2.925 kg/m²s.

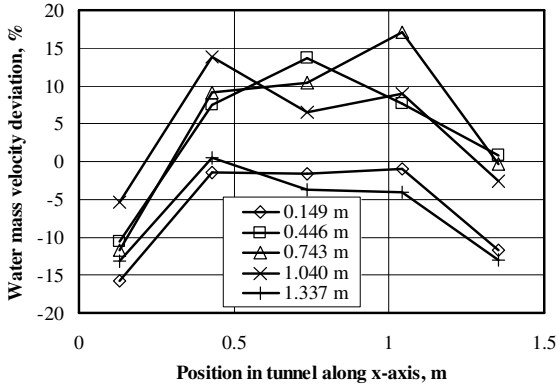

Figure E-15: Water mass velocity deviation under 1.22 m film fill with G_w = 1.502 kg/m²s.

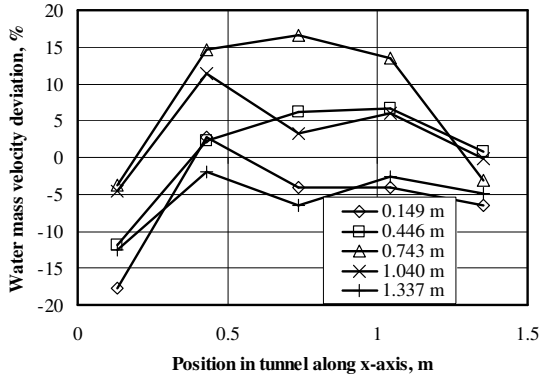

Figure E-16: Water mass velocity deviation under 1.22 m film fill with G_w = 2.924 kg/m²s.

Integrated G_w	1.554 kg/m²s
Flow meter G_w	1.502 kg/m²s
Percentage difference	3.450 %
Wall bypass G_w	0.048 kg/m²s
Percentage wall bypass	3.220 %
Christiansen coefficient	0.906

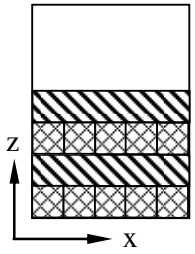

Integrated G_w	3.333 kg/m²s
Flow meter G_w	2.924 kg/m²s
Percentage difference	4.233 %
Wall bypass G_w	0.098 kg/m²s
Percentage wall bypass	3.362 %
Christiansen coefficient	0.916

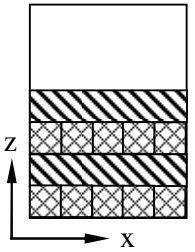

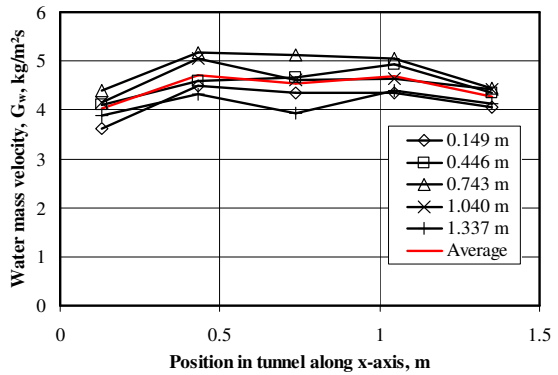

Figure E-17: Water mass velocity distribution under 1.22 m film fill with G_w = 4.396 kg/m²s.

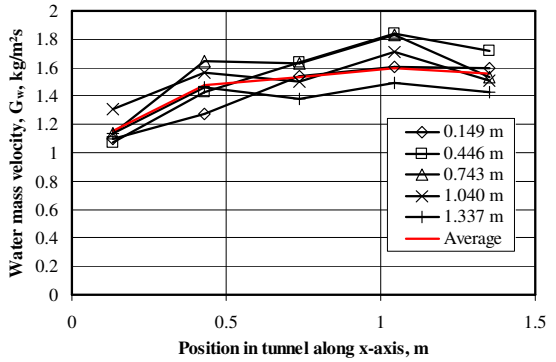

Figure E-18: Water mass velocity distribution under 1.83 m film fill with G_w = 1.493 kg/m²s.

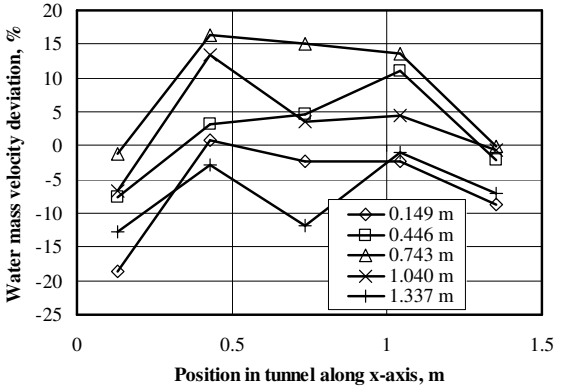

Figure E-19: Water mass velocity deviation under 1.22 m film fill with G_w = 4.396 kg/m²s.

Integrated G_w	4.612 kg/m²s
Flow meter G_w	4.396 kg/m²s
Percentage difference	4.909 %
Wall bypass G_w	0.162 kg/m²s
Percentage wall bypass	3.608 %
Christiansen coefficient	0.922

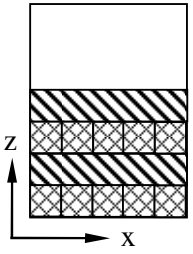

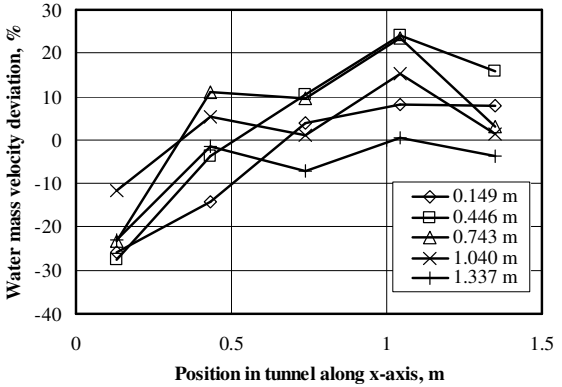

Figure E-20: Water mass velocity deviation under 1.83 m film fill with G_w = 1.493 kg/m²s.

Integrated G_w	1.529 kg/m²s
Flow meter G_w	1.493 kg/m²s
Percentage difference	2.493 %
Wall bypass G_w	0.058 kg/m²s
Percentage wall bypass	3.884 %
Christiansen coefficient	0.911

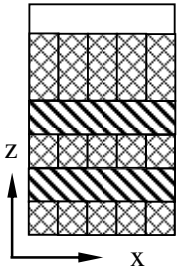

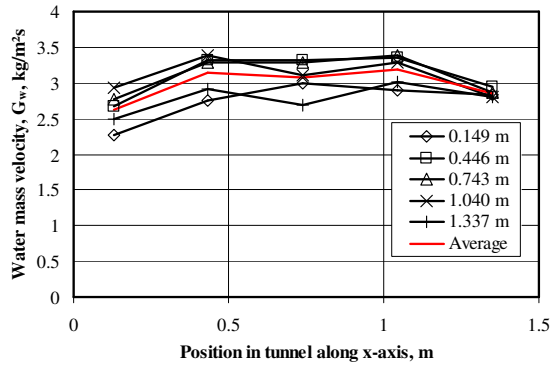

Figure E-21: Water mass velocity distribution under 1.83 m film fill with G_w = 2.98 kg/m²s.

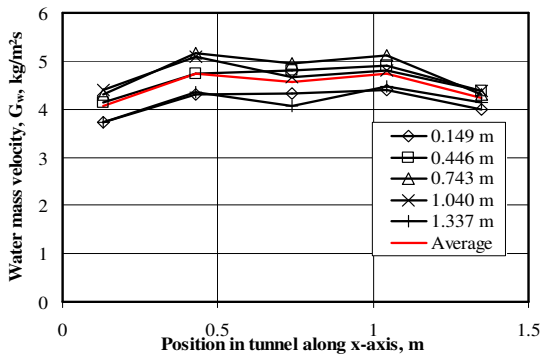

Figure E-22: Water mass velocity distribution under 1.83 m film fill with G_w = 4.396 kg/m²s.

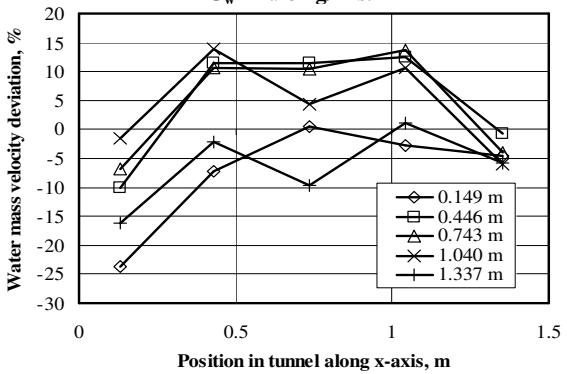

Figure E-23: Water mass velocity deviation under 1.83 m film fill with G_w = 2.98 kg/m²s.

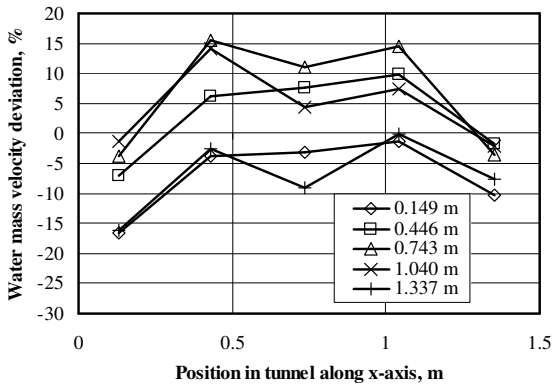

Figure E-24: Water mass velocity deviation under 1.83 m film fill with G_w = 4.396 kg/m²s.

Integrated G_w	3.113 kg/m²s
Flow meter G_w	2.980 kg/m²s
Percentage difference	4.471 %
Wall bypass G_w	0.139 kg/m²s
Percentage wall bypass	4.653 %
Christiansen coefficient	0.903

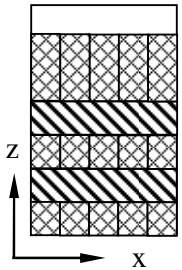

Integrated G_w	4.825 kg/m²s
Flow meter G_w	4.396 kg/m²s
Percentage difference	6.421%
Wall bypass G_w	0.215 kg/m²s
Percentage wall bypass	4.898 %
Christiansen coefficient	0.912

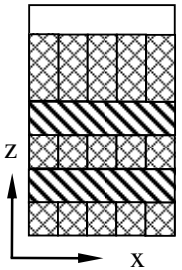

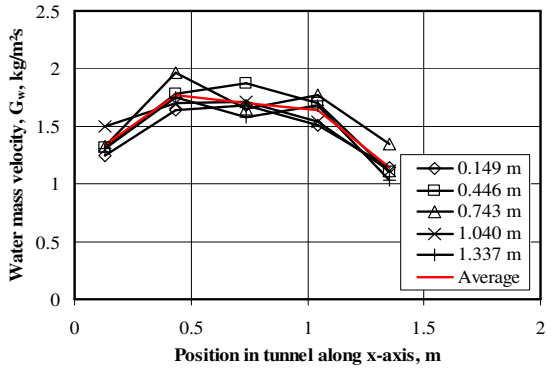

Figure E-25: Water mass velocity distribution under 0.5 m trickle fill with G_w = 1.494 kg/m²s.

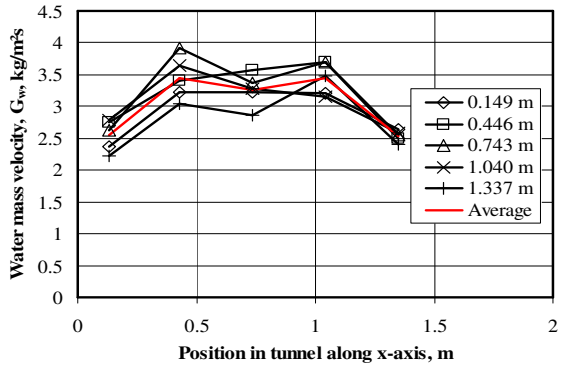

Figure E-26: Water mass velocity distribution under 0.5 m trickle fill with G_w = 3.006 kg/m²s.

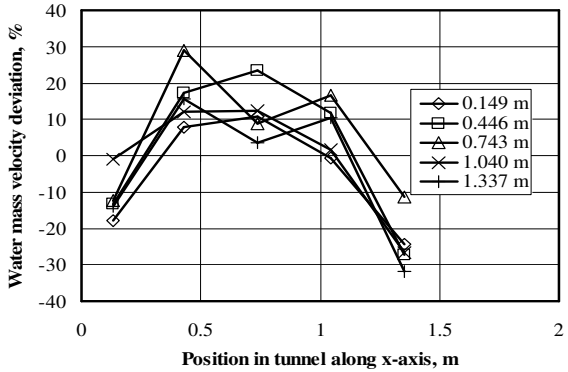

Figure E-27: Water mass velocity deviation under 0.5 m trickle fill with G_w = 1.494 kg/m²s.

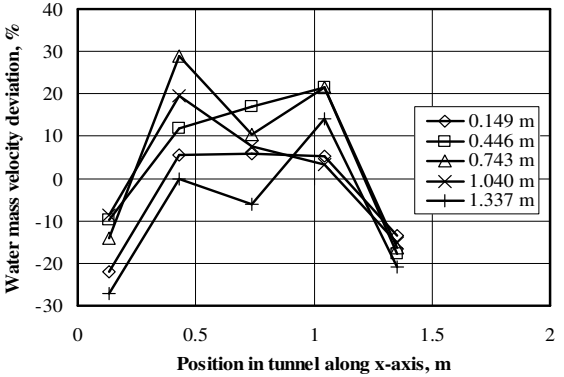

Figure E-28: Water mass velocity deviation under 0.5 m trickle fill with G_w = 3.006 kg/m²s.

Integrated G_w	1.518 kg/m²s
Flow meter G_w	1.494 kg/m²s
Percentage difference	1.653 %
Wall bypass G_w	0.036 kg/m²s
Percentage wall bypass	2.423 %
Christiansen coefficient	0.835

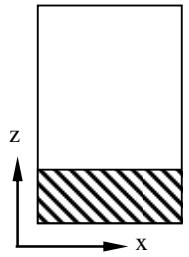

Integrated G_w	3.049 kg/m²s
Flow meter G_w	3.006 kg/m²s
Percentage difference	1.421 %
Wall bypass G_w	0.089 kg/m²s
Percentage wall bypass	2.945 %
Christiansen coefficient	0.844

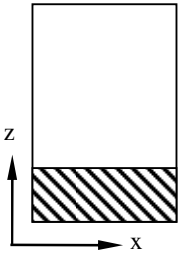

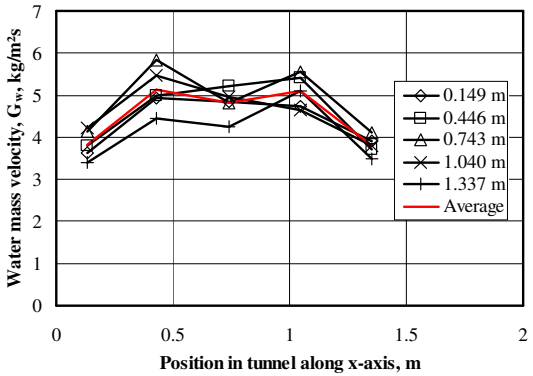

Figure E-29: Water mass velocity distribution under 0.5 m trickle fill with G_w = 4.468 kg/m²s.

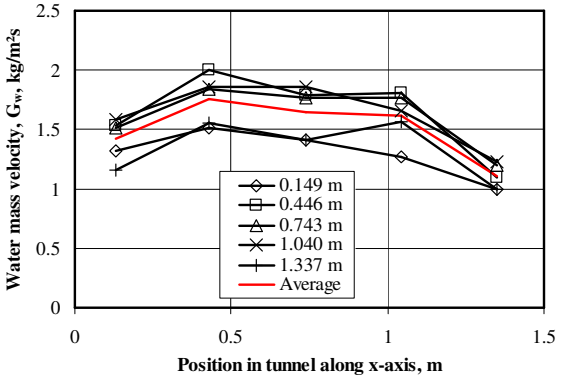

Figure E-30: Water mass velocity distribution under 1.0 m trickle fill with G_w = 1.496 kg/m²s.

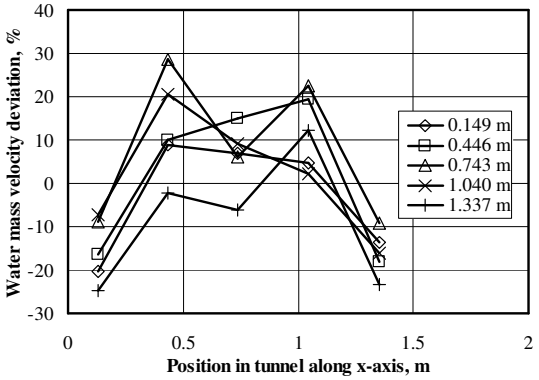

Figure E-31: Water mass velocity deviation under 0.5 m trickle fill with G_w = 4.468 kg/m²s.

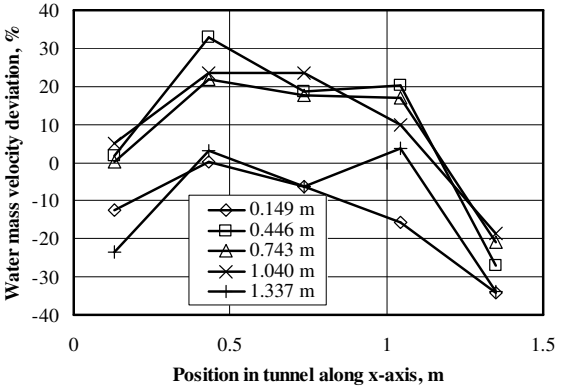

Figure E-32: Water mass velocity deviation under 1.0 m trickle fill with G_w = 1.496 kg/m²s.

Integrated G_w	4.537 kg/m²s
Flow meter G_w	4.468 kg/m²s
Percentage difference	1.543 %
Wall bypass G_w	0.1469 kg/m²s
Percentage wall bypass	3.287 %
Christiansen coefficient	0.849

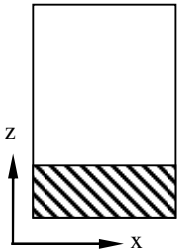

Integrated G_w	1.561 kg/m²s
Flow meter G_w	1.496 kg/m²s
Percentage difference	4.336 %
Wall bypass G_w	0.052 kg/m²s
Percentage wall bypass	3.477 %
Christiansen coefficient	0.828

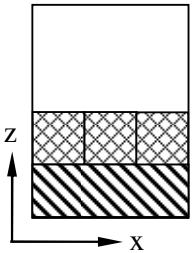

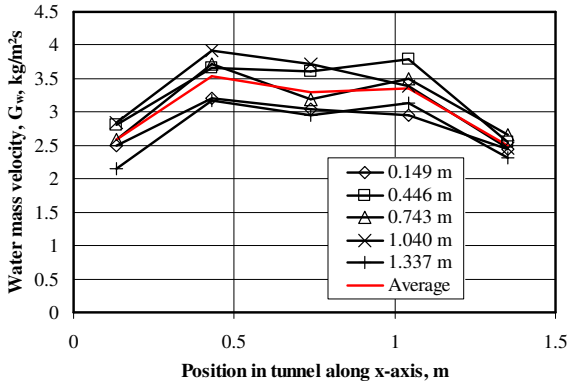

Figure E-33: Water mass velocity distribution under 1.0 m trickle fill with G_w = 3.041 kg/m²s.

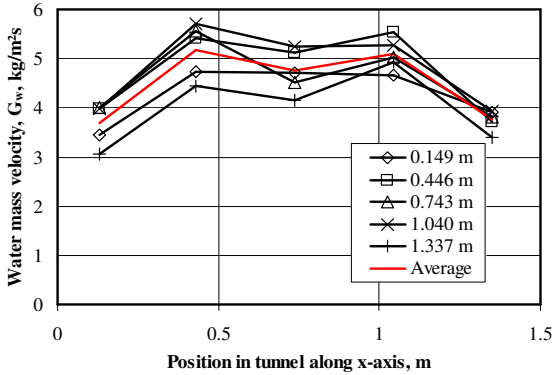

Figure E-34: Water mass velocity distribution under 1.0 m trickle fill with G_w = 4.504 kg/m²s.

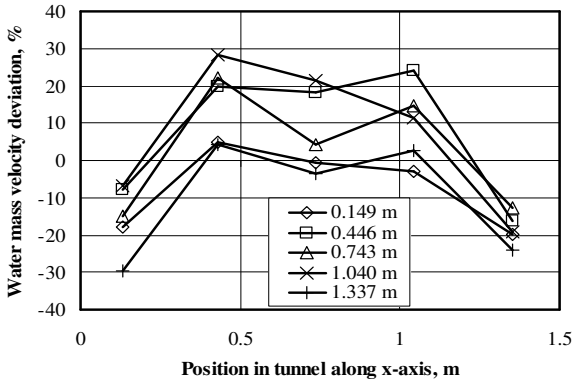

Figure E-35: Water mass velocity deviation under 1.0 m trickle fill with G_w = 3.041 kg/m²s.

Integrated G_w	3.174 kg/m²s
Flow meter G_w	3.041 kg/m²s
Percentage difference	4.377 %
Wall bypass G_w	0.125 kg/m²s
Percentage wall bypass	4.101 %
Christiansen coefficient	0.842

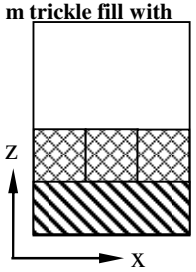

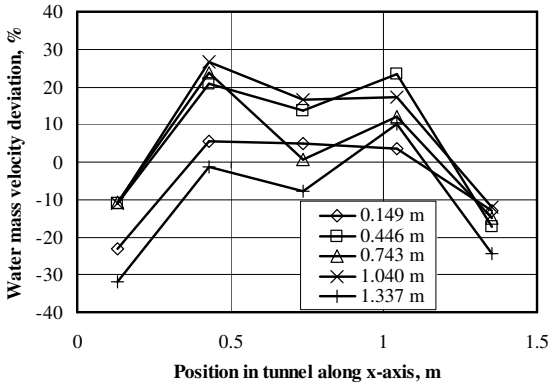

Figure E-36: Water mass velocity deviation under 1.0 m trickle fill with G_w = 4.504 kg/m²s.

Integrated G_w	4.678 kg/m²s
Flow meter G_w	4.504 kg/m²s
Percentage difference	3.880 %
Wall bypass G_w	0.184 kg/m²s
Percentage wall bypass	4.088 %
Christiansen coefficient	0.839

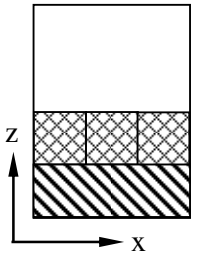

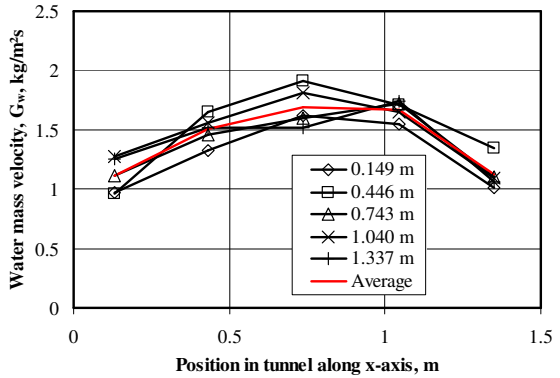

Figure E-37: Water mass velocity distribution under 1.5 m trickle fill with G_w = 1.491 kg/m²s.

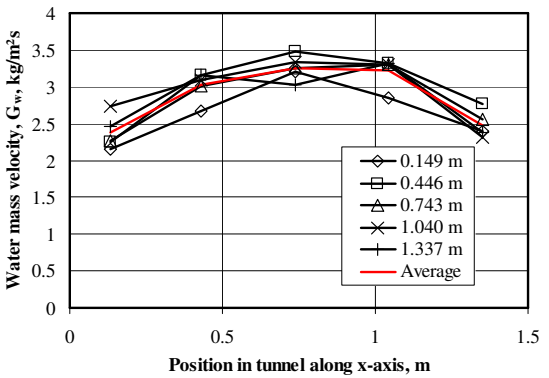

Figure E-38: Water mass velocity distribution under 1.5 m trickle fill with G_w = 2.997 kg/m²s.

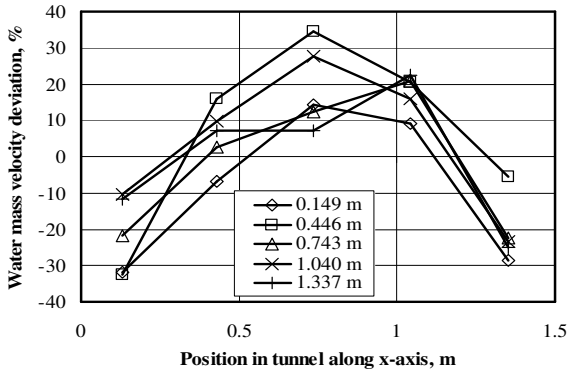

Figure E-39: Water mass velocity deviation under 1.5 m trickle fill with G_w = 1.491 kg/m²s.

Integrated G_w	1.530 kg/m²s
Flow meter G_w	1.491 kg/m²s
Percentage difference	2.605 %
Wall bypass G_w	0.108 kg/m²s
Percentage wall bypass	7.286 %
Christiansen coefficient	0.806

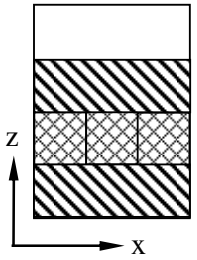

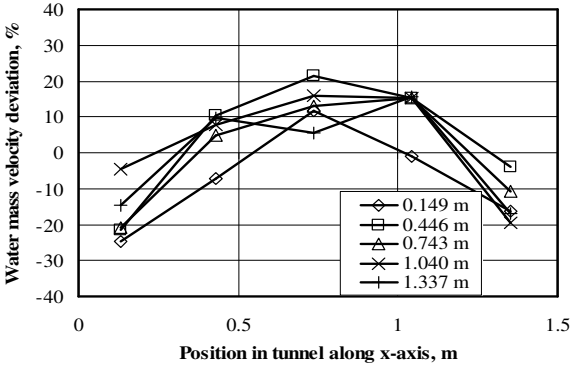

Figure E-40: Water mass velocity deviation under 1.5 m trickle fill with G_w = 2.997 kg/m²s.

Integrated G_w	3.108 kg/m²s
Flow meter G_w	2.997 kg/m²s
Percentage difference	3.714 %
Wall bypass G_w	0.237 kg/m²s
Percentage wall bypass	7.899 %
Christiansen coefficient	0.853

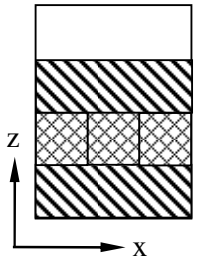

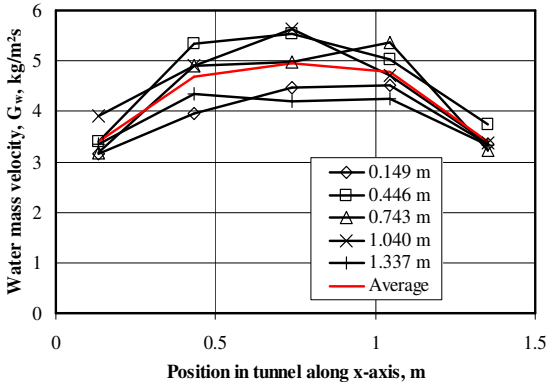

Figure E-41: Water mass velocity distribution under 1.5 m trickle fill with G_w = 4.423 kg/m²s.

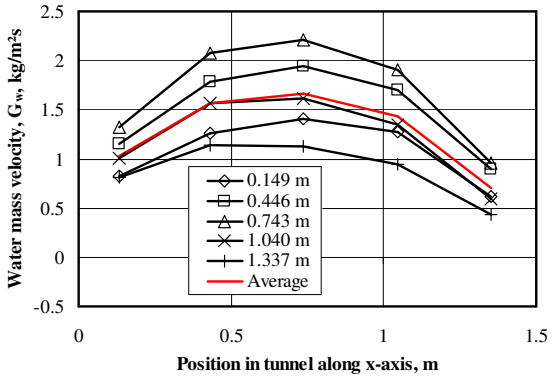

Figure E-42: Water mass velocity distribution under 2.04 m splash fill with G_w = 1.514 kg/m²s.

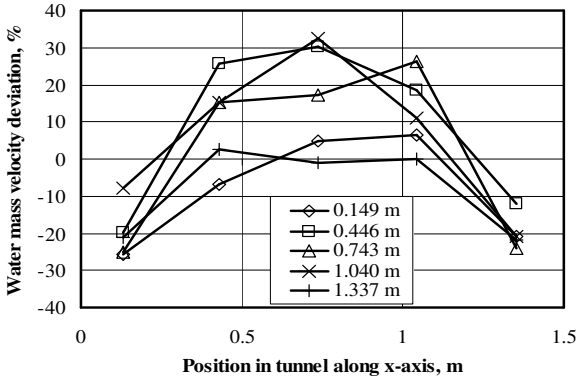

Figure E-43: Water mass velocity deviation under 1.5 m trickle fill with G_w = 4.423 kg/m²s.

Integrated G_w	4.590 kg/m²s
Flow meter G_w	4.423 kg/m²s
Percentage difference	3.776 %
Wall bypass G_w	0.342 kg/m²s
Percentage wall bypass	7.725 %
Christiansen coefficient	0.818

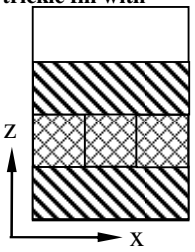

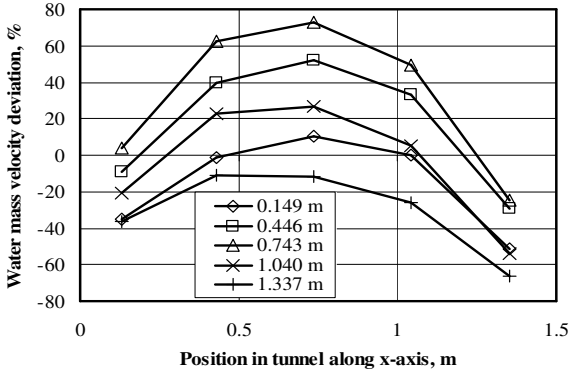

Figure E-44: Water mass velocity deviation under 2.04 m splash fill with G_w = 1.514 kg/m²s.

Integrated G_w	1.569 kg/m²s
Flow meter G_w	1.514 kg/m²s
Percentage difference	3.594 %
Wall bypass G_w	0.292 kg/m²s
Percentage wall bypass	19.252 %
Christiansen coefficient	0.683

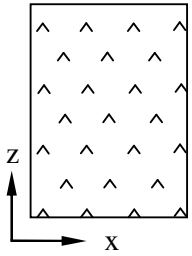

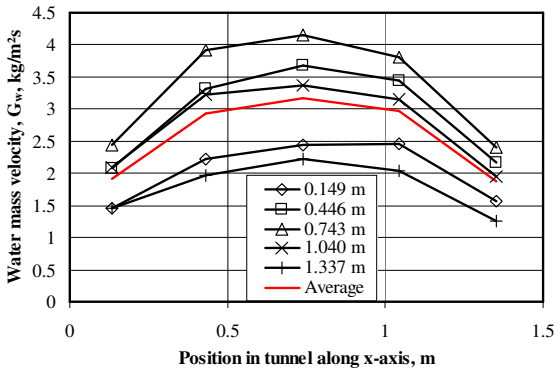

Figure E-45: Water mass velocity distribution under 2.04 m splash fill with G_w = 3.000 kg/m²s.

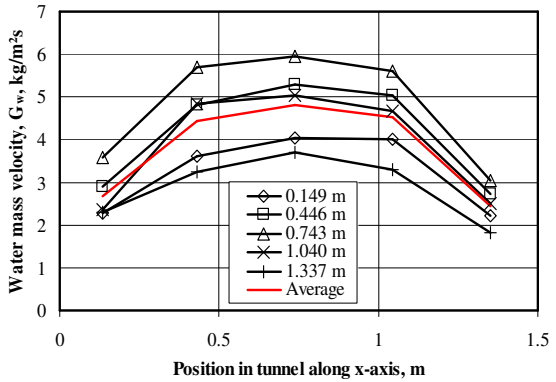

Figure E-46: Water mass velocity distribution under 2.04 m splash fill with G_w = 4.479 kg/m²s.

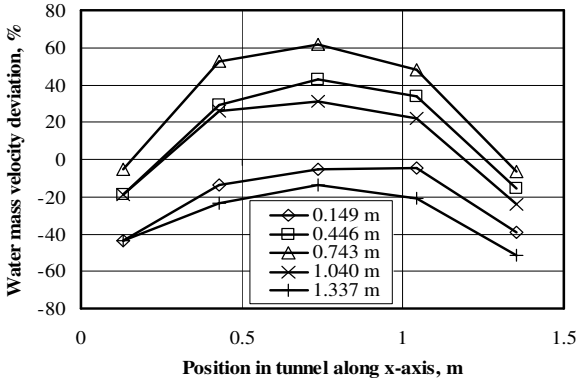

Figure E-47: Water mass velocity deviation under 2.04 m splash fill with G_w = 3.000 kg/m²s.

Integrated G_w	3.135 kg/m²s
Flow meter G_w	3.000 kg/m²s
Percentage difference	4.518 %
Wall bypass G_w	0.486 kg/m²s
Percentage wall bypass	16.189 %
Christiansen coefficient	0.708

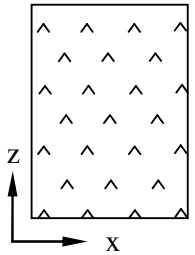

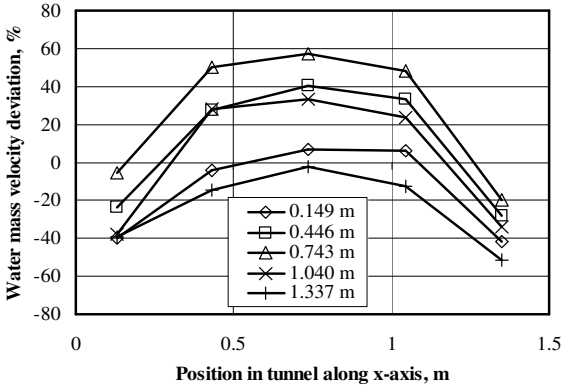

Figure E-48: Water mass velocity deviation under 2.04 m splash fill with G_w = 4.479 kg/m²s.

Integrated G_w	4.683 kg/m²s
Flow meter G_w	4.479 kg/m²s
Percentage difference	4.555 %
Wall bypass G_w	0.903 kg/m²s
Percentage wall bypass	20.148 %
Christiansen coefficient	0.701

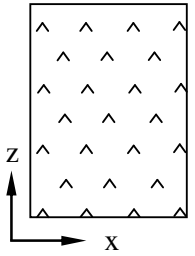

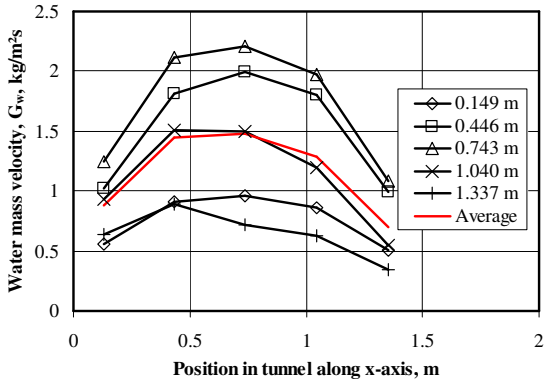

Figure E-49: Water mass velocity distribution under 3.04 m splash fill with G_w = 1.497 kg/m²s.

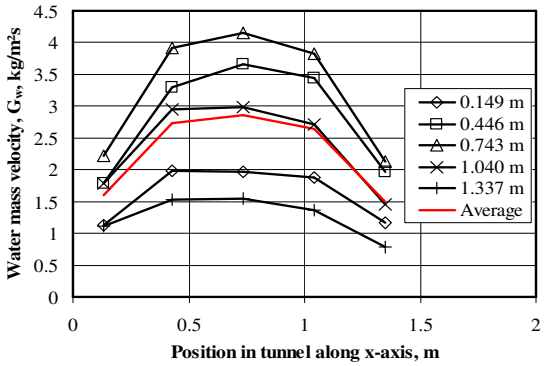

Figure E-50: Water mass velocity distribution under 3.04 m splash fill with G_w = 2.99 kg/m²s.

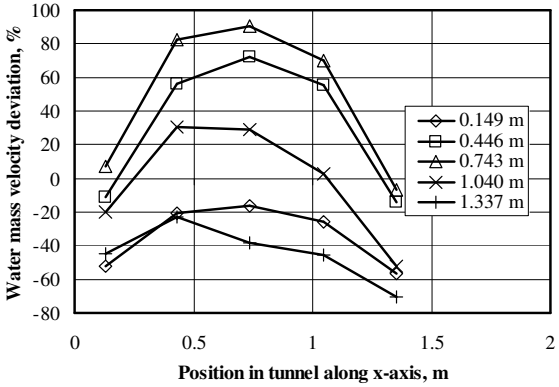

Figure E-51: Water mass velocity deviation under 3.04 m splash fill with G_w = 1.497 kg/m²s.

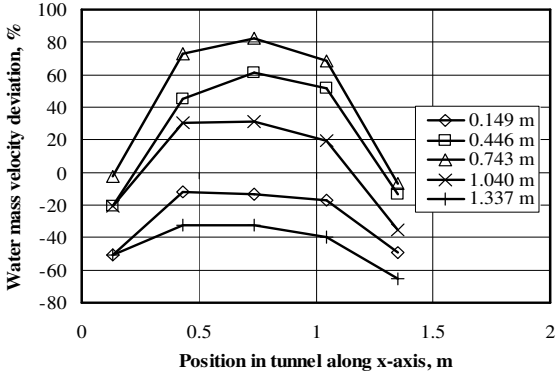

Figure E-52: Water mass velocity deviation under 3.04 m splash fill with G_w = 2.99 kg/m²s.

Integrated G_w	1.440 kg/m²s
Flow meter G_w	1.497 kg/m²s
Percentage difference	-3.825 %
Wall bypass G_w	0.283 kg/m²s
Percentage wall bypass	18.902 %
Christiansen coefficient	0.592

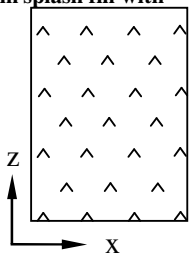

Integrated G_w	2.886 kg/m²s
Flow meter G_w	2.989 kg/m²s
Percentage difference	-3.456 %
Wall bypass G_w	0.615 kg/m²s
Percentage wall bypass	20.567 %
Christiansen coefficient	0.615

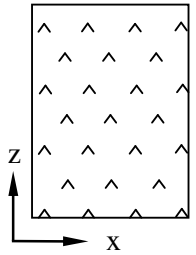

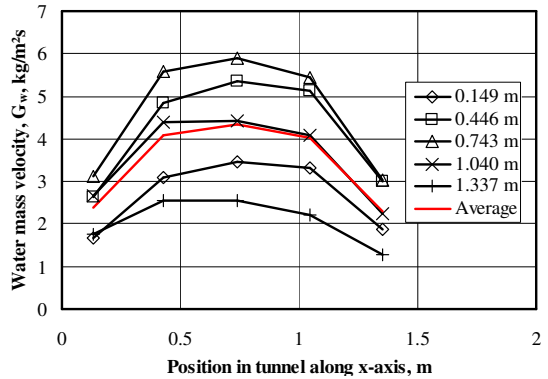

Figure E-53: Water mass velocity distribution under 3.04 m splash fill with G_w = 4.422 kg/m²s.

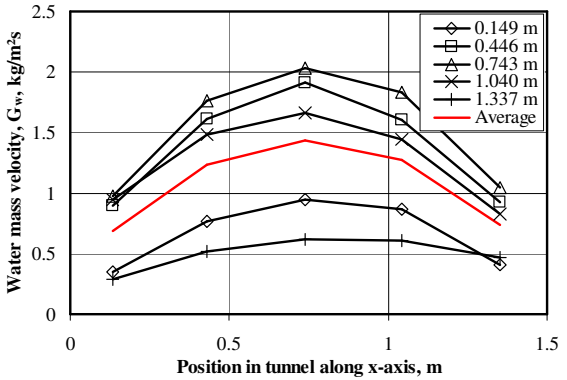

Figure E-54: Water mass velocity distribution under 4.04 m splash fill with G_w = 1.508 kg/m²s.

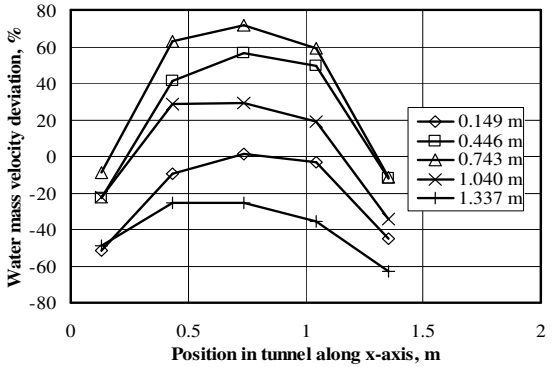

Figure E-55: Water mass velocity deviation under 3.04 m splash fill with G_w = 4.422 kg/m²s.

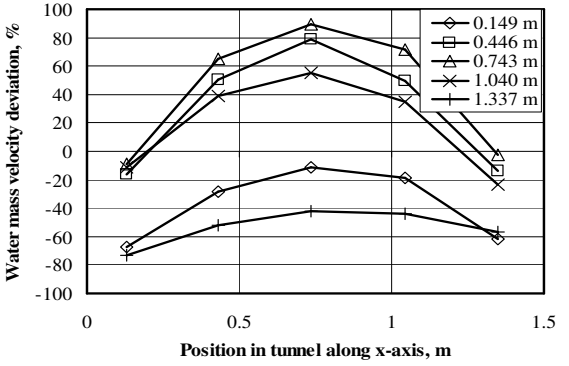

Figure E-56: Water mass velocity deviation under 4.04 m splash fill with G_w = 1.508 kg/m²s.

Integrated G_w	4.245 kg/m²s
Flow meter G_w	4.422 kg/m²s
Percentage difference	-4.006 %
Wall bypass G_w	0.823kg/m²s
Percentage wall bypass	18.61%
Christiansen coefficient	0.650

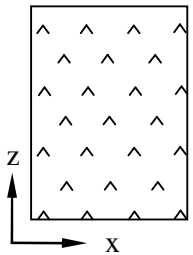

Integrated G_w	1.580 kg/m²s
Flow meter G_w	1.508 kg/m²s
Percentage difference	4.816 %
Wall bypass G_w	0.471 kg/m²s
Percentage wall bypass	31.233 %
Christiansen coefficient	0.560

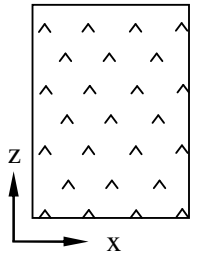

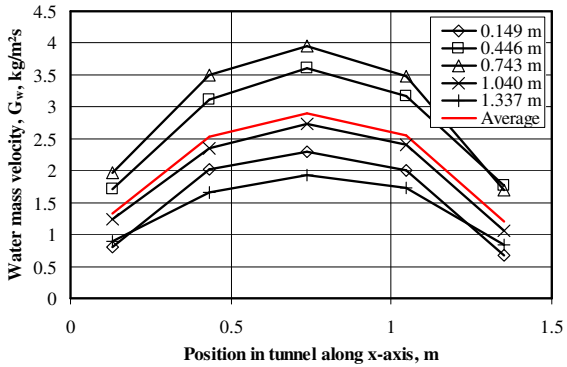

Figure E-57: Water mass velocity distribution under 4.04 m splash fill with G_w = 2.977 kg/m²s.

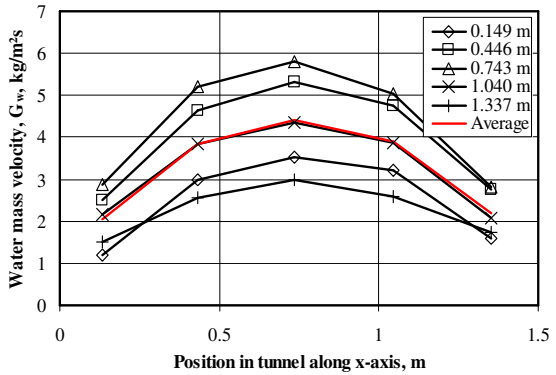

Figure E-58: Water mass velocity distribution under 4.04 m splash fill with G_w = 4.46 kg/m²s.

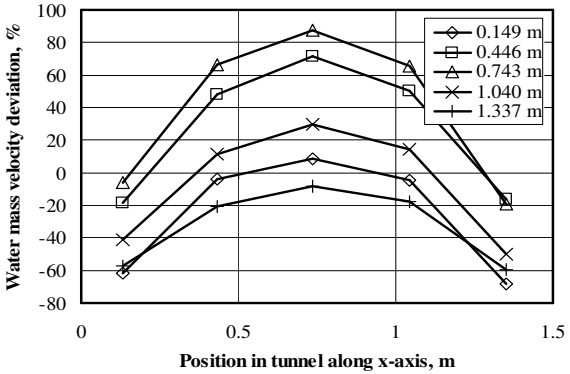

Figure E-59: Water mass velocity deviation under 4.04 m splash fill with G_w = 2.977 kg/m²s.

Integrated G_w	2.911 kg/m²s
Flow meter G_w	2.977 kg/m²s
Percentage difference	-2.215 %
Wall bypass G_w	0.807 kg/m²s
Percentage wall bypass	27.112 %
Christiansen coefficient	0.623

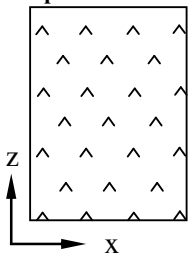

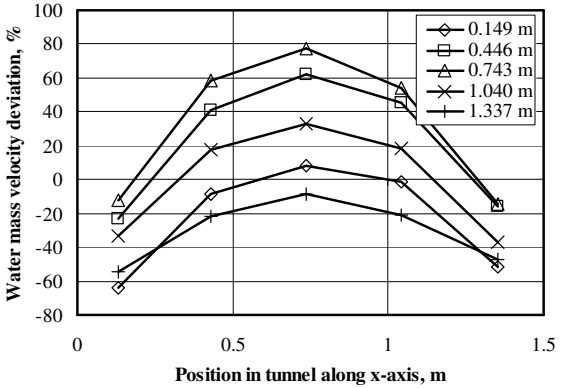

Figure E-60: Water mass velocity deviation under 4.04 m splash fill with G_w = 4.46 kg/m²s.

Integrated G_w	4.322 kg/m²s
Flow meter G_w	4.460 kg/m²s
Percentage difference	-3.097 %
Wall bypass G_w	1.107 kg/m²s
Percentage wall bypass	24.816 %
Christiansen coefficient	0.654

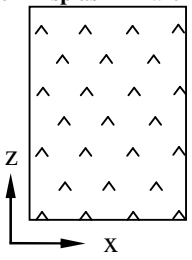

APPENDIX F. MERKEL NUMBER AND LOSS COEFFICIENT NUMERICAL EXAMPLE

Sample calculations illustrating how the Merkel number and loss coefficient are calculated for 1.22 m height of cross-fluted, mechanically bonded, treated film-type fill with spray frame water distribution, a 150 mm spray zone and two separate methods of measuring the water inlet and outlet temperatures enabling two independent Merkel numbers to be calculated. A water mass velocity of $G_w = 2.998$ kg/m^{2}s and an air mass velocity of $G_a = 2.5$ kg/m^{2}s are used in this example, as found in Table G-2. Figure F-1 illustrates the setup.

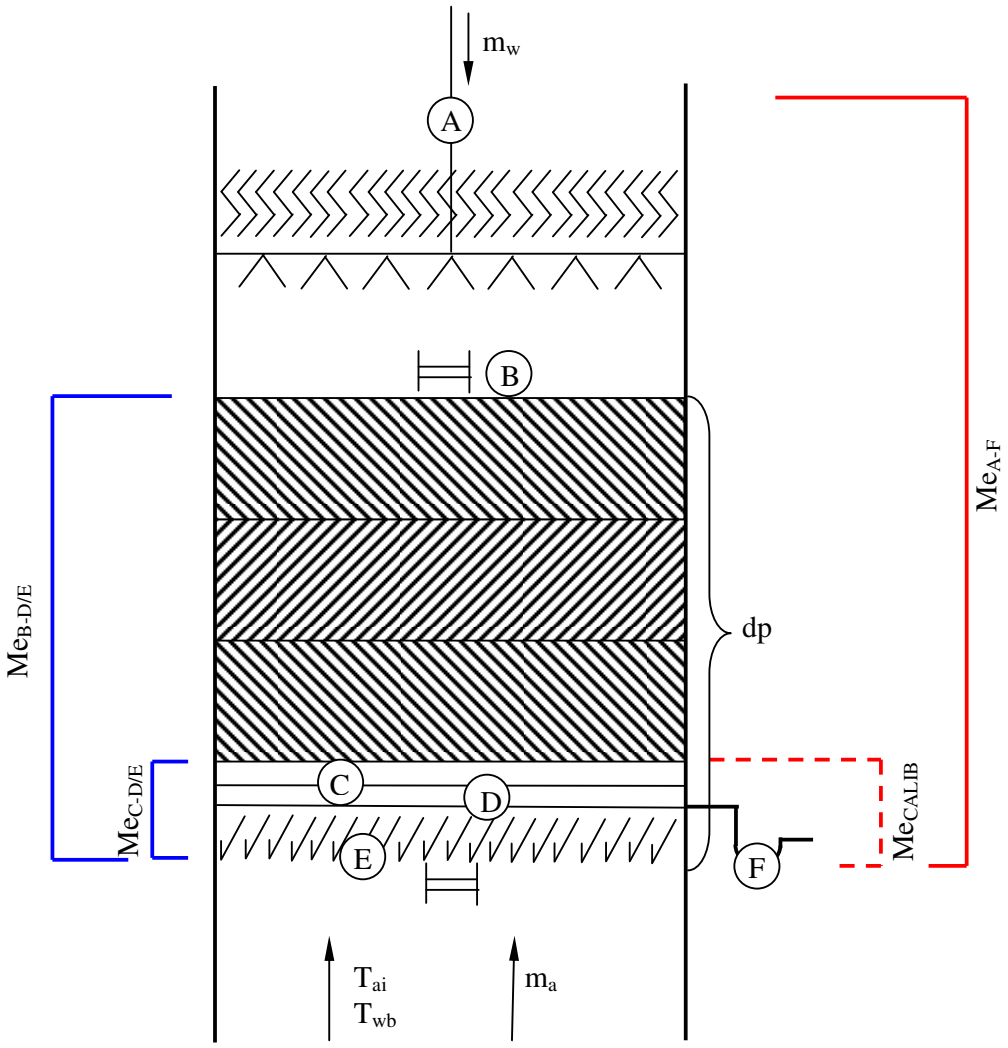

Figure F-1: Illustration of 1.22 m cross-fluted film fill test setup.

This sample calculation follows the example given in Kröger (2004). Hot water is sprayed through the spray frame into the test section. The water falls through the spray zone and lands in the fill. It moves downward through the fill and is eventually caught by the extraction troughs below the fill. Air is forced to flow uniformly upwards through the fill. The test fill pack has a cross-sectional area of 1.5 m x 1.5 m = 2.25 m².

The measured values associated with the test are:

Atmospheric pressure	$p_a = 100350$ N/m^2
Air inlet temperature	$T_{ai} = 14.2$ °C (287.35 K)
Air inlet temperature (wet-bulb)	$T_{wb} = 12.5$ °C (285.65 K)
Dry air mass flow rate	$m_a = 5.625$ kg/s
Water mass flow rate (in)	$m_w = 6.746$ kg/s

In calculating the Merkel number and loss coefficient it is assumed that the mean water mass flow rate is equivalent to the inlet water mass flow rate.

The Merkel equation is given as

$$\frac{h_d a_{fi} A_{fr} L_{fi}}{m_w} = \frac{h_d a_{fi} L_{fi}}{G_w} = \int_{Two}^{Twi} \frac{c_{pw}}{(i_{masw} - i_{ma})} dT_w$$

The term $h_d a_{fi} L_{fi}/G_w$ is identified as the Merkel number and is a dimensionless coefficient of performance or transfer characteristic.

The integral in the Merkel equation is solved using Chebyshev's solution, which uses values of the integrand at predetermined values within the interval over which the integral is solved. These predetermined values are selected such that the sum of these values multiplied by a constant gives the desired approximate integral. The four-point Chebyshev formula is

$$\int_a^b f(x)dx \approx \frac{(b-a)}{4}\left[f(x_1) + f(x_2) + f(x_3) + f(x_4)\right]$$

The values of f(x) have to be evaluated for values of x that are 0.102673, 0.406204, 0.593796 and 0.897327 of the interval (b-a). The values are rounded off to the nearest tenth and the results are still good. Values $f(x_1)$, $f(x_2)$, $f(x_3)$ and $f(x_4)$ have to be evaluated at the following x-values:

$f(x_1)$ = value of f(x) at x = a + 0.1(b-a)
$f(x_2)$ = value of f(x) at x = a + 0.4(b-a)
$f(x_3)$ = value of f(x) at x = a + 0.6(b-a)
$f(x_4)$ = value of f(x) at x = a + 0.9(b-a)

Applying the Chebyshev method to the Merkel equation gives:

$$\frac{h_d a_{fi} A_{fr} L_{fi}}{m_w} = \frac{h_d a_{fi} L_{fi}}{G_w} = \int_{T_{wo}}^{Twi} \frac{c_{pw}}{i_{masw} - i_{ma}} dT_w$$

$$\approx \frac{(T_{wi} - T_{wo})}{4}\left[\frac{c_{pw1}}{\Delta i_{(1)}} + \frac{c_{pw2}}{\Delta i_{(2)}} + \frac{c_{pw3}}{\Delta i_{(3)}} + \frac{c_{pw4}}{\Delta i_{(4)}}\right]$$

$$\approx \frac{c_{pwm}(T_{wi} - T_{wo})}{4}\left[\frac{1}{\Delta i_{(1)}} + \frac{1}{\Delta i_{(2)}} + \frac{1}{\Delta i_{(3)}} + \frac{1}{\Delta i_{(4)}}\right]$$

The calibrated Merkel number is first examined. The Merkel number of the entire setup is determined. This includes the effects of the spray zone, the fill and the water extraction troughs. Any effects of the tunnel on the Merkel number, other than the fill, are quantified by conducting thermal tests in the tunnel with no fill and a 150 mm spray zone above the extraction troughs, as described in Section 6.2.1. Here the water inlet temperature is measured at location A and the water outlet temperature is measured at location F. The temperature used for the Merkel number correction for the troughs is measured at location C in Figure F-1, according to the discussion in Section 6.2.1.

Water inlet temperature (location A)	T_{wi} = 40.85 °C (314 K)
Water outlet temperature (location F)	T_{wo} = 24.27 °C (297.42 K)
Water temperature in troughs (location C)	T_{wtr} = 25.75 °C (298.9 K)

The mean specific heat of the water c_{pwm} is evaluated at the mean water temperature or $(T_{wi} + T_{wo})/2 = (314 + 297.42)/2 = 305.707$ K using Equation (A.4.2)

$c_{pwm} = 8.15599 \times 10^{3} - 2.80627 \times 10 \times 305.768 + 5.11283 \times 10^{-2} \times 305.768^{2}$
$- 2.17582 \times 10^{-13} \times 305.768^{6} = 4177.707$ J/kg K

The enthalpy differentials, Δi, are dependent on the following intermediate temperatures:

$T_{w(1)} = T_{wo} + 0.1(T_{wi} - T_{wo}) = 297.42 + 0.1(314 - 297.42) = 299.075$ K
$T_{w(2)} = T_{wo} + 0.4(T_{wi} - T_{wo}) = 297.42 + 0.4(314 - 297.42) = 304.049$ K
$T_{w(3)} = T_{wo} + 0.6(T_{wi} - T_{wo}) = 297.42 + 0.6(314 - 297.42) = 307.365$ K
$T_{w(4)} = T_{wo} + 0.9(T_{wi} - T_{wo}) = 297.42 + 0.9(314 - 297.42) = 312.339$ K

The bracketed numbers one to four refer to the Chebyshev intervals in the four-point approximation.

The enthalpy per unit mass of dry air entering the fill is determined using Equation (A.3.4b). Certain thermophysical properties have to be determined at temperature $(T_{ai} + 273.15)/2 = (287.35 + 273.15)/2 = 280.251$ K.

Specific heat of dry air from Equation (A.1.2)

$c_{pai} = 1.045356 \times 10^{3} - 3.161783 \times 10^{-1} \times 280.251 + 7.083814 \times 10^{-4} \times (280.251)^{2}$
$- 2.705209 \times 10^{-7} \times (280.251)^{3} = 1006.429$ J/kg K

Specific heat of water vapour from Equation (A.2.2)

$c_{pvi} = 1.3605 \times 10^{3} + 2.31334 \times 280.251 - 2.46784 \times 10^{-10} \times (280.251)^{5}$
$+ 5.91332 \times 10^{-13} \times (280.251)^{6} = 1868.677$ J/kg K

Pressure of water vapour from Equation (A.2.1) evaluated at $T_{wb} = 285.65$ K with

$z = 10.79586(1 - 273.16/285.65) + 5.02808 \log_{10}(273.16/285.65)$
$+ 1.50474 \times 10^{-4} [1 - 10^{-8.29692\{(285.65/273.16) - 1\}}]$
$+ 4.2873 \times 10^{-4}[10^{4.76955(1 - 273.16/285.65)} - 1] + 2.786118312 = 3.16080101$

and

$p_{vi} = 10^{3.16080101} = 1448.108$ N/m^2

Humidity ratio from Equation (A.3.3)

$$w_i = \left(\frac{2501.6 - 2.3263(287.35 - 273.15)}{2501.6 + 1.8577(287.35 - 273.15) - 4.184(285.25 - 273.15)} \right) \times \left(\frac{0.6250 \times 1448.108}{100350 - 1.005 \times 1448.108} \right) - \left(\frac{1.00416(287.35 - 285.25)}{2501.6 + 1.8577(287.35 - 273.15) - 4.184(285.25 - 273.15)} \right)$$

$= 0.00845029497$ kg/kg dry air

Latent heat at 273.15 K follows from Equation (A.4.3)

$i_{fgwo} = 3.4831814 \times 10^{6} - 5.8627703 \times 10^{3} \times 273.15 + 12.139568 \times 273.15^{2}$
$- 1.40290431 \times 10^{-2} \times 273.15^{3} = 2501598.533$ J/kg

Upon substitution of the above properties into Equation (A.3.4b), find the enthalpy of the entering air.

$i_{mai} = 1006.429 (287.35 - 273.15)$
$+ 0.00845029497 [2501598.533 + 1868.677 (287.35 - 273.15)]$
$= 35655.789$ J/kg dry air

Similarly, to find the enthalpy of the saturated air at the local bulk water temperature $T_{w(1)}$ = 299.075 K, the following properties must be determined at $(T_{w(1)} + 273.15)/2 = (299.075 + 273.15)/2 = 286.11$ K.

Specific heat of dry air from Equation (A.1.2)

$$c_{pa(1)} = 1045.356 - 3.161783 \times 10^{-1} \times 286.11 + 7.083814 \times 10^{-4}(286.11)^2 - 2.705209 \times 10^{-7}(286.11)^3 = 1006.546 \text{ J/kg K}$$

Specific heat of water vapour from Equation (A.2.2)

$$c_{pv(1)} = 1360.5 + 2.31334 \times 286.11 - 2.46784 \times 10^{-10} \times (286.11)^5 + 5.91332 \times 10^{-13} \times (286.11)^6 = 1873.602 \text{ J/kg K}$$

Pressure of water vapour at $T_{w(1)}$ = 299.075 K from Equation (A.2.1) with

$$z = 10.79586(1 - 273.16/299.075) + 5.02808 \log_{10}(273.16/299.075) + 1.50474 \times 10^{-4}[1 - 10^{-8.29692\{(299.075/273.16) - 1\}}] + 4.2873 \times 10^{-4}[10^{4.76955(1 - 273.16/299.075)} - 1] + 2.786118312 = 3.524472$$

to give

$$p_{vi} = 10^{3.524472} = 3345.586 \text{ N/m}^2$$

Humidity ratio for saturated air at 304.683 K from Equation (A.3.3)
$w_{s(1)} = 0.62509 \times 3345.586 /(100350 - 1.005 \times 3345.586) = 0.02456245$ kg/kg dry air

The enthalpy of saturated air evaluated at the local bulk water temperature $T_{w(1)}$ = 299.075 K, follows Equation (A.3.4b)

$$i_{masw(1)} = 1006.546 (299.075 - 273.15) + 0.02456245 [2501598.5334 + 1873.602 (299.075 - 273.15)] = 81082.655 \text{ J/kg dry air}$$

The enthalpy of the air at $T_{w(1)}$ = 299.075 K is

$$i_{ma(1)} = m_w c_{pwm}(T_{w(1)} - T_{wo})/m_a + i_{mai} = 6.746 \times 4177.406 (299.075 - 297.707)/ 5.625 + 35655.789 = 43962.214 \text{ J/kg dry air}$$

With the above enthalpies, find
$\Delta i_{(1)} = (i_{masw(1)} - i_{ma(1)}) = 81082.655 - 43962.214 = 37120.441$ J/kg dry air

Similarly, the values of the other differentials are found to be
$\Delta i_{(2)}$ = 36768.864 J/kg dry air
$\Delta i_{(3)}$ = 39895.916 J/kg dry air
$\Delta i_{(4)}$ = 50983.897 J/kg dry air

With these values the Merkel equation for the spray zone, fill and troughs becomes

$$\frac{h_d a_{fi} L_{fi}}{G_w} \approx \frac{4177.707(314 - 297.417)}{4} \times \left[\frac{1}{37120.441} + \frac{1}{36768.864} + \frac{1}{39895.916} + \frac{1}{50983.897}\right]$$

$$Me_{A-F} = 1.711$$

The Merkel number contribution for the 150 mm spray zone and the troughs is correlated by Equation (6.2) from Section 6.2.1
$Me_{CALIB} = 0.386 G_w^{-0.742} G_a^{0.727} T_{wtr}^{-0.226}$
$Me_{CALIB} = 0.386(2.998)^{-0.742}(2.5)^{0.727}(298.896-273.15)^{-0.226}$
$= 0.160$

The resulting Merkel number of only the 1.22 m cross-fluted fill is
$Me = Me_{A-F} - Me_{CALIB} = 1.711 - 0.160$
$= 1.551$

Calculating this per metre fill results in

$Me_1 = 1.272\ m^{-1}$

The Merkel number calculation is repeated to calculate the Merkel number between points B and D/E, which represents the performance of the fill and the troughs. (The location of the inlet water temperature results in no compensation necessary for the spray zone, as the temperature measured is indeed the temperature of the water entering the fill.) The effects of the troughs are quantified by performing the Merkel number calculation again using location C as the water inlet temperature measurement location and location D/E as the water outlet temperature measurement location.

Similarly, for Merkel number B-D/E

Water inlet temperature (location B) T_{wi} = 40.12 °C (313.15 K)
Water outlet temperature (location D/E) T_{wo} = 24.13 °C (297.28 K)

$Me_{B-D/E} = 1.701$

Repeating the calculation for Merkel number C-D/E

Water inlet temperature (location C) T_{wi} = 25.75 °C (298.9 K)
Water outlet temperature (location D/E) T_{wo} = 24.13 °C (297.28 K)
$Me_{C\text{-}D/E}$ = 0.182

The resulting Merkel number of only the 1.22 m cross-fluted fill is
$Me = Me_{B\text{-}D/E} - Me_{C\text{-}D/E} = 1.701 - 0.182$

= 1.519

Calculating the Merkel number per metre fill gives
Me_1 = 1.245

Static pressure drop across fill and troughs is dp = 54.165 N/m^2 The resulting loss coefficient is determined as follows.

The measured pressure drop over the fill is attributed to frictional and drag resistances in addition to the acceleration of the air as a result of heating and mass transfer.

$$\Delta p_{fi} = \Delta p_{fd} + \left(\rho_{avo} v^2_{avo} - \rho_{avi} v^2_{avi}\right)$$

where the subscript fd refers to frictional and drag. The second term on the right-hand side of the equation represents the momentum change experienced by the air stream. The loss coefficient determined by frictional and drag effects can be defined in terms of the mean air-vapour flow rate and its density through the test section as

$$K_{fd} = \frac{2\Delta p_{fd}}{\rho v^2} = \frac{2\left[\Delta p_{fi} - \left(\rho_{avo} v^2_{avo} - \rho_{avi} v^2_{avi}\right)\right]}{\rho v^2_{avm}}$$

where $v_{avm} = m_{avm} / \rho_{avm} A_{fr}$ and $m_{avm} = \left(m_{avi} + m_{avo}\right)/2$

or

$$K_{fd} = 2\left[\Delta p_{fi} - \left(\rho_{avo} v^2_{avo} - \rho_{avi} v^2_{avi}\right)\right] \rho_{avm} A^2_{fr} / m^2_{avm}$$

To find the mean density of the air-vapour mixture through the fill, certain thermophysical properties must be determined.

According to Equation (A.3.1) the density of the inlet air at T_{ai} = 14.2°C is

$$\rho_{avi} = (1+\omega_i)[1-\omega_i/(\omega_i+0.62198)][p_a/287.08T_{ai}]$$
$$= (1+0.0084502949)\left[1-\frac{0.0084502949}{(0.0084502949+0.62198)}\right]\left[\frac{100350}{287.08(14.2+273.15)}\right]$$
$$= 1.210\ \text{kg/m}^3$$

The inlet air-vapour mass flow rate is
$m_{avi} = m_a + \omega_i m_a = 5.625 + 0.0084502949 \times 5.625 = 5.673$ kg/s

The corresponding velocity of the air entering the fill is
$v_{avi} = m_{avi}/\rho_{avi} A_{fr} = 5.673/(1.21 \times 1.5 \times 1.5) = 2.083$ m/s

According to the conservation of energy
$m_a(i_{mao} - i_{mai}) = m_w c_{pwm}(T_{wi} - T_{wo})$

Rearrange this equation to find and expression for the enthalpy of the outlet air.
$i_{mao} = m_w c_{pwm}(T_{wi} - T_{wo})/m_a + i_{mai}$
$= 6.746 \times 4177.707(313.997 - 297.417)/5.625 + 35655.789 = 118420.033$ J/kg dry air

Since it is assumed that the air leaving the fill (outlet air) is saturated, it follows from Equation (A.3.4b) that
$i_{mao} = i_{maos} = c_{pao}T_{ao} + \omega_{so}(i_{fgwo} + c_{pvo}T_{ao}) = 118720.033$ J/kg dry air

The thermophysical properties c_{pao}, ω_{so} and c_{pvo} are all functions of T_{ao}, and the latter can thus be determined from this equation by following an iterative procedure. Find T_{ao} = 33.15 °C (306.3 K).

To confirm that this is correct, evaluate the abovementioned thermophysical properties.

The mean specific heat of dry air is evaluated at 33.15/2 °C or 289.725 K according to Equation (A.1.2)
$$c_{pao} = 1.045356 \times 10^3 - 3.161783 \times 10^{-1} \times 289.725 + 7.083814 \times 10^{-4} \times 289.725^2$$
$$- 2.705209 \times 10^{-7} \times 289.725^3$$
$$= 1006.634\ \text{J/kgK}$$

Similarly the specific heat of water vapour at the temperature follows from Equation (A.2.2)

$$c_{pvo} = 1.3605\times10^{3} + 2.31334\times289.725 - 2.46784\times10^{-10}\times289.725^{5} + 5.91332\times10^{-13}\times289.725^{6} = 1876.687 \text{ J/kgK}$$

The pressure of the saturated water vapour at T_{ao} = 33.15 °C (306.3 K) is given by Equation (A.2.1)

$z = 10.79586(1 - 273.16/306.3) + 5.02808 \log_{10}(273.16/306.3)$
$+ 1.50474 \times 10^{-4} [1 - 10^{-8.29692\{(306.3/273.16) - 1\}}]$
$+ 4.2873 \times 10^{-4}[10^{4.76955(1 - 273.16/306.3)} - 1] + 2.786118312$
$= 3.70524985$

Thus

$p_{vo} = 10^{3.70524985} = 5072.825 \text{ N/m}^2$

The humidity ratio of the saturated air at this temperature is given by Equation (A.3.3)

$$\omega_{so} = \frac{0.62509\times5072.825}{100350 - 1.005\times5072.825} = 0.0332904 \text{ kg/kg dry air}$$

Substitute these properties into Equation (A.3.4b) and find

$i_{maos} = 1006.634 \times (306.3 - 273.15)$
$+ 0.0332904 \times (2501598.5334 + 1876.687 \times (306.3 - 273.15))$
$= 118720.033$ J/kg dry air

This value is in agreement with the value obtained for i_{mao}, which means that the given value of T_{ao} = 33.15 °C is correct.

The density of the outlet air at this temperature is, according to Equation (A.3.1),

$$\rho_{avo} = (1 + 0.0332904)\left[1 - \frac{0.0332904}{0.0332904 + 0.62198}\right]\left[\frac{100350}{287.08\times306.3}\right] = 1.119 \text{ kg/m}^3$$

The outlet air mass flow rate is

$$m_{avo} = m_a + \omega_{so} m_a = 5.625 + 0.0332904\times5.625 = 5.812 \text{ kg/s}$$

The corresponding velocity of the air leaving the fill is

$$v_{avo} = m_{avo}/(\rho_{avo} A_{fr}) = 5.812/(1.119\times1.5\times1.5) = 2.308 \text{ m/s}$$

The arithmetic mean air mass flow rate through the fill is thus

$$m_{avm} = \frac{m_{avi} + m_{avo}}{2} = \frac{5.672 + 5.812}{2} = 5.742\,\text{kg/s}$$

The harmonic mean density of the air through the fill is

$$\rho_{avm} = 2\left(\frac{1}{\rho_{avi}} + \frac{1}{\rho_{avo}}\right)^{-1} = 2\left(\frac{1}{1.21} + \frac{1}{1.119}\right)^{-1} = 1.163\,\text{kg/m}^3$$

Substitute these values into the equation defining the loss coefficient for the spray zone, fill and troughs

$$\begin{aligned} K_{fdm\_total} &= 2\left[\Delta p_{fi} - \left(\rho_{avo} v^2{}_{avo} - \rho_{avi} v^2{}_{avi}\right)\right]\rho_{avm} A_{fr}{}^2 \Big/ m^2{}_{avm} \\ &= 2\left[54.165 - \left(1.119 \times 2.308^2 - 1.21 \times 2.083^2\right)\right]1.163 \\ &\quad \times (1.5 \times 1.5)^2 \Big/ 5.742^2 \\ &= 19.291 \end{aligned}$$

The loss coefficient contribution for the 150 mm spray zone and the troughs is correlated by the Equation (6.6) in section 6.2.2.

$$\begin{aligned} K_{tr} &= 3.581 G_w{}^{0.243} G_a{}^{-0.388} \\ &= 3.581(2.998)^{0.243}(2.5)^{-0.388} \\ &= 3.278 \end{aligned}$$

with the resulting Merkel number of just the 1 m V-bar fill as

$K_{fdm} = K_{fdm\_total} - K_{tr} = 19.291 - 3.278$

$= 16.013$

Calculating the loss coefficient per metre fill gives

$K_{fdm1} = 13.126\ \text{m}^{-1}$

APPENDIX G. FILL TEST RESULTS

Table G-1: Sample of experimental data for empty tunnel tests.

p_a	L_{fi}	G_w	G_a	$Me_{(A-F)}$	$Me_{(B-C)}$	K_{dfm}	T_{noz_db}	T_{noz_wb}	T_{fill_db}	T_{fill_wb}	dp_{noz}	dp_{fi_ave}	$T_{wi(A)}$	$T_{wi(B)}$	$T_{wi(C)}$	$T_{wo(F)}$	$T_{wo(D/E)}$
N/m²	m	kg/m²s	kg/m²s				°C	°C	°C	°C	N/m²	N/m²	°C	°C	°C	°C	°C
100400	0.00	1.51	1.03	0.12	0.01	3.89	17.55	13.25	17.29	13.39	48.73	1.88	51.46	48.88	48.45	45.77	43.97
100400	0.00	1.50	1.51	0.14	0.01	3.29	17.71	13.17	17.42	13.12	105.53	3.42	51.24	47.99	47.50	44.40	42.48
100400	0.00	1.49	2.01	0.17	0.02	3.01	17.72	13.44	17.70	13.46	186.89	5.50	50.98	47.25	46.59	43.13	41.27
100400	0.00	1.49	2.50	0.21	0.02	2.81	17.71	13.26	17.95	13.38	287.53	7.90	50.74	46.51	45.57	41.80	40.22
100400	0.00	1.48	3.00	0.24	0.02	2.68	17.46	13.34	17.98	13.53	413.95	10.82	50.53	45.35	44.57	40.57	39.24
100400	0.00	1.50	3.50	0.31	0.02	2.55	17.47	13.47	18.26	13.79	563.38	14.09	50.34	43.59	42.76	38.59	37.43
100400	0.00	3.02	1.04	0.08	0.00	4.97	17.37	13.34	17.62	13.95	49.40	2.46	50.34	48.71	48.53	46.51	45.37
100400	0.00	3.01	1.52	0.10	0.01	3.95	17.19	13.38	17.53	13.81	106.59	4.20	50.23	48.19	47.85	45.59	44.34
100400	0.00	3.00	2.00	0.12	0.01	3.45	17.14	13.28	17.44	13.58	184.92	6.35	49.97	47.52	47.13	44.63	43.37
100400	0.00	2.98	2.52	0.14	0.01	3.14	17.07	13.30	17.64	13.73	292.51	9.11	49.74	46.91	46.42	43.74	42.50
100400	0.00	2.97	3.01	0.15	0.01	3.02	17.01	13.32	17.66	13.69	416.18	12.43	49.55	46.30	45.90	43.01	41.69
100400	0.00	2.99	3.51	0.17	0.02	2.90	16.94	13.44	17.84	13.84	566.26	16.20	49.37	45.86	45.25	42.27	40.85
100400	0.00	4.52	1.03	0.06	0.00	5.83	16.90	13.39	17.75	14.63	48.65	2.85	49.01	48.02	47.97	46.37	45.57
100400	0.00	4.51	1.50	0.08	0.00	4.49	16.88	13.35	17.49	14.20	103.96	4.67	48.69	47.40	47.26	45.43	44.56
100400	0.00	4.51	2.01	0.09	0.01	3.85	16.82	13.43	17.47	14.16	185.64	7.12	48.35	46.79	46.59	44.58	43.62
100400	0.00	4.50	2.51	0.10	0.01	3.51	16.78	13.37	17.69	14.21	290.55	10.13	48.03	46.23	46.02	43.84	42.83
100400	0.00	4.50	3.02	0.12	0.01	3.31	16.73	13.48	17.72	14.16	420.72	13.77	47.80	45.73	45.47	43.17	42.11
100400	0.00	4.49	3.51	0.13	0.01	3.18	16.69	13.35	17.72	13.92	567.00	17.80	47.53	45.19	44.91	42.47	41.36

Table G-2: Sample of performance evaluation data for film fill.

p_a	L_{fi}	G_w	G_a	$Me_{1(A-F)}$	$Me_{1(B-C)}$	K_{dfm1}	T_{noz_db}	T_{noz_wb}	T_{fill_db}	T_{fill_wb}	dp_{noz}	dp_{ftot}	dp_{fi}	$T_{wi(A)}$	$T_{wi(B)}$	$T_{wi(C)}$	$T_{wo(F)}$	$T_{wo(D/E)}$
N/m^2	m	kg/m^2s	kg/m^2s	m^{-1}	m^{-1}	m^{-1}	°C	°C	°C	°C	N/m^2	N/m^2	N/m^2	°C	°C	°C	°C	°C
100350	1.22	1.50	1.00	1.28	1.24	15.17	13.69	12.13	14.11	12.74	45.39	10.57	8.74	44.66	43.95	28.49	26.43	26.19
100350	1.22	1.49	1.51	1.72	1.68	13.43	13.66	12.10	14.00	12.52	103.65	20.84	17.35	44.06	42.80	23.96	22.24	21.97
100350	1.22	1.50	2.00	2.13	2.10	12.63	13.52	11.92	13.95	12.28	182.00	33.76	28.31	43.68	41.92	20.99	19.56	19.24
100350	1.22	1.50	2.50	2.52	2.49	12.05	13.56	11.94	14.09	12.30	284.87	49.64	41.88	43.54	41.23	18.91	17.76	17.44
100350	1.22	1.51	3.00	2.86	2.88	11.74	13.49	11.91	14.24	12.33	410.06	68.66	58.29	43.19	40.36	17.36	16.51	16.19
100350	1.22	1.51	3.51	3.13	3.27	11.62	13.46	11.86	14.47	12.35	561.22	91.78	78.51	43.22	39.45	16.11	15.66	15.28
100350	1.22	3.00	1.00	0.61	0.61	16.56	13.58	11.91	14.38	12.98	45.57	11.85	9.66	42.92	42.80	34.86	32.98	32.77
100350	1.22	2.98	1.50	0.85	0.84	14.42	13.53	11.87	14.19	12.70	102.30	22.83	18.68	42.31	41.99	31.07	29.27	29.05
100350	1.22	3.00	2.01	1.08	1.05	13.33	13.54	11.93	14.17	12.58	183.47	37.22	30.64	41.61	41.07	28.10	26.44	26.28
100350	1.22	3.00	2.50	1.27	1.24	12.71	13.46	11.84	14.20	12.50	284.31	54.17	44.86	40.85	40.12	25.75	24.27	24.13
100350	1.22	3.01	3.01	1.46	1.45	12.36	13.47	11.84	14.30	12.43	412.20	75.17	62.70	40.04	39.15	23.76	22.47	22.29
100350	1.22	3.00	3.50	1.64	1.66	12.24	13.46	11.84	14.46	12.44	557.71	99.26	83.44	39.43	38.38	22.15	21.06	20.81
100350	1.22	4.51	1.01	0.34	0.38	17.84	13.48	11.83	14.46	13.26	45.98	12.64	10.25	38.20	38.26	34.53	33.16	32.96
100350	1.22	4.48	1.50	0.52	0.54	15.27	13.47	11.86	14.23	12.95	102.38	23.94	19.42	37.26	37.26	31.78	30.39	30.20
100350	1.22	4.49	2.01	0.69	0.70	14.04	13.42	11.83	14.17	12.72	184.40	39.24	32.01	36.70	36.61	29.51	28.19	28.05
100350	1.22	4.49	2.51	0.86	0.86	13.34	13.40	11.83	14.18	12.70	286.23	57.26	47.01	36.34	36.13	27.64	26.44	26.33
100350	1.22	4.48	3.01	0.98	0.99	12.94	13.44	11.87	14.36	12.65	412.29	79.07	65.37	35.94	35.67	26.11	24.99	24.86
100350	1.22	4.50	3.50	1.11	1.14	12.82	13.37	11.81	14.45	12.56	557.73	104.71	87.27	35.73	35.34	24.81	23.80	23.57

Table G-3: Sample of performance evaluation data for trickle fill.

p_a	L_{fi}	G_w	G_a	$Me_{1(A-F)}$	$Me_{1(B-C)}$	K_{dfm1}	T_{noz_db}	T_{noz_wb}	T_{fill_db}	T_{fill_wb}	dp_{noz}	dp_{ftot}	dp_{fi}	$T_{wi(A)}$	$T_{wi(B)}$	$T_{wi(C)}$	$T_{wo(F)}$	$T_{wo(D/E)}$
N/m²	m	kg/m²s	kg/m²s	m^{-1}	m^{-1}	m^{-1}	°C	°C	°C	°C	N/m²	N/m²	N/m²	°C	°C	°C	°C	°C
101410	1.0	1.520	1.005	0.937	0.856	11.74	13.28	11.00	13.36	11.57	45.31	7.49	5.65	50.15	48.92	33.25	30.34	30.13
101410	1.0	1.493	1.500	1.178	1.093	10.69	13.33	10.97	13.35	11.37	100.93	14.63	11.20	49.64	47.72	29.21	26.46	26.13
101410	1.0	1.496	2.006	1.417	1.336	10.11	13.37	10.96	13.43	11.26	180.54	24.08	18.67	49.18	46.68	26.14	23.69	23.37
101410	1.0	1.507	2.497	1.632	1.572	9.80	13.44	11.09	13.67	11.35	280.03	35.42	27.77	48.92	45.83	23.82	21.79	21.51
101410	1.0	1.502	3.003	1.843	1.756	9.69	13.37	10.97	13.83	11.27	404.75	49.55	39.32	48.62	44.92	22.14	20.15	20.02
101410	1.0	1.496	3.500	2.041	1.967	9.66	13.48	11.06	14.20	11.45	550.10	65.92	52.90	48.38	43.83	20.69	18.98	18.81
101410	1.0	2.989	1.004	0.533	0.497	13.42	13.59	10.97	14.08	12.22	45.27	8.73	6.53	47.45	47.04	38.49	36.10	35.88
101410	1.0	2.997	1.504	0.694	0.636	11.58	13.46	10.95	13.91	11.96	101.58	16.63	12.47	47.12	46.40	35.15	32.72	32.65
101410	1.0	2.986	2.001	0.837	0.777	10.78	13.42	10.95	13.82	11.66	179.71	26.75	20.25	46.62	45.56	32.39	30.04	29.93
101410	1.0	2.996	2.502	0.972	0.905	10.34	13.36	10.95	13.92	11.65	280.99	39.36	30.11	46.34	44.99	30.26	28.00	27.97
101410	1.0	2.980	2.999	1.082	1.038	10.18	13.42	10.93	14.05	11.52	403.63	54.41	42.14	45.95	44.35	28.37	26.33	26.16
101410	1.0	2.981	3.490	1.188	1.152	10.18	13.38	10.92	14.22	11.49	546.76	72.18	56.61	45.47	43.62	26.92	24.94	24.63
101410	1.0	4.478	1.000	0.361	0.371	15.22	13.33	10.96	14.31	12.62	44.89	9.68	7.28	44.96	44.86	39.55	37.81	37.52
101410	1.0	4.484	1.509	0.496	0.490	12.71	13.38	11.00	14.10	12.31	102.26	18.32	13.72	44.26	43.93	36.66	34.82	34.49
101410	1.0	4.483	1.989	0.593	0.592	11.62	13.38	10.94	13.96	11.94	177.56	28.68	21.57	43.76	43.30	34.48	32.65	32.26
101410	1.0	4.468	2.491	0.699	0.682	11.06	13.48	10.99	13.95	11.84	278.52	42.05	31.92	43.24	42.64	32.57	30.70	30.42
101410	1.0	4.482	2.994	0.787	0.765	10.85	13.40	10.99	14.15	11.79	402.50	58.42	44.86	42.60	41.86	30.92	29.08	28.84
101410	1.0	4.488	3.471	0.865	0.844	10.82	13.51	11.05	14.35	11.74	541.17	76.86	59.74	42.06	41.22	29.59	27.77	27.53

Table G-4: Sample of performance evaluation data for splash fill.

p_a	L_{fi}	G_w	G_a	$Me_{1(A-F)}$	$Me_{1(B-C)}$	K_{dfm1}	T_{noz_db}	T_{noz_wb}	T_{fill_db}	T_{fill_wb}	dp_{noz}	dp_{ftot}	dp_{fi}	$T_{wi(A)}$	$T_{wi(B)}$	$T_{wi(C)}$	$T_{wo(F)}$	$T_{wo(D/E)}$
N/m^2	m	kg/m^2s	kg/m^2s	m^{-1}	m^{-1}	m^{-1}	°C	°C	°C	°C	N/m^2	N/m^2	N/m^2	°C	°C	°C	°C	°C
101340	3.04	1.509	1.005	0.26	0.34	11.73	13.31	11.27	13.72	12.02	45.44	18.46	16.64	48.33	47.09	31.60	30.97	28.48
101340	3.04	1.504	1.499	0.31	0.39	9.22	13.29	11.23	13.59	11.73	101.01	32.00	28.59	48.18	46.20	28.26	27.80	25.38
101340	3.04	1.505	2.007	0.35	0.44	8.45	13.23	11.18	13.60	11.57	181.00	51.81	46.41	48.03	45.26	26.00	25.63	23.31
101340	3.04	1.503	2.496	0.38	0.47	8.38	13.20	11.19	13.70	11.60	279.99	78.12	70.52	47.65	44.31	24.51	24.07	21.69
101340	3.04	1.493	3.005	0.40	0.50	8.88	13.12	11.22	13.85	11.67	405.54	117.49	107.32	47.28	43.34	23.44	23.03	20.38
101340	3.04	1.497	3.509	0.42	0.53	9.53	13.08	11.30	14.12	11.82	553.05	169.15	156.15	46.88	42.06	22.43	22.16	19.39
101340	3.04	3.024	1.003	0.15	0.20	17.01	13.11	11.38	13.94	12.62	45.18	26.48	24.30	46.37	46.05	37.47	36.20	34.70
101340	3.04	3.016	1.509	0.20	0.25	12.75	13.04	11.34	13.70	12.34	102.36	44.92	40.76	46.10	45.46	34.13	33.14	31.52
101340	3.04	3.008	2.014	0.23	0.28	11.59	12.96	11.32	13.63	12.13	182.18	71.71	65.17	45.67	44.70	31.68	30.84	29.11
101340	3.04	3.009	2.503	0.25	0.31	12.16	12.93	11.36	13.76	12.16	281.31	113.71	104.52	45.28	43.98	30.15	29.38	27.32
101340	3.04	3.007	2.995	0.26	0.35	13.25	12.97	11.33	13.92	12.10	402.89	173.85	161.65	45.11	43.39	28.48	28.39	25.52
101340	3.04	2.994	3.499	0.26	0.40	12.86	12.94	11.30	14.13	12.04	549.73	228.35	212.79	44.84	42.78	26.87	27.54	23.86
101340	3.04	4.499	0.997	0.10	0.14	22.29	12.84	11.04	14.29	13.06	44.56	33.65	31.28	44.21	44.15	38.97	37.84	36.79
101340	3.04	4.502	1.501	0.14	0.19	16.29	12.40	10.60	13.62	12.22	100.87	55.96	51.42	43.85	43.61	36.03	35.10	33.90
101340	3.04	4.492	1.983	0.17	0.22	14.87	12.27	10.45	13.31	11.78	175.90	88.25	81.19	43.69	43.28	34.02	33.18	31.84
101340	3.04	4.492	2.512	0.18	0.25	16.49	12.35	10.47	13.36	11.68	282.40	153.37	143.13	43.57	42.88	32.26	31.79	29.77
101340	3.04	4.490	3.023	0.19	0.30	16.65	12.37	10.44	13.42	11.50	408.88	221.09	207.40	43.40	42.44	30.46	30.85	27.74
101340	3.04	4.489	3.502	0.19	0.36	15.32	12.36	10.43	13.59	11.39	548.73	272.10	254.84	43.23	41.93	28.78	30.04	25.98

APPENDIX H. SPLASH FILL DETAILS

The V-bar splash tested is shown in Figure H-1.

Figure H-1: Photograph of V-bar splash fill in test facility.

The fill is packed in a staggered arrangement with a vertical pitch of 200 mm and a horizontal pitch of 100 mm, as shown in Figure H-2.

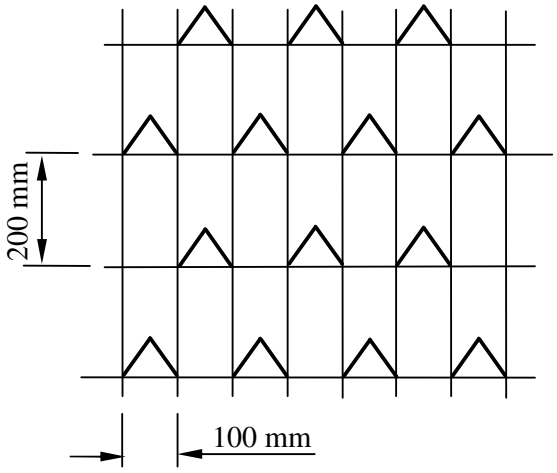

Figure H-2: Staggered layout of V-bar splash fill.

The dimensions of a single V-bar are shown in Figure H-3.

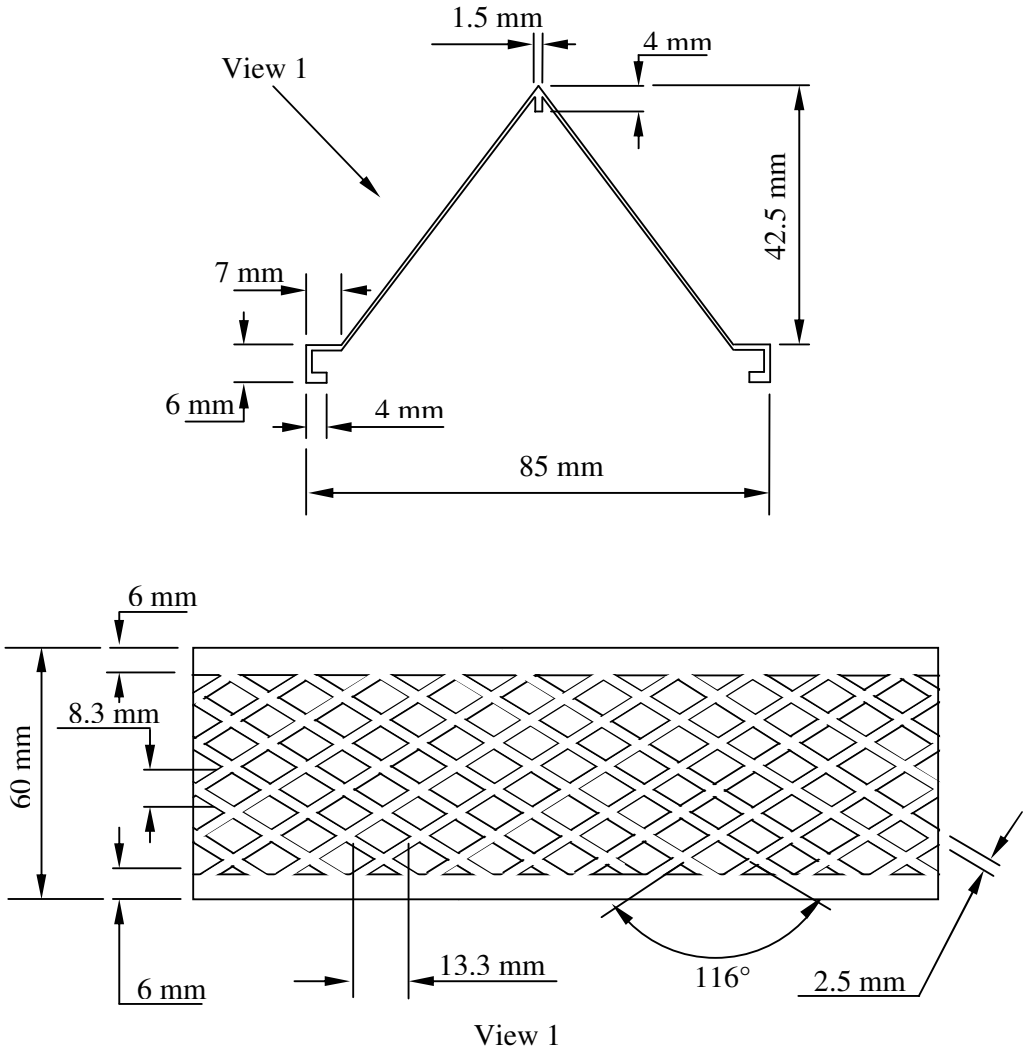

Figure H-3: Detail dimensions of V-bar splash fill.